Morphometric analysis of the gull *Larus* (Aves:Laridae) with implications for small theropod diversity in the Late Cretaceous

by

Michel Haché

A thesis submitted to the Faculty of Graduate and Postdoctoral Affairs in partial fulfillment of the requirements for the degree of

Master of Science

in

Earth Science

Carleton University
Ottawa, Ontario

Abstract

This project analyzed morphological diversity in the modern gull (Aves: Charadriiformes) genus *Larus*. Measurements of the post-cranial skeletons were made on specimens from six species of *Larus* and analyzed using Principal Component Analysis (PCA). Similar analyses were conducted on a series of theropod taxa. Landmark-based geometric morphometric analysis was also conducted on select skulls of gulls and analyzed using PCA. The results show that most of the gull species are very similar for the morphological parameters analyzed, only differing in overall body size, and, thus cannot be easily distinguished based on their skeletal morphology. These results were used as a modern analogue for inferring species diversity in the theropod fossil record. The implications of this study suggest that skeletal morphology, without the addition of soft tissue and behavior data available for modern birds, may not be able to distinguish closely related species of interbreeding, non-avian theropods in the fossil record. This suggests that the species diversity of extinct non-avian theropods was likely higher than can be of determined from their skeletal remains.

Acknowledgements

I would like to thank my supervisors, Dr. Michael Ryan and Dr. Tim Patterson for their support over the past two years. I would like to thank Elizabeth Anderson for her patience and for helping me with writing this thesis. I would also like to thank Michel Goselin and the staff of the Canadian Museum of Nature for helping me with my data collection and allowing me access to the museum's collection. I would like to thank Mark Peck for helping me with the data collection of the specimens at the Royal Ontario Museum. I also want to thank Dr. Phil Currie for providing me with his database of theropod measurements. I want to thank everyone in the Patterson Research Group for their help and support. A special thank you to all my friends and family for all the support they've given in the past three years. This research was, in part, supported by a NSERC Discovery Grant to Tim Patterson.

Table of Contents

List of Tables

List of figures

List of Appendices

Chapter 1: Introduction

1.1 Introduction

All living birds are dinosaurs belonging to the clade Avialae, a branch-based clade that includes modern birds and all species more closely related to them than to deinonychosaurs (Naish, 2012, Gauthier, 1986). Small-bodied theropods (Dinosauria: Theropoda) are among the most studied dinosaurs, with multiple new taxa being described every year, (e.g., Benson and Carrano, 2010; Ryan *et al*., 2012), but our understanding of their rich natural history is affected by preservation and the completeness of their fossil record that frequently only preserves fragmentary specimens, especially for material derived from North American deposits (e.g.: Ryan *et al*., 2012; Larson, 2008). Taphonomic size biases ensure that larger-bodied taxa are commonly more complete as fossils, and will preserve more readily than smaller-bodied taxa (e.g., Brown 2013). Theropods are typically diagnosed based on hard tissue characters (skeletal elements and teeth) and soft tissues are only rarely preserved in some taxa (e.g., Ji *et al*., 2001, Longrich, 2006, Xu *et al*., 2012). There are rare cases of exceptional preservation where soft tissues are preserved, such as the Solnhofen limestones of Germany (e.g., *Archaeopteryx*) or the Jehol fauna from the Liaoning deposits of China (containing multiple complete skeletons from birds and small theropods) that can preserve feathers and stomach contents (e.g., Zhang, *et al.* 2010; Bada, *et al.* 1994). Many of these, such as the recently discovered *Zhenyuanlong suni* (Hu *et al*., 2009, Zanno, 2010, Lü and Brusatte

2015), provide new insights into the evolutionary history of modern birds through the description of new anatomical details. However, since almost all small theropod taxa are described exclusively based on their skeletal characteristics, this has resulted in most genera being monospecific.

By contrast, species recognition of modern animals is not uniquely based on skeletal features, but uses molecular, behavioural and morphological data, such as integument type and colour and general body size (e.g., Griffiths *et al*., 1998; Haddrath and Baker 2001; Hebert *et al*., 2004). The only skeletal related character that is frequently used to diagnose extant birds is size, which has limited utility in fossil taxa where the effects of ontogeny can rarely be fully considered (e.g., Dwight, 1925).

Extant Aves are described either exclusively, or primarily, on soft-tissue features (i.e., feather colour and patterning), behavior (i.e., mating behaviour and songs (Emlen, 1972; Slabbekoorn and Smith, 2002), and genetic differences (mDNA and chromosomal differences, e.g., Prum, *et al*., 2015). These characters allow for a level of taxon discrimination unavailable for fossils such that for the vast majority of modern birds genera, multiple species are recognized, with many having overlapping geographical occurrences (e.g., Kubetzki and Garthe, 2003; Norell and Makovicky, 2004). Recent work in molecular phylogeny has further suggested that the number of species within some groups should at least be doubled because morphologically and behaviorally identical taxa have proven to be genetic distinct (e.g., Jetz *et al*., 2012, Lemme and Erbacher, 2013).

Despite the limitations of the fossil record, there are currently ~1100 valid non-avian dinosaurs known from the 186 million years of the Mesozoic, with 527 genera currently described (Starrfelt and Liow 2016). By comparison, there are more than 10,600 (Hoyo *et al*., 2013) modern dinosaurs (Aves) alive today. If we can assume that every bird taxa has a 1 million year time span, and that bird diversity for the Jurassic and Cretaceous was similar to what it is today, then we can estimate that approximately 1.4 million species have existed since the end of the Triassic, If dinosaur diversity in the Jurassic and Cretaceous matched that of modern birds, then we can estimate that only 0.1% of the dinosaur species that actually existed after the end of the Triassic are currently known. When we acknowledge that most living theropod (bird) species are only recognized based on non-fossilizing features, then we can hypothesize that the fossil material that is known for extinct, non-avian theropods cannot capture the diversity we would expect for any diagnosed genera.

Species concepts

The ability to recognize and diagnose species in fossilized taxa has been an on-going debate in biology ever since Linnaeus formalized a system of taxonomic nomenclature and the concept of a dichotomously branching 'tree' to represent the relationships between taxa (Queiroz, 1997, Reece *et al*., 2009). In such a system, the lengths of the 'branches', and the distance between them, were rough indications of the implied evolutionary relationships between groups (Reece *et al*., 2009). Mayr (1942) formulated the biological species concept as follows: ‘’*Species are groups of actually or potentially interbreeding natural populations, which are reproductively isolated from other such populations”.* he later revised this basic definition in 1969 and 1982 by omitting the ‘’actually and potentially’’ interbreeding clause. He also added that species ‘’*occupy a specific niche in nature”* (Mayr 1982). The key to the biological species concept is that species are not defined based on their appearance, but on their breeding potential (Mayr 1942, Mayr, 1957; Mayden, 1997).

Recognizing the difficulty in determining interbreeding potential in the fossil record, Simpson (1951) defined the evolutionary species concept as "*…a lineage (an ancestral-descendent sequence of populations) evolving separately from others and with its own unitary evolutionary role and tendencies”*. This concept does not consider the breeding potential of a species or it’s ecological niche (Mayden 1997). Multiple additional definitions have been coined, including the phylogenetic species concept, the genetic species concept, the morphological species concept, all of which have varying systematic utility

depending on the group being investigated and the questions of relationships being asked. Some of the other species concepts are summarized below:

Morphological Species Concept: This concept groups species based on morphological and anatomical criteria (Reece *et al*., 2011). It typically uses skeletal morphology to infer taxonomic relationships. It is also used to characterize species that do not reproduce sexually, or for species that are known only as fossils (Mayr *et al* 1963).

Phylogenetic/cladistic species concept: This concept considers the evolutionary relationships among organisms. It relies on evolutionary history and common ancestry to define species (Reece *et al*., 2011). Since paleontologists lack access to the breeding potential and most soft tissue features of the fossils that they study, they typically use hard tissue characters to construct hypotheses of relationships relative to a common ancestor, thus incorporating, in part, the morphological species concept when describing fossil organisms. Geographic, stratigraphic, and ontogenetic considerations can also be incorporated as characters in these analyses.

Genetic Species Concept: This concept defines species based on their genetic similarity or distance. Genetic analyses can uncover cryptic species, which cannot be distinguished using morphological analyses. This concept incorporates the biological species concept by assuming that a species is a group of

genetically compatible, interbreeding natural populations that are genetically isolated from other populations (Baker and Bradley, 2006).

Paleontologists lack access to assessing the breeding potential of the fossils that they study, so they typically implicitly use the phylogenetic species concept (Reece *et al*., 2011). The inferred relationships within the phylogenetic hypotheses illustrated by phylograms are generated almost exclusively on hard tissue characters.

In the modern era of paleontology, inferences of relationships between taxa based on the cladistical method developed by Hennig (1965) which categorizes organisms based on shared, derived characters, and illustrated using branching diagrams called cladograms. Under this system, discrete characters are compared within a group assumed to have a common evolutionary ancestry. The analytical methods of cladistics have been refined using complicated mathematical algorithms that can be run using specific computer software (e.g., NTSSYS-pc, PHYLIP, PAUP etc.) on powerful computing systems, and can incorporate a range of characters including morphologic, genetic, geographic and stratigraphic.

1.2 Project goals

This project assumes that modern birds can be used as analogues for their related non-avian theropod relatives (based on the extant phylogenetic bracketing methodologies of Bryant and Russell, 1992; and, Witmer, 1995), and that inferences made about the skeletal basis for recognizing modern species

can be applied to build hypotheses about recognizing species, and thus, species diversity, in the fossil record. The goal of this research is to analyze the morphological diversity within one multispecific bird genus to determine if these species can be distinguished exclusively on a select set of skeletal parameters alone. If they cannot be distinguished, this will suggest that, perhaps, within small, non-avian theropods there may be a hidden diversity that also cannot be determined without access to soft-tissue and behavioral data.

To examine this question, I analyzed species within one genus (*Larus*) of the most common group of shorebirds, the gulls (Aves: Charadriiformes) for a limited number of characters of the skull and postcrania to determine if they can be distinguished morphologically. Since the species to be studied are well established, I will test the null hypothesis (H_o) that the species cannot be distinguished morphologically. If rejected, I will accept the alternative hypothesis (H_1) that the species can be distinguished morphologically using morphometrics analyses. I will also conduct analyses of the post crania for the best available data set of small maniraptoran dinosaurs to determine if they can be distinguished (H_o) by the same parameters. If they cannot, I will not reject the null hypothesis (Ho); I can then infer, that like the modern birds examined, the fossil sample set may contain more species than is currently recognized.

1.3 Gulls

Gull phylogenetic relationships used in this research are based on the cladistic analysis of Chu (1998). His analysis was based on morphological

characters of the skeleton and integument. Gulls (or seagulls) are among some of the best-studied shorebirds, with a worldwide distribution. They are genetically and behaviorally diverse but very similar morphologically (see: Chu 1998; Baker *et al*., 2007; Thomas *et al*., 2004a, Thomas *et al*., 2004b), making them an excellent group on which to explore the utility and limitations of morphological characters in identifying species (Chu 1998). Laridae (gulls) is the sister clade to Sternidae (terns) within the clade Lari in the clade (order) Charadriiformes (Chu 1998, Cane 1994, Wetmore 1960). Charadriiformes is diagnosable by the following shared characters: schizognathous palate (having the maxilla-palatine bones separate from each other and from the vomer, which is pointed in front) and further similarities in syrinx and leg tendons (Brooke and Birkhead 1991). They are distantly related to auks, skimmers and waders (Chu 1998, Crochet *et al*., 2000, Livezey 2010). They have medium-to-large sized bodies that are typically white to grey in integument colour, often with black tipped wings and/or heads, long bills and webbed feet. Their unhinged jaws allow them to feed on large prey items of fish and marine invertebrates (Colewell 2010). Gulls are typically coastal animals. They nest in large, densely packed colonies of between 50 to hundreds of individuals. They lay two to three eggs in nests composed of vegetation (Burger 2006).

Most taxa take two years to develop adult plumage, going through several plumage states during their lifespan (Olsen and Larsson, 2010), although medium and large-sized gulls may take three or four years, respectively to reach maturity (Olsen 2010). Plumage is used to assess age in the field.

1.4 Avian evolution

The gull *Larus* was chosen because it is a large (~1.5 kg) genus - making it easy to measure parameters - with multiple species. Ideally, a flightless bird taxon would have been chosen as, lacking well-developed tails and being flightless, it more closely resemble their non-avian theropod ancestors; however, most flightless taxa are monospecific, and they are poorly represented in museum collections, making it difficult to amass a statistically significant data set. Birds evolved from small-bodied maniraptoran dinosaurs during the mid- to late Jurassic with the earliest accepted bird being *Archaeopteryx lithographica* (Padian, 2004). Most of the features that characterize birds first evolved in small-bodied maniraptorans, such as feathers, sternum, furcula and hollow limb bones, and are now generally considered to be adaptations for fast running (Padian, 2004, Holtz, 2012). During the Late Cretaceous, birds diversified very rapidly with most of the major clades evolving within the short span of 0.5 to 5 million years (McCormack *et al*., 2013).

Gauthier (1986) coined the term Avialae for the branch-based clade that includes modern birds and all species more closely related to them than to deinonychosaurs (Naish, 2012, Gauthier, 1986), with the term ‘Aves’ being used to describe the crown group of birds. Modern birds (Neornithes), are divided into three major groups: Paleognathae (*Tinamous* and flightless ratites), Galloanserae (gamebirds and waterfowls) and Neognathae (other modern birds) (Naish, 2012, Prum, 2015). Neognathae includes the clade Neoaves which

represents the majority of all avian diversity (about 95% of all species) (Mayr and Clarke, 2003). Paleognathae and Neognathae form the group Neornithes (Naish, 2012; Padian, 2004; Mayr and Clarke, 2003).

Sibley and Ahlquist (1990) made major advances in bird taxonomy when they applied DNA hybridization to determine the degree of similarity between taxa. This technique compares the entire genome of species to determine how closely related various species are. Hackett (2008) conducted a phylogenomic analysis of 169 species of birds to determine their evolutionary history (fig 1). His analysis showed support for much of the previously established clades of birds (like land birds, charadriiformes, water birds and galloanserae).

A recent comprehensive phylogenetic analysis of Neornithes (Prum *et al*. 2015) refined the proposed relationships between major clades and defined the synapomorphies that support them (fig 2 and 3). They erected the new clade Aequorlitornithes within Neoaves, which includes the majority of waterbirds, including Charadriiformes (waders and shorebirds, including gulls), Mirandornithes (flamingos and grebes) and Ardeae (Eurypygimorphae and Aequornithes).

The sister group of the shorebirds is the ‘land birds’, which is an informal name for a large and diverse group supported only by molecular characters (Hackett *et al*., 2008, Ericson *et al*., 2006). This group contains most (but not all) of the familiar land birds, including the Passeriformes (a group that includes more than half of all bird species) (Hackett *et al*., 2008).

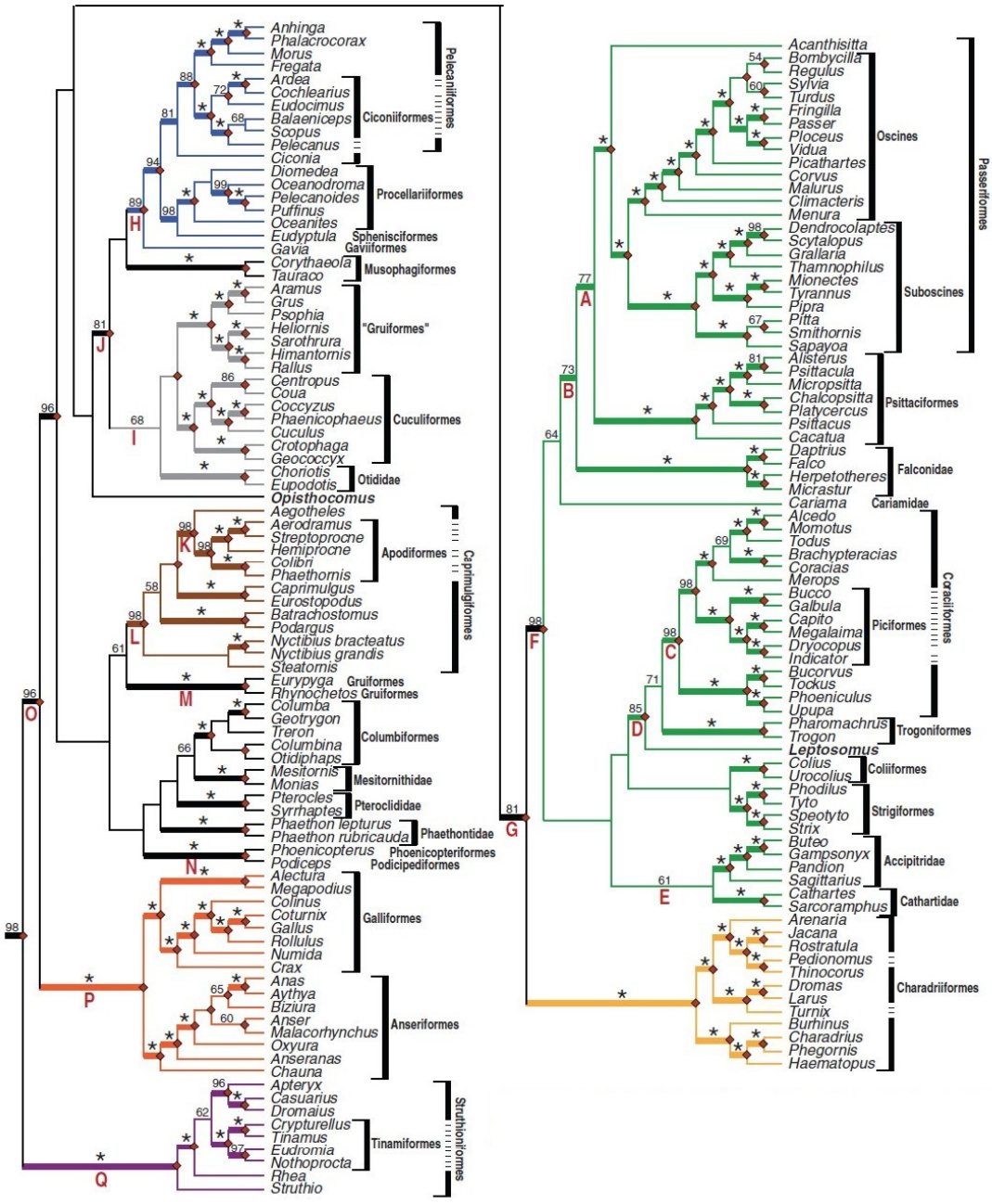

Figure 1: Fig. 2 from Hacket *et al.,* 2008 showing avian taxonomy

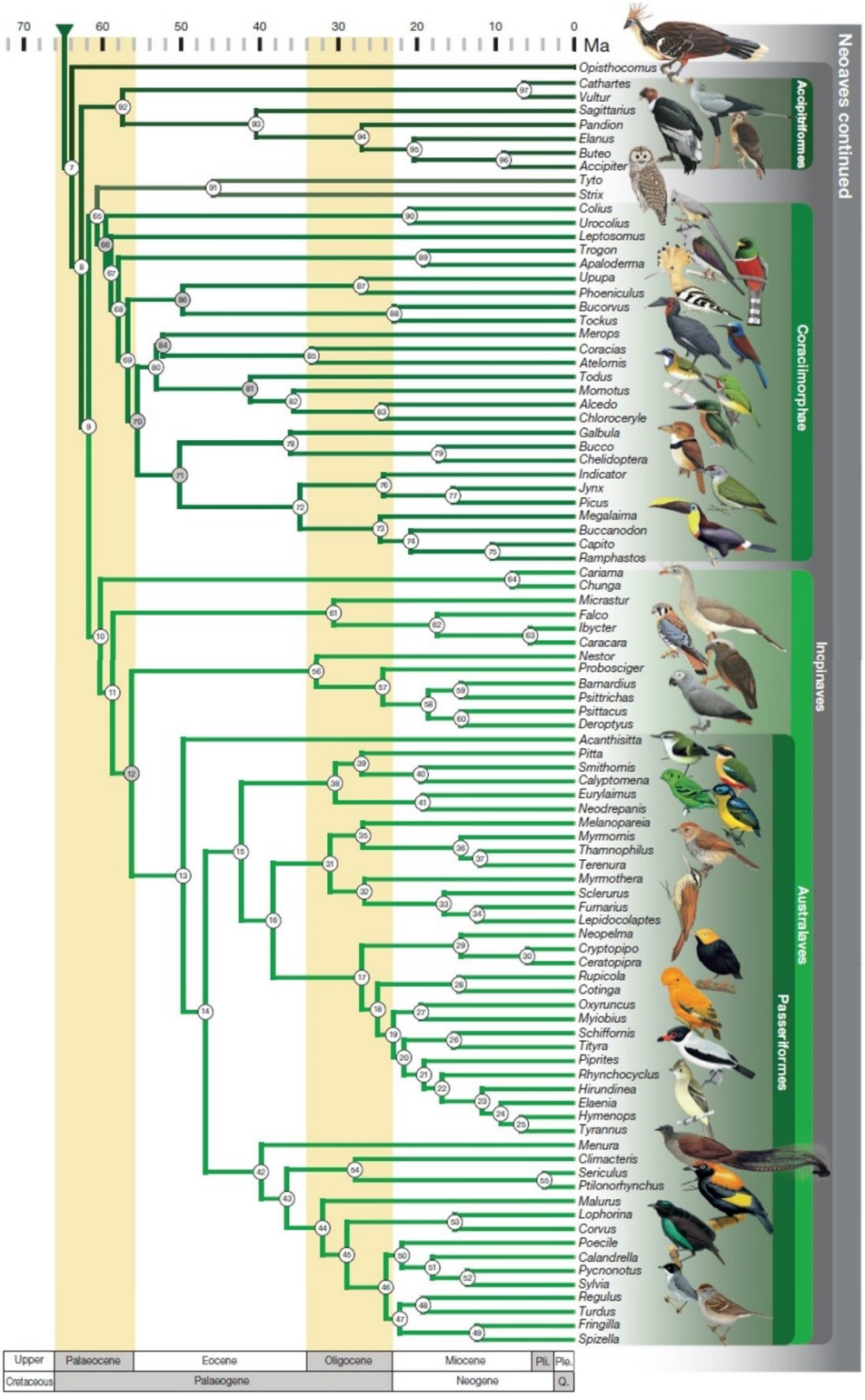

Figure 2: Taxonomy of the birds based on Prum *et al.*, 2015 pt. 1

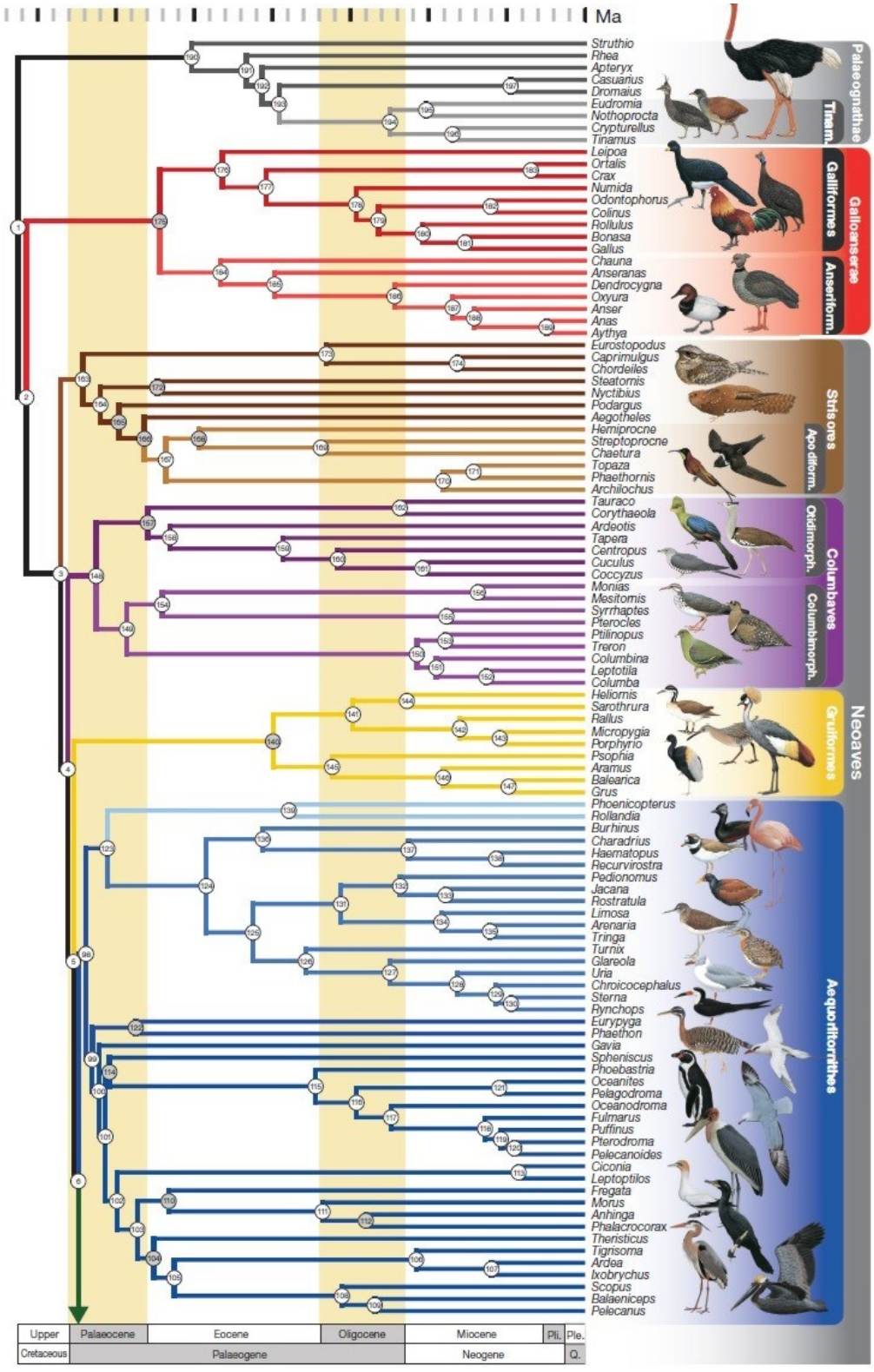

Figure 3: Avian taxonomy based on Prum *et al.*, pt. 2

1.5 Laridae taxonomy

The systematics of Laridae (comprising skuas, terns, gulls and skimmers) have been studied for more than a century, beginning with early 19th century non-phylogenetic studies (Coues,1862). Most previous morphological analyses carried out on species within the genus *Larus* (gulls) were based on non-morphometric data. Typically, the data used focused on external characters, such as plumage coloration. One of the first avian analyses to include gulls obtained poor resolution within 'gulls' and could not distinguish between gull species (Dwight, 1925; fig. 1). Dwight grouped the gulls into two genera, *Larus* and *Hydrocoloeus* with four and five species, respectively. He further subdivided the largest bodied species into subspecies. The first hypothesis of gull systematics based on qualitative morphological features (plumage and bill coloration) and display behavior was proposed by Moynihan (1959; fig. 4). He recognized 10 genera of gulls comprised of 9 species.

Hudson *et al*. (1969) conducted a non-cladistical numerical analysis of shorebirds using characters of the appendicular musculature of gulls. Their results supported the recognition of gulls as a monophyletic group, but had poor resolution. Schnell (1970) conducted a principal component analysis and a phenetic study of Lari (gulls, skuas, terns and skimmers) using a combination of skeletal and integumentary data to generate over a dozen phenograms that he used to differentiate skimmers and terns from gulls and skuas by characters of the bill. However, only one of Schnell's analyses (using external characters of the

feathers) was able to cluster all the gulls together to the exclusion of all other shorebirds.

Hoffman (1984) also performed a qualitative analysis of the postcranial skeleton, but he could not resolve their relationships (Fig. 5). Cane (1994) analyzed the ontogeny of bill shape and hind limbs in a variety of shorebirds that indicated a close relationship between gulls and skuas (Fig. 6B and 6C). Chu (1998) conducted an analysis of gulls using 117 skeletal and 64 integumentary characters and obtained one best, fully resolved tree (Fig. 7), although the recovered clades are poorly supported statistically. Chu's results suggest that the genus *Larus* is not monophyletic. In order to make nomenclature reflect the phylogeny that he generated, Chu suggested subdividing the gulls into six genera; *Larus, Xema, Rissa, Pagophila, Hydrocoloeus* and *Chroicocephalus*.

Chu (1998) also compared the utility of osteological vs. integumentary characters in his analysis of the gulls using a total-evidence analysis. The total-evidence methodology uses character congruence to look for the best fitting phylogenetic hypothesis for all the available characters (Eernisse and Kluge, 1993). Chu analyzed 117 qualitative characters from the skeleton and scored them according to character states (e.g., presence/absence of the character). He did several analyses using, 1., only the osteology, 2., using only integuments, and then, 3., using thevcombiined osteology and integument data. The osteology-only data set recovered 25% of the most parsimonious trees using a total evidence approach, while the integument-data set only had 30% congruence. Chu found that in the gull groups, osteological change is minimal

compared to other groups of birds (e.g., the auks). If only the gulls are considered, then the osteology-only data set included approximately 7% of the clades. This suggests for gulls, osteology is important in reconstructing higher-level phylogenies, but the integument is more useful for lower-level phylogenetic reconstructions.

The gulls constitute a well-studied group of birds that include over 28 extant species within a single genus (Sibley and Ahlquist 1990). Support for what is now considered to be the natural gull group has been the outcome of several studies (e.g. Hudson *et al*., 1969; Schnell, 1970; Hoffman, 1984; Hackett, 1989; Sibley and Ahlquist, 1990; Crochet *et al*., 2000), and continues to be refined within the context of both more detailed analyses (e.g., Laridae; Pons *et al*., 2005), and broader analyses of all Aves (e.g., Livezey *et al*., 2007). This ongoing research uses a variety of data types, including morphological analysis (e.g., Chu, 1998), comparative parasitology (Timmermann, 1957; Hugot *et al*., 1991), protein electrophoresis and DNA-DNA hybridization (Hackett, 1989, Sibley and Ahlquist, 1990), and behavioural analysis (Burger and Gochfeld, 1990). Some of these analyses have produced differing in-group relationships for Laridae (e.g., Chu, 1998, Hacket, 1984) and different sister group relationships within Aves. Laridae is currently placed as a sister clade to Sternidae (terns) within the clade Lari in the order Charadriiformes (Pons *et al*., 2005).

1.6 Previous morphometric analyses of dinosaurs

There have been numerous morphometric (shape) analyses conducted on dinosaurs to investigate such functions as cranial kinesis (e.g., Holliday and Witmer, 2008), jaw and neck mechanics (e.g., Snively and Russell, 2007) and locomotion (e.g., Gatesy and Middleton, 1997). Foth and Rauhut (2013) used geometric morphometrics to evaluate theropod cranial diversity and its relation to phylogeny, ecology and function, but not species level recognition. Some morphometrics of teeth have been used to recognize dinosaur taxa (e.g. Smith *et al* 2005, Larson 2008).

Dodson (1993) conducted some of the first dinosaurian morphometric analyses when he compared the cranial morphology of several species of ceratopsians. In 1993, he used 16 specimens from 12 taxa to test whether phyletics produced similar clustering results as cladistics. Dodson digitized 21 landmarks on each skull specimens and His analysis determined that specific diagnostic characters can be found on all parts of the skull and that they are not sexually dimorphic. His analysis was also recovered the clade Ceratopsidae clade indicating that morphometrics is a valid method for recovering and recognizing higher level dinosaur clades.

Hedrick and Dodson (2013) conducted 3D geometric morphometric analysis on *Psittacosaurus* specimens to understand their individual and taphonomic variations. They sampled 30 skulls from three species of Psittacosauridae (*P. lujiatunensis*, *P. major*, and *Hongshanosaurus houi*) from the Lujiatun beds of the Yixian Formation. Their results showed that most of the

variation between the species results from individual and taphonomic variation. They concluded that there is only one species of *Psittacosaurus* within the Lujiatun beds and that the three species previously identified represent different taphomorphotypes of *P. lujiatunensis*. This implies that the range of variation found in other dinosaurian groups may also be related to taphonomic distortion, rather than interspecific variation (Hedrick and Dodson, 2013).

Maiorino *et al*. (2013) conducted geometric morphometrics on *Triceratops* and *Torosaurus* to determine whether these taxa are congeneters. They examined the cranial morphology of 28 skulls and 36 squamosals of *Nedoceratops hatcheri, Triceratops sp*. and *Torosaurus sp.* using landmark-based morphometrics. Their results showed that *Torosaurus* is a distinct and valid taxon, whether looking at the entire skull, the skull without the frill, frill alone, or squamosals separately. *Torosaurus* has different morphologies and distinct allometric trajectories compared to *Triceratops*. These results indicate that extinct dinosaur taxa can be recognized using morphometric analyses.

Maiorino *et al*., (2013) also c geometric morphometrics to investigate the shape change in the squamosals of 155 ceratopsian specimens, representing 27 species of Chasmosaurinae and Centrosaurinae. The results indicate that the ceratopsian squamosal is highly constrained in phylogeny. There is an evolutionarily significant allometric signal between the two clades, but not within each clade. Chasmosaurines, compared to centrosaurines, show a more derived squamosal morphology, with a trend towards a blade that is strongly expanded

dorsoventrally and with a narrower angle between the infratemporal process and the caudoventral margin (Maiorino *et al*. 2013).

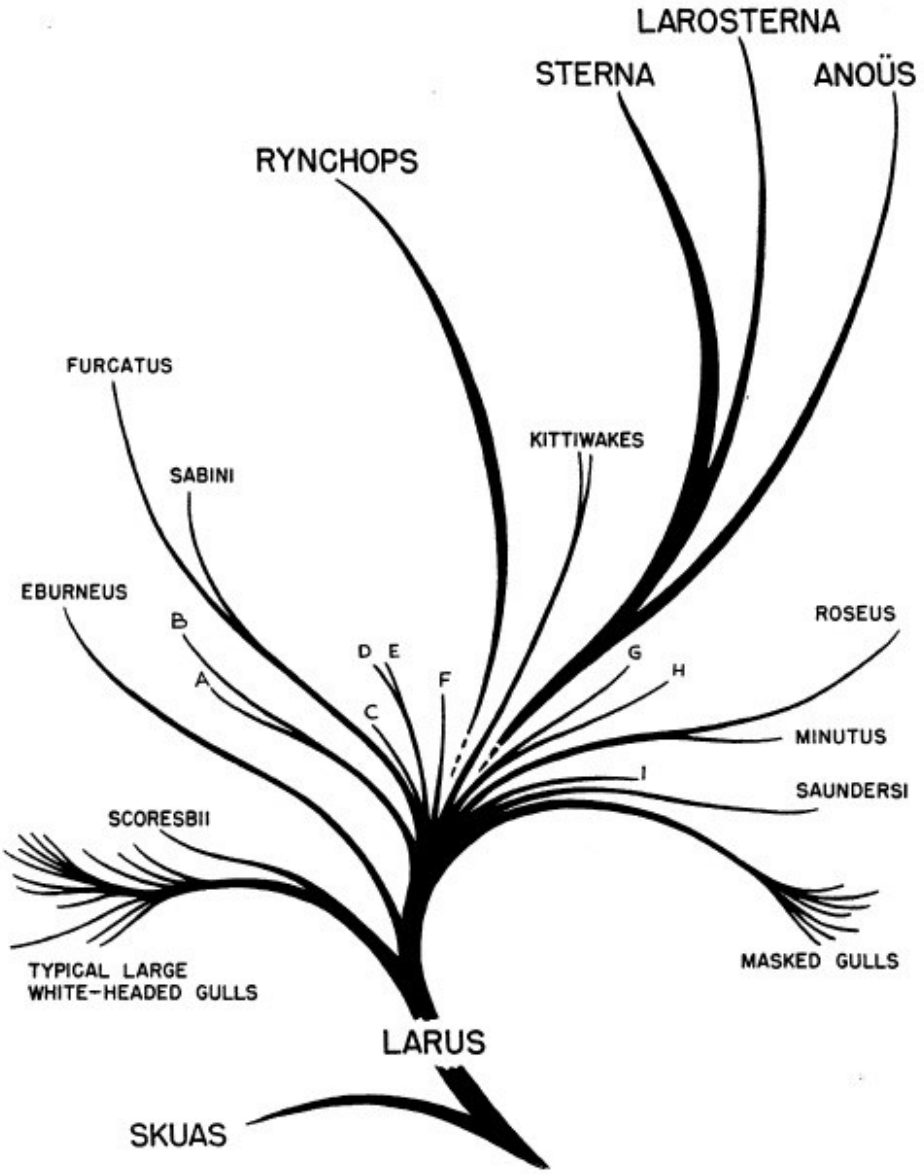

Figure 4: a rough family tree generated by Moyniham (1959) showing the inferred releationship between each gull taxa. A: *Larus heermanni*, B: *Larus modestus*, C: *Larus fuliginosus*, D: *Larus hemprichi*, E: *Larus leucopthalmus*, F: *Larus atricilla*, G: *Larus ichtyaetus*, H: *Larus pipixcan*, I: *Larus melanocephalus*. A: *Larus heermanni*, B: *Larus modestus*, C: *Larus fuliginosus*, D: *Larus hemprichi*, E: *Larus leucopthalmus*, F: *Larus atricilla*, G: *Larus ichtyaetus*, H: *Larus pipixcan*, I: *Larus melanocephalus.*

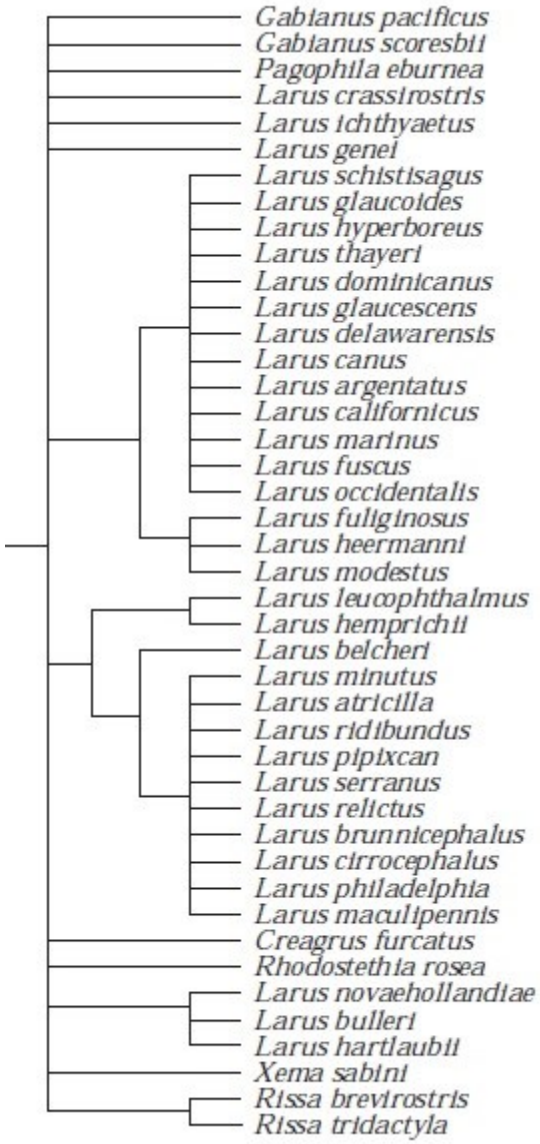

Figure 5: Hoffman's (1984) phylogeny of the gulls showing the relationships of each gull taxa.

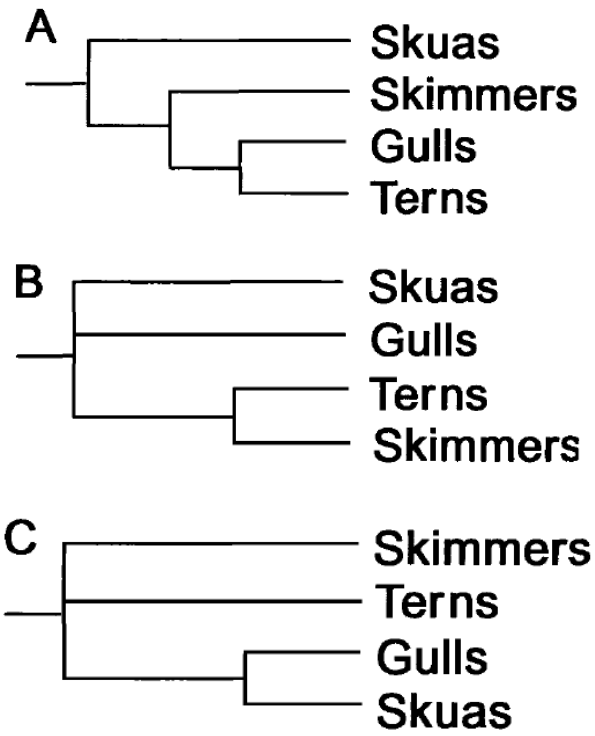

Figure 6: Three common theories on shorebird taxonomy, A being the one that is currently accepted (from Cane 1994). A) Terns and gulls are more closely related to each other than to skimmers and skuas. These relationships are supported by molecular analyses (ex: Hackett 1989). B and C have been suggested by comparative parasitology (Timmermann 1957) and analyses of skeletal morphology (Strauch 1978)

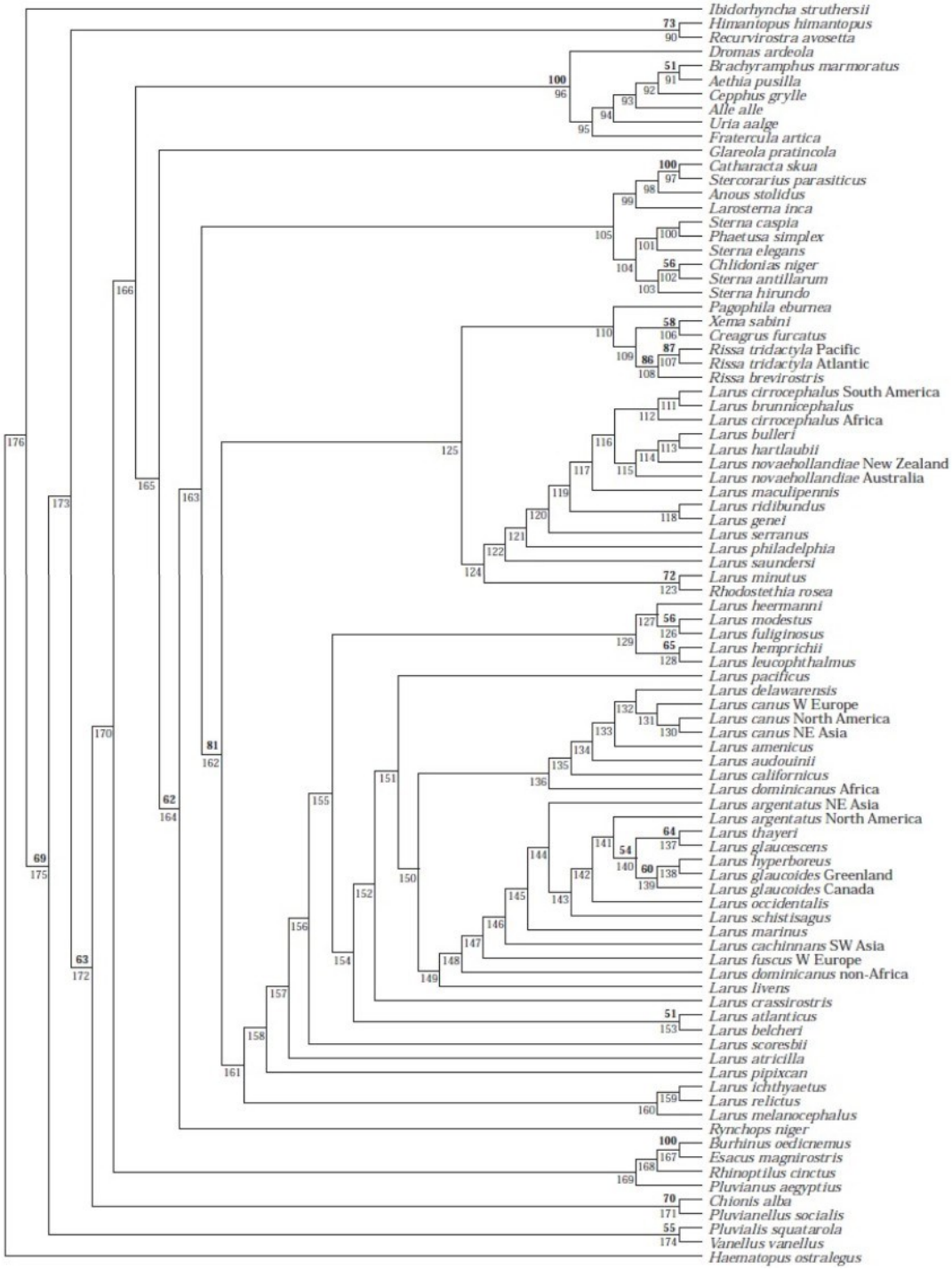

Figure 7: Phylogeny of gulls as proposed by Chu (1998).

1.7 Theropod taxonomy

Theropoda (‘’beast-footed ones’’) are some of the most well-studied dinosaurs and various hypotheses regarding their phylogenetic relationships are illustrated in Figs. 8 - 11. They are a diverse and globally distributed group of saurischian dinosaurs comprised of some of the largest terrestrial carnivores ever to exist, such as *Spinosaurus, Tyrannosaurus* and *Giganotosaurus*. Other theropods were quite small, such as *Microraptor* and *Epidendrosaurus* (Holtz, 2012). Theropods represent the most successful group of dinosaurs in that their descendants, the birds, survived the terminal extinction at the end of the Cretaceous (Cooper and Penny, 1997; Holtz, 2012).

The earliest theropod-bearing deposits are found in the upper Triassic Ischigualasto formation of Argentina, (Sereno *et al*. 1993; Sereno ,1997; Benton, 2004; Irmis, 2010; Benton, 2012). The closest outgroups to Dinosauria are found in South-America, suggests that dinosaurs originated in South-America (Brett-Surman *et al*. 2012).

Theropoda is defined as *Passer domesticus* (the European house sparrow) and all taxa sharing a more recent common ancestor with it than with *Cetiosaurus oxoniensis* (Holtz and Osmólska, 2004). A recent revision has suggested replacing *Passer domesticus* with *Allosaurus fragilis* (Kischlat, 2000). There are several characters that unite Theropoda, including: prezygapophyses in the distal caudals extending one quarter or more the length of the previous caudal; the humerus is shorter than 60% of the length of the femur; the proximal ends of the metacarpals are joined to each other (but don not overlap); the shaft

of metacarpal IV is much more slender than the other metacarpals; the fifth digit of the hand does not have phalanges (Benton, 2012).

Most theropods belong to the clade Averostra (=Neotheropoda *sensu* Bakker, 1986) and belong to one of two major clades, Ceratosauria and Tetanurae (Benson, 2009, Brusatte and Sereno, 2008, Langer *et al*., 2014, Carrano *et al*., 2012). Since the theropods of interest to this project are within Tetanurae, the phylogeny of ceratosaurs will not be discussed. For a complete discussion of Ceratosauria phylogeny, see Carrano and Sampson (2008).

Tetanurae systematics

Tetanurae (‘’stiff tails’’) is composed of three major clades; Megalosauroidea, Carnosauria and Coelurosauria (Fig. 11), with the last two comprising Avetheropoda (Holtz, 2012). The coelurosaurs originated during the Middle Jurassic (Holtz. 2000, Rauhut. 2003), or earlier (e.g., Barrett. 2009) and include the Maniraptora and all living birds (Avialae; Holtz, 2012). Some of the characteristics of tetanurans include having teeth restricted to the front of the jaws, proportionally larger hands, and interlocking tail vertebrae in the distal half of the tail (Holtz, 2012).

Maniraptoriformes, which includes famous groups such as the dromaeosaurs and birds, is a group of theropods characterized by a reduction of skull size relative to body size; a reduction in tooth size; an increase in tooth count, an increase in brain size (based on skull size); elongated forelimbs; a large, bony sternum for the attachment of the muscles that pull the arms inward;

and a semilunate carpal (a pulley-shaped block of wrist bones that allowed greater folding motion while sacrificing motion in the other plane).

Eumaniraptora (often synonymized with Paraves) is one of the last major groups of extinct theropods to have radiated and includes Deinonychosauria and Avialae, and is defined by the following synapomorphies: greatly reduced prefrontals; margin of the external antorbital fenestra on the craniolateral surface of the descending ramus flattens out and is not continued on the surface of the jugal; vertical columnar process is present on the retroarticular process; vertebral centra of caudal vertebrae I – V are box-like with increased mobility; glenoid articulation of the pectoral girdle is oriented laterally in basal dromaeosaurids, basal troodontids and basal birds; coracoid is subrectangular; coracoid forms a sharp angle at the point of articulation with the scapula; pubic tubercle is spine-or crest-like and points cranially; distal articular surface of the tibia is rectangular and more than three times as wide transversely as craniocaudally (Holtz and Osmólska, 2004).

Avialae is the group of theropods that includes *Archaeopteryx* and modern birds (Neornithes). Current taxonomy shows that birds evolved within Maniraptora, approximately 150 million years ago (Padian 2004). The earliest divergence within Neornithes occurred between Neognathae (fowls, ducks and most modern birds) and Paleognathae (emus, ostriches and relatives) (Tuinen 2009, Edwards *et al*., 2005). Avialans are distinguished from other vertebrates by a number of features, including: an elongate prenarial portion of the premaxilla; the breaking down of the postorbital bar; absence of dental serrations and the

presence in the teeth of a characteristic constriction; enlargement of the cranial cavity; caudal tympanic recess opening within the columnar recess; presence of a caudal maxillary sinus; fewer tail vertebrae, with the prezygapophyses reduced distally; ossified uncinate processes on the edge of their vertebral ribs (Witmer 2002). Other features of birds include a keeled sternum; furcula; hollow limb bones and double-condyled quadrates that articulate with the prootic (Padian, 2004). Many of these features first evolved in small maniraptorans as adaptations for fast running and ground dwelling. Feathers were originally thought to be an avian synapomorphy for at least Coelosauria, but are now recognized as a symplesiomorphy (an ancestral trait shared by two or more taxa or group). This is due, in part, to the presence of a feather-like integument in a number of non-theropod dinosaur groups, including *Psittacosaurus* and *Tianyulong* (an Early Cretaceous heterodontosaurid) (Norell and Xu. 2005, Godefroit *et al*. 2014, Zheng *et al*. 2009).

Archaeopteryx represents one of the earliest eumaniraptorans and one of the earliest members of Avialae. It is the sister taxon to Deinonychosauria+Avialae (Mayr *et al*., 2005). *Anchiornis* from the Late Jurassic of China was originally described as a basal bird older than *Archaeopteryx*, but has more recently been identified as a non-avian troodontid by Hu *et al*. (2009). *Archaeopteryx* is represented by seven skeletons and isolated feathers, all of which were discovered in the Solnhofen limestone in Germany. Even though they retained the long tail and teeth of reptiles, the fossils were recognized as early

birds because of the fact that they retained feathers, a boomerang-shaped furcula, and hollow bones (Padian 2004).

Avialae (*sensu* Gauthier, 1986) is defined as a stem group to encompass living birds and maniraptorans closer to them than to *Deinonychus.* Defining characters of Avialae include: enlarged brains; long slender, tridactyl manus; curved chevrons making the distal part of the tail slender and long; and narrow metatarsals (Holtz, 2012, Larsson *et al*. 2000). The term ‘’birds’’ is still used to encompass *Archaeopteryx* and all the more derived members of Avialae (with Neornithes considered the crown taxon) (Padian, 2004, Gauthier, 1986).

Our understanding of the evolution and radiation of early birds has been growing exponentially in recent years. This is due in part to the discovery of several early bird fossils that have come out of China, including the *Archaeopteryx*-like *Xiaotingia zhengi* and *Jeholornis prima* (O’Connor and Zou 2015, Xu *et al*., 2011). Ever since the discovery of *Archaeopteryx,* very few new avian fossil have been discovered until quite recently (Fountaine *et al*., 2005). With these recent additions more than 70 genera of Mesozoic fossil birds are known from sites distributed globally (Chiappe and Dyke 2002).

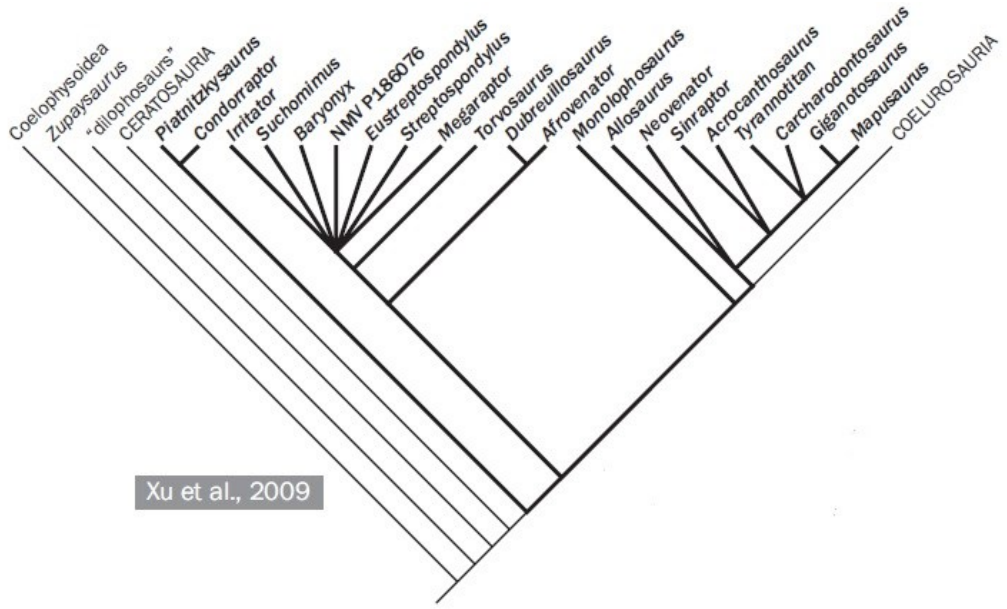

Figure 8: Phylogeny of theropods as proposed by Xu *et al.,* 2009.

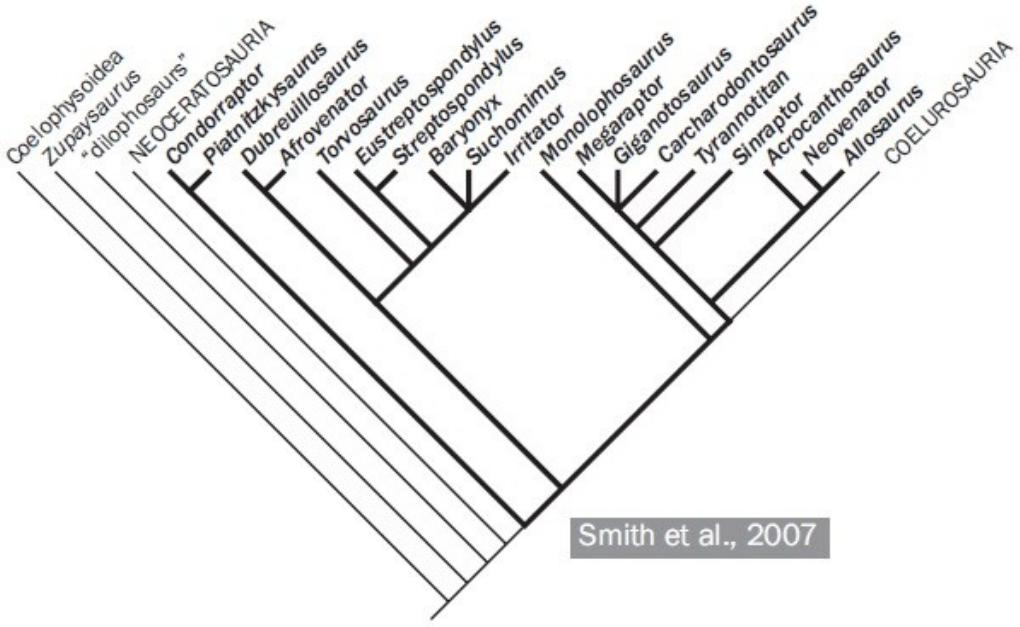

Figure 9: Phylogeny of theropods as proposed by Smith *et al*., 2007.

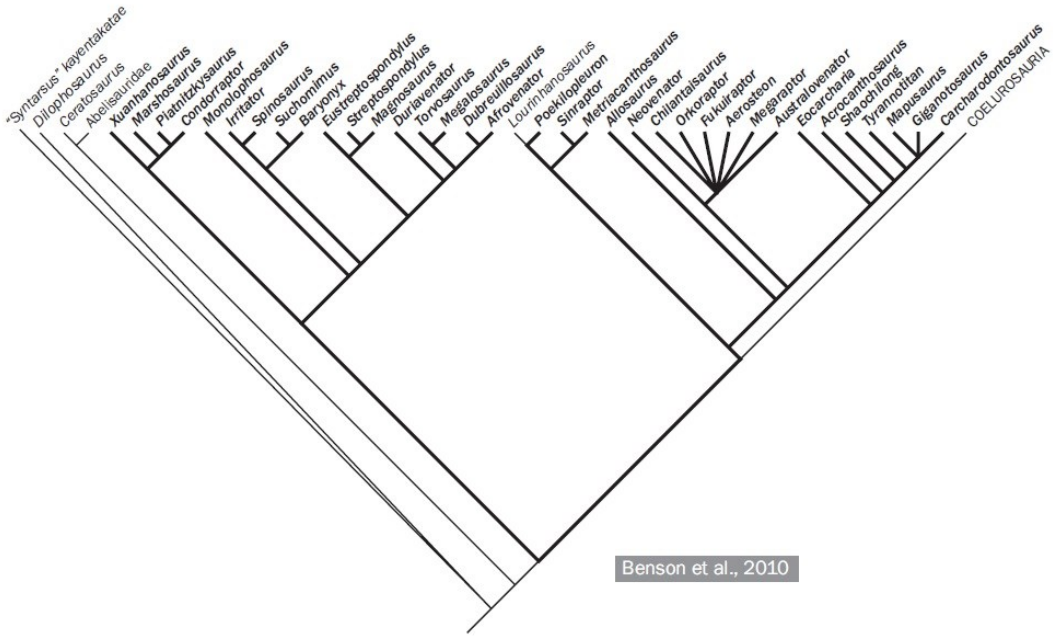

Figure 10: Phylogeny of theropods as proposed by Benson *et al*., (2010)

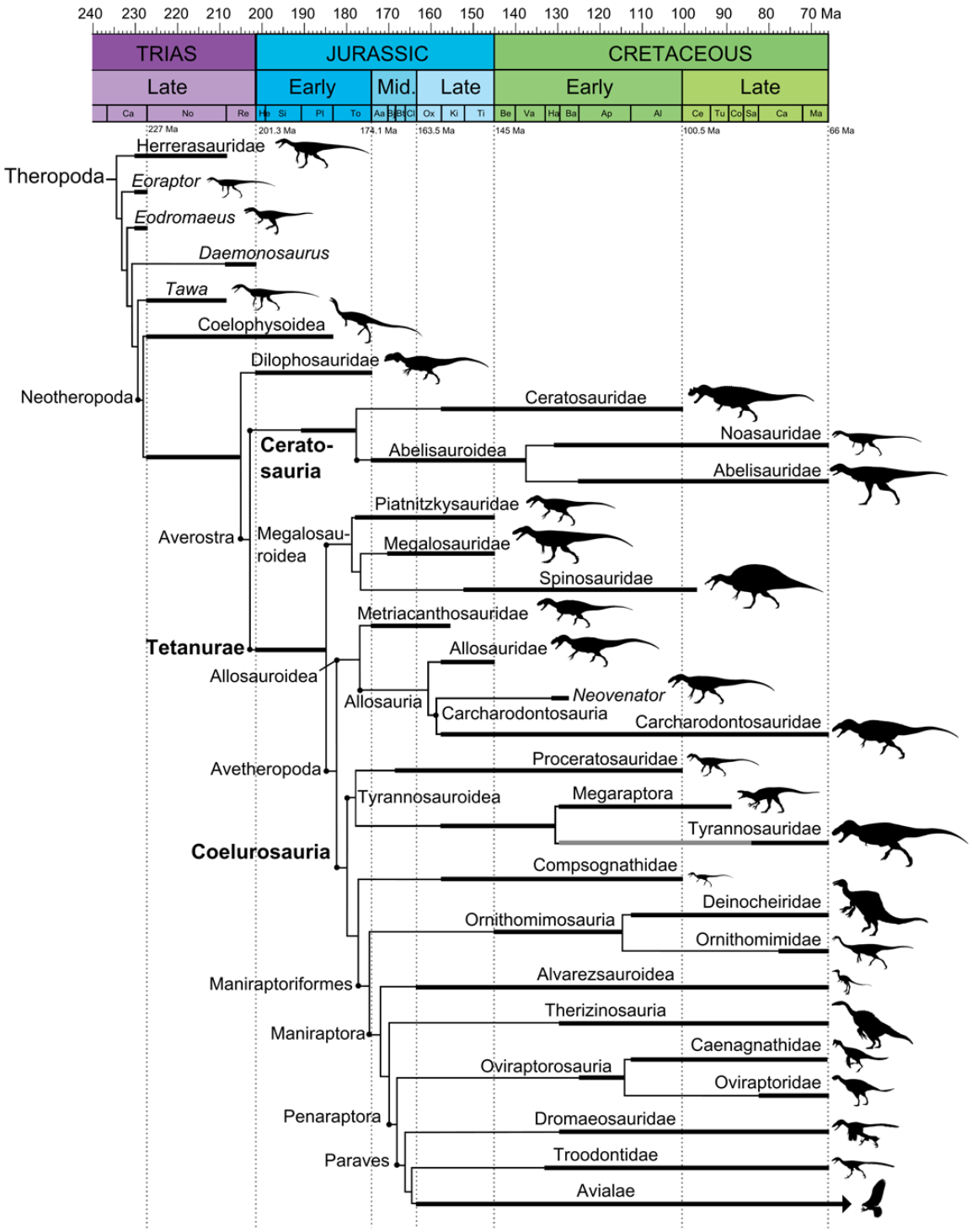

Figure 11: Theropod phylogeny from Hendrickx *et al.*, 2015.

Chapter 2: Materials and Methods

2.1 Gull species analyzed

Gulls are part of the family Laridae and are defined by several characteristics, including: exposed culmen (the upper part of a bird's beak) is less than one and a quarter times as long as the tarsus; tarsus is more than one-tenth as long as the wing; tail is usually truncate or rounded, rarely forked, and sometimes wedge shaped or graduated (Ridgeway and Friedmann, 1919, p. 561). The genus *Larus* is distinguished by the following characteristics: medium to very large Laridae with well-developed hallux entirely free from the inner toe; tibia has at least the lower half unfeathered; tarsus is longer than the middle toe without claw; tail is truncate or very slightly rounded; in adults, the tail and under belly is almost entirely white; and the bill is shorter than the head (Ridgeway and Friedmann, 1919, p. 581). The original description of *Larus* was made by Linneaus (1758): Bill straight, sharp edged and hooked at the tip; lower mandible convex below the tip; nostrils linear, broader near the fore-part and placed in the middle of the bill. The original description of *Larus* was made by Linnaeus (1758): the bill is straight, with sharp edges and hooked at the tip; the lower mandible convex bellow the tip; nostrils linear, broader near the fore-part and placed in the middle of the bill

A short description of each gull species analyzed based on field guides is included in Table 1. The gull species analyzed during this project include:

Larus delawarensis (Ring-billed gull): Their most defining feature is the black ring around their bills (Rideway and Friedmann, 1919).

Larus argentatus (European Herring gull) (Pontoppidan 1763): The original description roughly translates to: *Larus argentatus* has a black spot on the end of the outer wing. There is a red dot on the lower beak (Pontoppidan 1763). Most of the defining characters of *L. argentatus* are integumentary in nature (refer to Table 1).

Larus glaucoides (Iceland gull) (Meyer 1822): The original description roughly translates to: the beak is yellow, with the base greenish gray. The lower jaw has a bright red spot. The beak is slightly shorter than in *L. argentatus*. The feet are yellow. The shoulder and wing coverts are pale blue gray, the edge of the wings are white. The Flight feathers are white without black (Meyer 1822).

Larus glaucescens (Glaucous-winged gull) (Naumann 1840): They are mostly defined based on their feather coloration (refer to Table 1). Their bills are yellow, whitish at the tip with a subterminal red spot on the lower mandible.

Larus hyperboreus (glaucous gull) (Gunnerus 1767): This species is typically larger in size compared to other gull species (Ridgeway and Friedmann 1919, P. 581) (refer to Table 1 for description).

Larus thayeri (Thayer's gull) (Brooks 1915): described as being about the size of *Larus kumlienis*, but differeing primarily in the color of the mantle, primary flight feathers and having a larger and heavier bill. The color of its mantle is intermediate between *L. kumlieni* and *L. argentatus* (see Table 1) (Brooks 1915, p.373).

Table 1: description of each *Larus* species analyzed during this project (from Hayman *et al* 1986 and Sibley 2003

Species	Size (M= males, F= females)	Physical description	Geographic range
Larus argentatus	Length M: 60 – 66cm F: 56 – 62cm Weight M: 1000 – 1250g F: 800 – 980g	Both sexes have similar plumage. First year young have all brown plumage. Yellow beak with red spot on lower mandible. Beak is long and slender with peak on rear crown. Pink or flesh coloured legs. Wing feathers are black with white spots. Long narrow wings. Eyes are golden with yellow ring of skin.	Entire northern hemisphere. Native to Nearctic and palearctic regions. Live in coastal regions near body of water.
Larus delawarensis	Length M: 46 – 54cm F: 43 – 50cm Weight M: 400 – 700g F: 300 – 700g	Adults have an average wingspan of 127cm. Pale bluish back with white heads. White wings and their belly is white. They have a narrow black band around their bills. Their bill is fairly short and slim. First year young have whitish feathers with brown flecks. Morphologically similar to herring gulls.	Ranges from the southern shores of Alaska to the gulf coast to Cuba. Found in inland waterways
Larus glaucoides	Length 55 – 64cm Wingspan 125 – 130cm Weight 557 – 863g	Relatively small with round head and short bill. Round bodies with short bills, short legs and relatively broad but pointed wings which create an overall stocky appearance.	Breeds in arctic regions of Canada and Greenland. Winters in the northernmost states of the USA, in Iceland and on the coast of Norway
Larus hyperboreus	Length 64 – 77cm Weight 1070 – 1820g Wingspan 132 – 142cm	As large as the Great Black Backed gull. Plumage is lighter in coloration, light gray in coloration. Back and wings are pale blue-gray, belly and wingtips are white. Often confused with the similar, but smaller, Iceland Gull. Their heads are flatter, back of their head us less rounded. Legs more pinkish.	Lives in the arctic regions of the northern hemisphere, Northern Europe and Asia.
Larus thayeri	Length 56 – 69cm Weight 846 – 1152g Wingspan 130 – 140cm	White headed with pale gray mantle. Bill is yellow with red gonydeal spot. Legs are dark pinkish. Some scientists consider it to be a subspecies of herring gull. It is considered as its own species in this project.	Breeds in high arctic of Canada. Found on the western coast of the united states and Canada.
Larus glaucescens	Length 61 – 69cm Weight 900 – 920g Wingspan 130 – 142cm	Males larger than females. Adults are white with pale gray backs. Wings pale gray with small white patches. Large body and large bill, but extremely variable: some are more slender than others.	Lives near salt or brackish water along coasts and bays. Nests on rocky cliffs of the coastal northern pacific, from Alaska to the Aleutians

2.2 Theropod taxa analyzed

All the theropod measurements were taken from a database of measurements provided courtesy of Dr. Philip J. Currie. The database contains over 2000 theropod specimens from 150 genera including seven tyrannosaurids, six maniraptorans and the earliest birds *Archaeopteryx lithographica* and *Confuciusornis sanctus*. They range in size from very large theropods to small-bodied birds. Only the most complete specimens, a total of 52, were analyzed. The species listed below and described subsequently were analyzed during this project:

Tyrannosauridae (large-bodied theropods)

- *Albertosaurus sarcophagus*
- *Daspletosaurus torosus*
- *Gorgosaurus liberatus*
- *Raptorex kriegsteini*
- *Tarbosaurus bataar*
- *Nanotyrannus lancensis*
- *Tyrannosaurus rex*

Eumaniratpora: Dromaeosauridae (small to medium-sized theropods)

- *Sinosauropteryx prima*
- *Bambiraptor feinbergi*
- *Deinonychus antirrhopus*
- An unidentified dromaeosaurid
- *Velociraptor mongoliensis*
- *Saurornitholestes langstoni*

Aves ('basal birds') (small-bodied theropods)

- *Archaeopteryx lithographica*
- *Confuciusornis sanctus*

Tyrannosauridae

Tyrannosauridae (Albertosaurinae+Tyrannosaurinae) is a derived clade of large-bodied theropods that lived at the end of the Cretaceous in North America and Asia. They are characterized by large skulls with a highly specialized heterodont dentition, a derived squamosal-quadratojugal flange, and a highly pneumatic basicranium. They also have greatly reduced forelimbs (both in size and in number of digits) and elongated hindlimbs. The hindlimbs have a pinched third metatarsal (the arctometatarsus) (Holtz, 2004).

Albertosaurinae

Albertosaurus sarcophagus (Osborne 1905): Occurs in the early Maastrichtian Horseshoe Canyon Formation of Alberta (Tanke and Currie, 2010; Russell, 1970; Currie and Eberth, 2010; Holtz, 2001). It is smaller than tyrannosaurids from the Late Maastrichtian (i.e., *Tarbosaurus* and *Tyrannosaurus*) (Holtz, 2004).

*Gorgosaurus libratus (*Lambe, 1914): Occurs in the Dinosaur Park Formation of Alberta, with referred specimens coming from the Two Medicine and Judith River formations of Montana (Holtz, 2004, Erickson *et al*. 2006).

Tyrannosaurinae:

Daspletosaurus torosus (Russell, 1970): Occurs in the Campanian Oldman and Dinosaur Park formations of Alberta, and the Two Medicine Formation of Montana (Holtz, 2004).

Tarbosaurus bataar (Maleev, 1955): Occurs in the Late Cretaceous (?Maastrichtian) of Mongolia, with referred material from China (Holtz, 2004).

Raptorex kriegsteini (Sereno *et al*., 2009): A *nomen dubium* of uncertain provenience that is probably a juvenile *Tarbosaurus* (Fowler *et al*., 2011).

Nanotyrannus lancensis (Bakker *et al*., 1988): The holotype (CMNH 754) comes from the Hell Creek Formation of Montana (Larson, 2013).

Compsognathidae:

Sinosauropteryx prima (Ji and Ji, 1996)***:*** *Sinosauropteryx* was a small-bodied compsognathid discovered in China. It is the first nonavialan dinosaur discovered to have integumentary structures (Holtz *et al*., 2004; Ji and Ji, 1996). Given the phylogenetic position of compsognathids, the structures found on *Sinosauropteryx* are interpreted as the precursors to feathers (Holtz *et al*., 2004; Ji and Ji, 1996). It is known from the Yixian Formation in the Liaoning province of North East China (Holtz, 2004). *Sinosauropteryx* is comparable in size to *Compsognathus* (Currie and Chen, 2001). Both species share several

morphological characters that indicate a close relationship (Currie and Chen, 2001).

Eumaniratpora: Dromaeosauridae

Dromaeosaurs are a group of highly diverse, small to mid-sized maniraptorans that are characterized by the presence of a recurved claw on the second pedal digit (the raptorial claw) as well as a stiffened tail (Gianechini and Apesteguia, 2011). Dromaeosaurs are closely related to the group Avialae.

Bambiraptor feinbergi: Bambiraptor is a Late Cretaceous bird-like dromaeosaurid theropod from the Two Medicine Formation of Montana. The holotype specimen consists of the well preserved skeleton of a juvenile individual. It has several features that are more birdlike than those of other dromaeosaurids (Holtz 2004, Burnham, 2000). Most of those features might be due to the fact that the specimen is a juvenile and not a fully developed adult. The species highly resembles *Saurornitholestes* and only differs in aspects of the frontal bone (Holtz, 2004).

Deinonychus antirrhopus: Deinonychus is a species of carnivorous dromaeosaurid from the late-Aptian to middle-Aptian (Early Cretaceous) (Norell and Makovicky, 2004; Ostrom, 1969). It was approximately 1 meter tall and nearly 3 meters in total length. It was first discovered in the Cloverly Formation of Montana and Wyoming. It shares several features of dromaeosaurine dinosaurs,

such as laterally compressed, serrated teeth, a raptorial manus, a raptorial second pedal digit, and a long tail stiffened by hypertrophied prezygapophyses and chevron processes (Ostrom 1969; Brinkman *et al*., 1998). Several specimens have been collected in assemblages that contained several disarticulated specimens, which leads paleontologists to believe that *Deinonychus* was a gregarious pack hunter (Norell and Makovicky, 2004; Brinkman *et al*., 1998).

Velociraptor mongoliensis: Velociraptor is probably the best-known dromaeosaurid dinosaur. More than a dozen articulated specimens have been recovered. It lived approximately 71 to 75 million years ago during the later part of the Cretaceous period (Osborn, 1924, Norell and Makovicky, 1997). It shares several features with other dromaeosaurids, such as a caudolateral process on the squamosal, an enlarged quadrate foramen, elongated cranial processes on the prezygapophyses of the distal caudals and chevrons and a raptorial second pedal digit (Norell and Makovicky, 2004; Norell *et al*., 1997). It was originally discovered in 1923 in the Gobi by an expedition from the American Museum of Natural History. The taxon is known from the Djadokhta Formation of Mongolia and the Minhe Formation of China (Norell and Makovicky, 2004).

Sinornithosaurus millenii: Sinornithosaurus is a genus of dromaeosaurid dinosaur from the Early Cretaceous period (early Aptian). It is found in the Yixian Formation of China and is one of the smallest dromaeosaurids known from a

near complete skeleton (Xu *et al*., 1999). Xu *et al* (1999) recovered *Sinornithosaurus millenii* as the sister taxon to the velociraptorine-dromaeosaurine group. The specimen preserves elongated integumentary structures associated with the skeleton (Norell and Makovicky 2004).

Aves

The definition of birds used for this project will follow that of Padian (2004): birds comprise *Archaeopteryx* and all its living descendents. Data from only two early birds were available for this project:

Archaeopteryx lithographica: Archaeopteryx is considered the first commonly accepted true bird (e.g., Padian 2004; Longrich *et al*., 2012; Martin *et al*., 1998). . The first discovery of *Archaeopteryx* (a feather) was made in 1860, and all subsequent skeletons have come from the Late Jurassic Solnhofen limestones of Germany (Padian, 2004)*Archaeopteryx lithographica* shares multiple synapomorphies with modern birds, including: elongated, narrow and pointed premaxillae, with long nasal processes; the double condyled quadrate articulates with the prootic; the teeth are reduced in size and are not serrated; the coracoid has a pronounced sternal process; the forelimbs are nearly as long as, or longer, than the hindlimbs; in the pelvis, the cranial process of the ischium is reduced or absent; the caudal margin of the naris nearly reaches or overlaps the rostral border of the antorbital fossa (Padian 2004).

Confuciusornis sanctus: Confuciusornis (Hou *et al*., 1995) is a species of early crow-sized bird from the Early Cretaceous of China. Similar to modern birds,

Confuciusornis has a toothless beak and has a pygostyle. The specimen is well represented by hundreds of specimens collected from the Lower Cretaceous beds of Northeastern China. In certain specimens, there is a pair of blade-like rectrices that have been interpreted as an early example of sexual dimorphism (Feduccia 1996).

2.3 Data collection

Measurements of specimens

A total of 72 specimens from the collections of the Canadian Museum of Nature (Gatineau, QC) and the Royal Ontario Museum (Toronto, ON) were examined and measured from 6 species (Appendices A and B); *L. argentatus* (18 specimens), *L. delawarensis*, (15 specimens); *L. thayeri* (18 specimens); *L. hyperboreus* (10 specimens)*; L. glaucescens* (5 specimens); *L. glaucoides* (2 specimens). All the specimens were measured using a Vernier Digital Caliper and photographed using a Nikon 8200 series camera.

The following linear measurements were taken on each specimen; femur (total length, proximal, distal, and midshaft width), tibiotarsus (total length, proximal and distal widths), tarsometatarsus (total length, proximal and distal widths), and the total lengths of humeri, radii, ulnae; these are diagrammed in figures 12 and 13. Each measurement was taken three times and an average value calculated. This was done to reduce the potential error in the measurements. The sex, age, location and year of collection for each specimen, and all measurements taken are recorded in Appendix A. Measurements of the

theropods were obtained by Dr. Phil Currie and include: femur length, tibiotarsus length, length of third metatarsus, length of radius, length of ulna and length of humerus. Only length measurements were used, because most of the width measurements were missing or incomplete.

Thirty-five skulls from *L. argentatus*, *L. delawarensis* and *L. glaucescens* were selected for landmark-based geometric morphometrics to determine whether there are any morphological differences between the gull species. Each skull was photographed in dorsal and ventral views using the camera mounted on a Zerene stackshot rail and remotely operated using a computer to eliminate any movement that could be caused by manual release of the shutter. The camera was mounted approximately 50 cm away from each specimen. The specimens were placed on a semi-transparent ‘’photo table’’ and illuminated using a series of LED spotlights. In each orientation, between five to eight photographs were taken at different focal points which were then processed in the ‘’zerene stacker’’ program to generate a completely in-focus photograph of each specimen. These were then used for the geometric morphometric analyses.

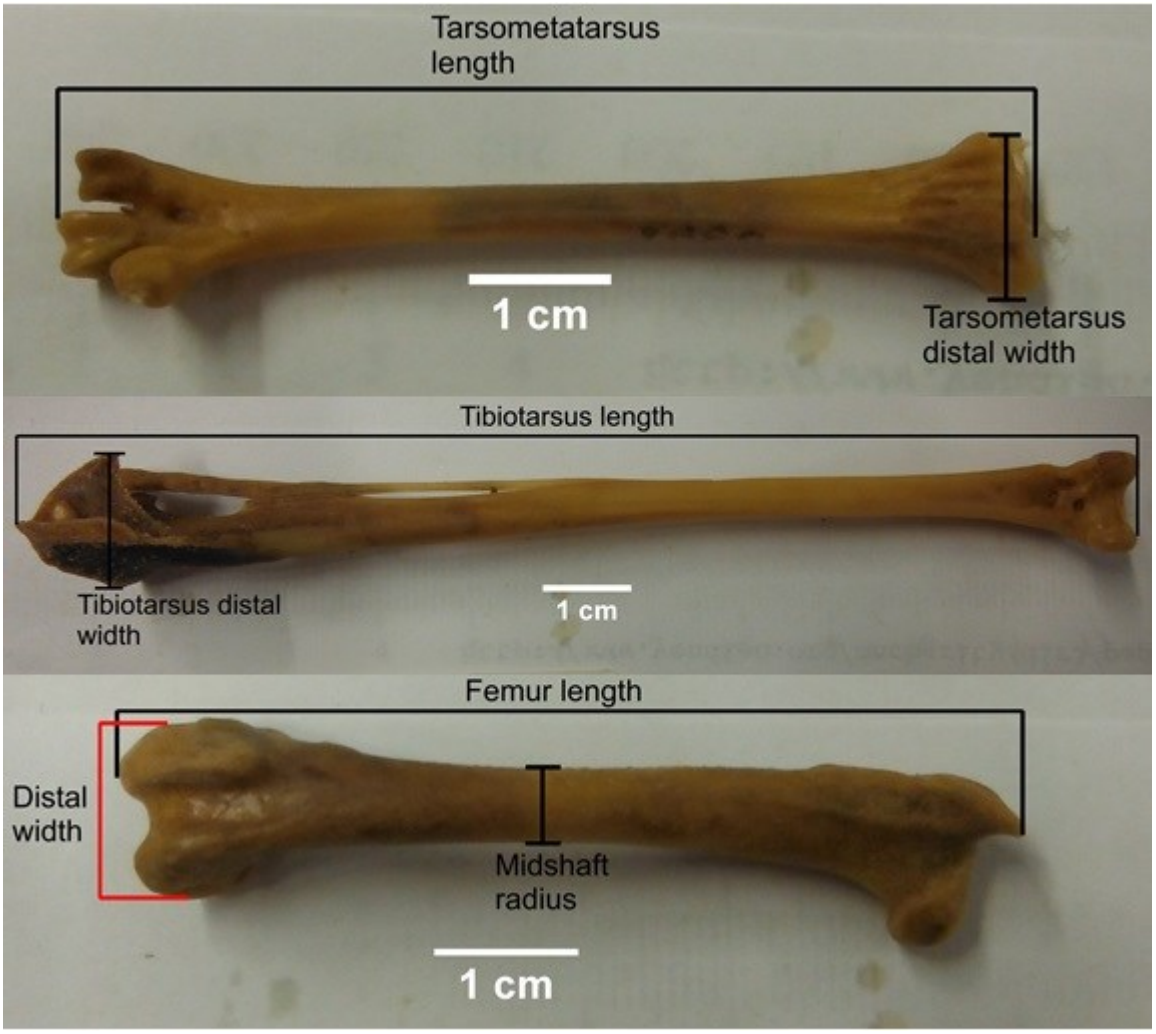

Figure 12: photograph depicting measurements taken on each skeletal element of the gull specimens

Figure 13: measurements taken on the forelimb elements of each gull specimen

Landmark selection

Consistent landmarks (e.g., at sutural junctions or discrete morphological features) that would best represent the shape of the skull were indentified and plotted on each of the photograph. Fourteen landmarks were selected on the dorsal view and 15 on the ventral following the methodology of Cullen (2014) and using some of the methodology suggested by Webster and Sheets (2010). These landmarks were then used to conduct shape-based analyses to determine morphological differences between the specimens. Appendix E illustrates the location of the landmarks that were digitized on each skull. All landmarks were digitized using TPSdigs. Prior to analyzing the landmarks, pocrustes superimposition was performed on the landmarks using the Coordgen8 This was done to reduce the effects of overall size differences while also aligning the coordinates. The data were then analyzed using PCA to identify major trends in the morphological data. The superimposed landmark data was imported into PCAgen8 and deformation grids were extracted for each component to visualize the change in shape of the skulls.

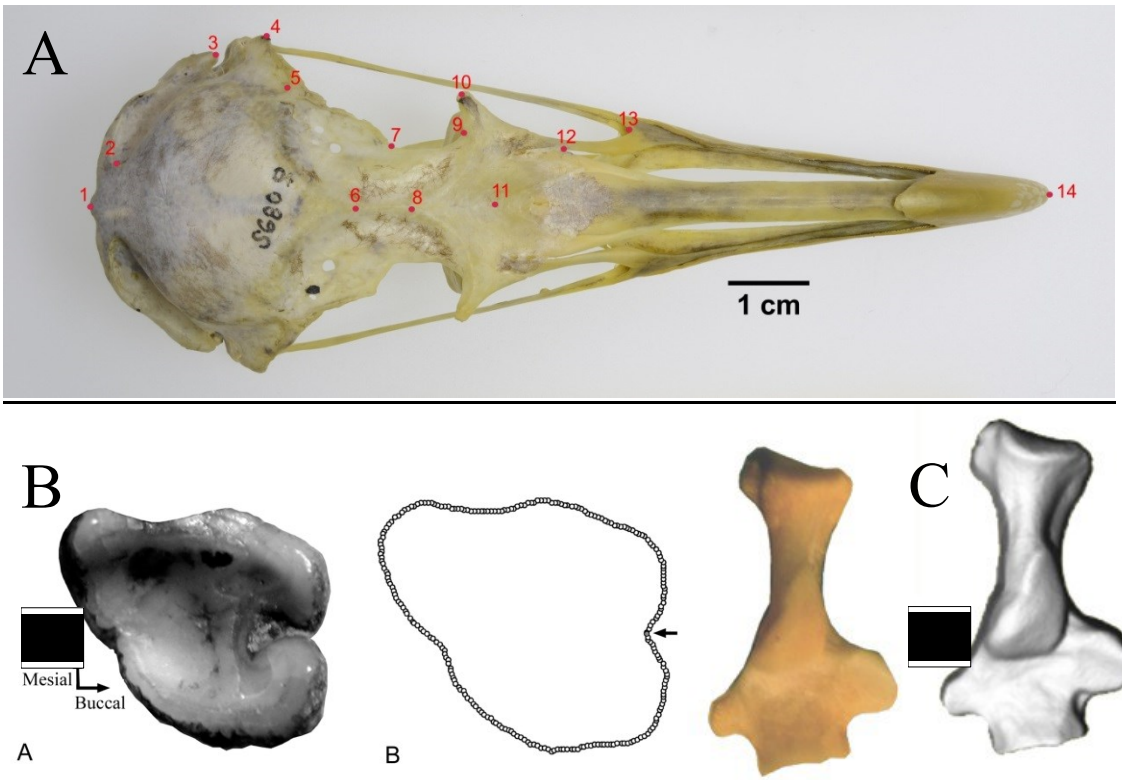

Figure 14: types of landmarks. A) 2-dimensional landmarks, B) semi-landmarks, C) 3-dimensional surface

Geometric Morphometric Analysis

Morphometrics are any quantitative analysis of morphological form, size and/or shape (e.g., Rohlf and Marcus, 1993, Webster and Sheets, 2010). There are three types of morphometric analyses: 1, traditional morphometrics use linear measurements along with multivariate statistics to compare shapes (Marcus 1990, Webster and Sheets 2010), 2, geometric morphometric uses landmark configurations to summarize shape variations, and, 3, morphometric analysis is frequently used in biology to describe organisms (e.g.,Gunduz *et al* 2007). Outline-based geometric morphometrics summarizes the shape of open or closed curvatures (perimeters) (Webster and Sheets, 2010).

An inherent problem with traditional morphometric is that it doesn't adequately capture the overall shape and is sometimes hard to interpret. Landmark-based morphometrics typically capture more of the shape variation and can be easier to visualize. In geometric morphometrics, landmarks are any points described with Cartesian coordinates (x, y and sometimes z) that are used to describe a shape. Figure 14 illustrates the differences in landmark types. Typically, landmarks are placed on a biologically or geometrically homologous point or structures. Semi-landmarks are points placed using algorithms, usually by defining endpoints at biologically homologous points and by placing semi-landmarks between them, e.g., placing two points at either end of a limb bone and then placing a set number of points around the bone (Bookstein 1997, Webster and Sheets, 2010).

Outline-based geometric morphometrics involves summarizing the shape of an object mapping landmarks on the perimeter of the object, typically without using fixed landmarks.

There are three types of landmarks:

Type I: a mathematical point whose claimed homology from case to case is supported by the strongest evidence, such as local patterns of tissue overlap, or small patches of unusual histology (Zelditch, 2004).

Type II: a mathematical point whose claimed homology from case to case is only supported by geometric evidence, not histology (e.g., the sharpest curvature of a structure) (Zelditch, 2004),

Type III: a landmark that has at least one deficient coordinate, for example: either ends of a longest diameter or the bottom of a concavity. Type III landmarks characterize more than one region of the shape (Zelditch, 2004).

2.4 Analysis

Data processing/statistical analysis:

The measurements were standardized by subtracting its mean from that variable and dividing it by its standard deviation:

$$Z_{ij} = \frac{X_{ij} - \bar{x}_j}{s_j}$$

Where:

X_{ij} = data for variable *j* in sample unit *i*

$\bar{x}_j$ = Sample mean for the variable *j*

S_j = Sample standard deviation for variable *j*

This is done so that variables that have higher variance will not have more emphasis than the variables that have less variance.

Principal Component Analyses (PCA) were conducted on the standardized measurements of the gulls and the theropods. PCA is a multivariate method used to emphasize variation and show patterns in a dataset. PCAs maximize variation while reducing dimensionality in a dataset. It works by converting a set of observations of possibly correlated variables into a set number of linearly uncorrelated variables called principal components (PC) (Wold *et al*., 1987). The PCAs were run using a variance-covariance matrix. Twelve PC (PC_g) were extracted for the gull analysis and 6 for the theropod analyses. All PCAs were

conducted using minitab. The components are plotted against each other to show the morphological variation between each species. In a PCA, specimens that clump together will show similar trends. Two sets of PCAs were conducted on the gull postcrania: one included all the species of gulls, the second only analyzed individual specimens from *L. argentatus, L. delawarensis* and *L. thayeri*. The analyses of individual species were conducted to analyze the extent of intraspecific morphological variations. Two sets of analyses were conducted on the theropod postcranial data: one included all specimens available, the other excluded the tyrannosaurs.

For the cranial analysis of the gulls, the coordinates of the digitized landmarks were analyzed in CoordGEN8. The data were then rotated using partial Procrustes superimposition to remove size difference between landmark configuration (Webster and Sheets, 2010). This makes comparison of landmark configuration easier by removing variation associated with differences in their location, orientation and size (Webster and Sheets, 2010). PCA deformation grids were generated for each quadrant of the PCA plots using PCAgen8. These grids use the information in the landmark coordinates to help visualize shape changes (Webster and Sheets, 2010).

Chapter 3: Results

3.1 Gull postcranial morphometric analysis

The PCA results for the postcranial skeletal elements of the gulls are shown in figures 15 – 17. The figures are scatter plots generated with the PCA using standardized data. Table 2 provides the loading of each principal component (PC_g). Table 3 provides the eigenvalues and percent of variance of each PC_g. The first component explains most of the variation in the analysis (Table 2). PC_g1 shows high and positive loading for all of the variables (Table 2, appendix D). This suggests that PC_g1 represents a size variation. PC_g2 is highly and positively correlated with the tibiotarsus length, tibiotarsus distal width and tarsometatarsus length. It is also negatively correlated with the humerus length, humerus distal width, ulna length and ulna distal width. This suggests an inverse correlation between elements of the hindlimb and elements of the forelimb (Table 2, Appendix D). As the forelimb elements increase in size, the hindlimb elements decrease in size (Fig. 15). This suggests that specimens with larger hindlimbs will have relatively smaller forelimb elements.

Table 2: eigenvalues and percent variance of the components

PC_g	Eigenvalue	% variance
1	11.0511	93.426
2	0.24198	2.0457
3	0.168343	1.4232
4	0.114514	0.9681
5	0.06964	0.58873
6	0.057711	0.48789
7	0.045269	0.3827
8	0.028761	0.24315
9	0.02415	0.20416
10	0.014902	0.12598
11	0.008444	0.071382
12	0.003918	0.03312

Table 3: loadings of each principal component

	PC_g 1	PC_g 2	PC_g 3	PC_g 4
left femur length	0.29554	0.019803	-0.1924	-0.20311
left femur distal width	0.29582	0.01209	-0.2091	-0.18222
left femur midshaft radius	0.27903	-0.15339	0.007996	0.45266
left tibiotarsus length	0.29727	0.23656	-0.05962	-0.06968
left tibiotarsus distal width	0.28398	0.12954	-0.63438	0.37949
left tarsometatarsus length	0.27491	0.74524	0.17756	-0.33297
left tarsometatarsus distal width	0.2893	-0.16404	-0.31193	-0.09115
left humerus length	0.29234	-0.04565	0.23429	0.18763
left humerus distal width	0.29196	-0.26858	0.16919	-0.03481
left radius length	0.28566	-0.01121	0.39478	0.27399
left ulna length	0.293	0.01681	0.37734	0.18201
left ulna distal width	0.28436	-0.49626	0.051237	-0.55495

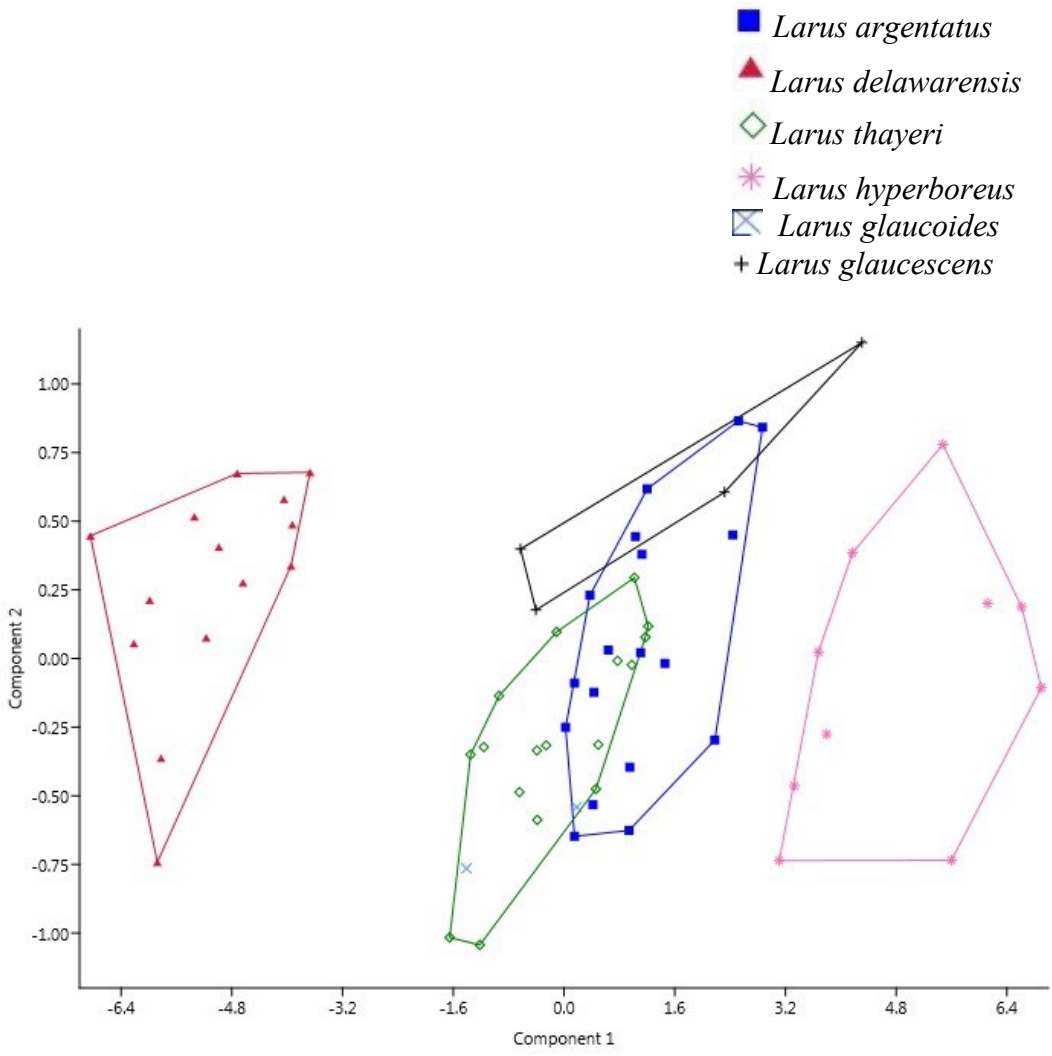

Figure 15: scatter plot showing the results of the post cranial PCA analysis. Components 1 and 2 are shown.

Figure 15 shows the resulting scatter plot for the first two components of the analysis. Principal component (PC_g) 1 accounts for approximately 93% of the total variance in the analysis. PC_g 2 accounts approximately 2% of the total variance. Specimens plotting on the left side of graph will be smaller than those plotting on the right side of the graph. For example, the *Larus delawarensis* specimens plot as a group on the left section (Fig.15), suggesting that they are smaller compared to the other species. *L. hyperboreus* plots on the far right of the graph, suggesting it is larger compared to all other species. *L. delawarensis*, being the smaller species, plots on the left hand side of the scatter plot. The other species of gulls, being of similar size, plot in a seemingly uniform group near the center of the plot. PC_g2 shows an inverse relationship between elements of the forelimb and elements of the hindlimb. Specimens plotting higher on PC_g2 (the Y axis in Fig.15) will have larger hindlimb and smaller forelimb elements. The specimens lower on the Y axis will have relatively larger forelimb elements.

There is less variation along the second axis of the analysis. There is one noticeable outlier in Fig. 15. Specimen CMNAV S-484 (see appendix B) plotted away from all the other specimens and was also outside of the 95% confidence ellipse. The information on the specimen card did not specify the age of the specimen. Because juvenile gulls are noticeably smaller compared to adults, it is possible that any juvenile measured in the analysis would potentially plot far away from all the other specimens. Since it cannot be confirmed whether the specimen is juvenile or not, the specimen is considered to be an experimental or

measurement error and will not be considered in the analysis. The other outlier in the analysis was an immature female CMNAV S-1785 (see Appendix B).The immature nature of the specimen could explain why it is plotting outside of the 95% confidence ellipse as an outlier.

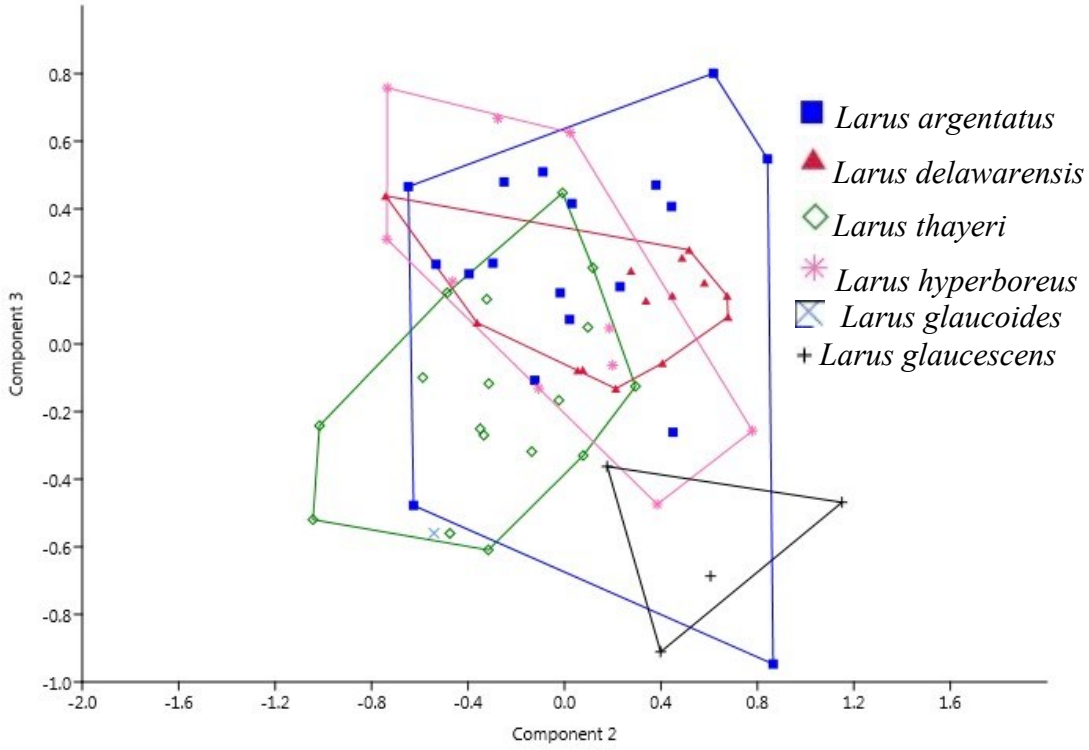

Figure 16: Scatter plot of the post cranial skeleton showing components 2 and 3.

The PCA results for the PC_g 2 and PC_g 3 are shown in Figure 16. The graph was plotted with a 95% confidence ellipse. The samples are all grouping in the center of the graph. PC_g 2 accounts for approximately 2% of total sample variance. PC_g 3 represents approximately 1% of the total sample variance. The variance in PC_g 3 (Table 2) is characterized by positive loadings of tarsometatarsus length, ulna length and distal width, humerus length and distal width, radius length and ulna length and distal width. PC_g3 also shows strong negative correlation with tibiotarsus distal width and tarsometatarsus length (Table 2).

In a typical morphometric analysis, comparing PC 2 and PC 3 will show the shape variation within the dataset. Considering that PC 2 and PC 3 only account for a total of 3% of the sample variance, shape variation is not significant in these species of gulls. What little shape variation is present is seen most notably in the tibiotarsus and tarsometatarsus, as these have the highest loading on PC_g2 and 3 (Table 2). Because of the inverse relationship between tarsometatarsus length and distal width, specimens plotting on the right side of the graph will have longer and narrower tarsometatarsus.

3.2 Intraspecific morphological variation

Individual scatter plots were generated to analyze the morphological variation within each individual species. Only the species with a significant number of specimens were used for the analysis. The results are shown in Figures 18 through 20 as bivariate plots generated from the PCA.

Table 4: eigenvalues and percent variance of the *L. argentatus* PCA.

PC	Eigenvalue	% variance
1	0.934015	61.382
2	0.257388	16.915
3	0.136616	8.9781
4	0.08678	5.703
5	0.038666	2.5411
6	0.030332	1.9934
7	0.01607	1.0561
8	0.008219	0.54014
9	0.005695	0.37426
10	0.004837	0.31786
11	0.001992	0.13091
12	0.001041	0.068396

Table 5: loadings on the PC of the *L. argentatus* analysis

	PC 1	PC 2	PC 3
left femur length	0.29987	0.067409	-0.21213
left femur distal width	0.33657	-0.22746	0.044216
left femur midshaft radius	0.23067	0.17003	0.66941
left tibiotarsus length	0.31356	0.068144	-0.27531
left tibiotarsus distal width	0.35246	-0.22045	-0.00611
left tarsometatarsus length	0.58341	0.302	-0.36811
left tarsometatarsus distal width	0.25583	-0.70771	0.16969
left humerus length	0.10819	0.17399	0.12799
left humerus distal width	0.10241	0.038671	0.32915
left radius length	0.1435	0.35481	0.24569
left ulna length	0.15996	0.2788	0.23576
left ulna distal width	0.21644	-0.18471	0.15533

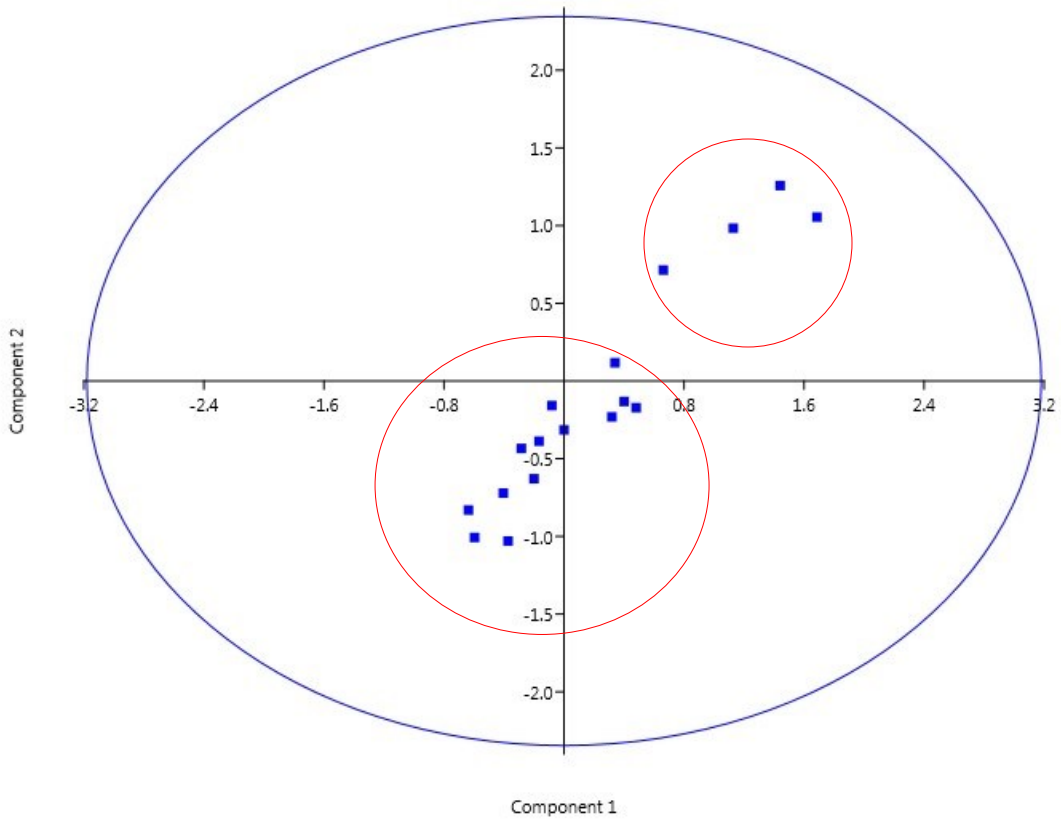

Figure 17: PCA scatter plot for *Larus argentatus* that shows two different grouping of specimen. The lower left specimens are females and the upper right specimens are all males.

Figure 17 shows the PCA results for *Larus argentatus*. PC1 accounts for 61.4% of the sample variation (Table 5). All the variables are positively correlated in PC1 (Table 4). The tarsometatarsus length has the highest loading on PC 1, followed by the femur length and distal width and the tibiotarsus length and distal width. Elements of the forelimbs (humerus, radius and ulna) show lower loading on PC1 than elements of the hindlimbs. Specimens plotting on the right side of the graph (far right on the x axis) will therefore be larger in their hindlimbs and forelimbs. PC2 accounts for 16.91% of the total variation (Table 5). The tarsometatarsus distal width has a high and negative loading on component 2. The ulna, tibiotarsus and femur distal width are weakly negatively correlated with PC2. The radius and ulna lengths have a strong positive correlation on PC2 (Table 4). Specimens plotting on the upper part of the graph (positive on the y axis) will have longer and narrower skeletal elements. Those plotting lower on the graph (negative on the y axis) have shorter, broader skeletal elements.

The specimens plot in two separate groups. This graph demonstrates that *L. argentatus* specimens exhibit sexual size dimorphism. The females plot on the lower central part of the graph and the males plot in the upper right quadrant of the graph.

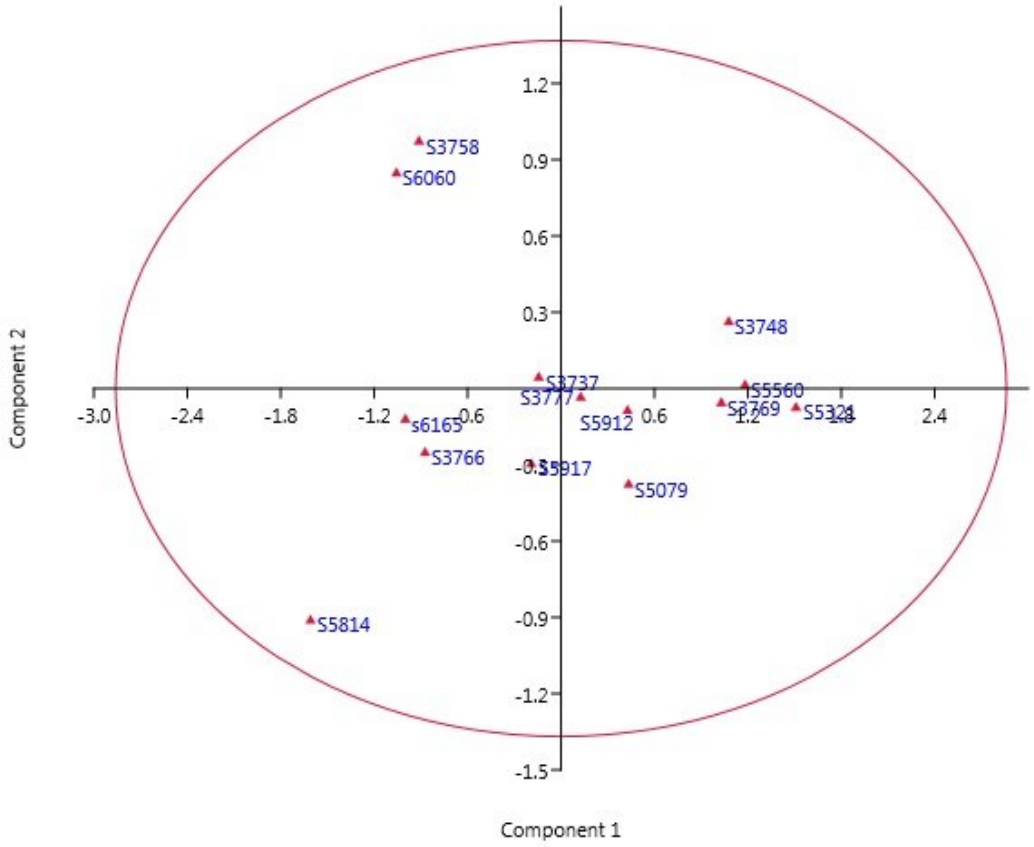

Figure 19: PCA scatter plot for *L. delawarensis* species showing Components 1 and 2.

Figure 18 shows the PCA results of the *L. delawarensis* species. Component 1 explains 70.8% of the total variance in the dataset. Component 2 explains 16.2% of the variance (Table 7). PC1 is positively correlated with all the variables. The strongest loading is in the tarsometatarsus length. The weakest loading is shown in the ulna width. All other elements show similar, positive loadings on PC1 (Table 6). PC2 is strongly and positively correlated with the distal width of the ulna. The tarsometatarsus width, humerus width and ulna length are weakly and positively correlated with PC2. The femur width and midshaft radius, tibiotarsus length and width and tarsometatarsus length all have weak and negative loading on PC2. Components plotting on the upper portion of the graph will exhibit wider ulnae, narrower femora, short and narrow tibiotarsi and short, wider tarsometatarsi. There doesn't appear to be sexual dimorphism in PC 1 and 2.

Table 6: loading of each component of the *L. delawarensis* PCA

	PC 1	PC 2
left femur length	0.28053	0.028659
left femur distal width	0.33811	-0.07357
left femur midshaft radius	0.29989	-0.11865
left tibiotarsus length	0.31431	-0.08553
left tibiotarsus distal width	0.2466	-0.06894
left tarsometatarsus length	0.4683	-0.14581
left tarsometatarsus distal width	0.21486	0.11516
left humerus length	0.27767	-0.06942
left humerus distal width	0.28829	0.0654
left radius length	0.22965	0.018625
left ulna length	0.25315	0.074326
left ulna distal width	0.12228	0.95819

Table 7: Eigenvalue and percent variance of the *L. delawarensis* PCA

PC	Eigenvalue	% variance
1	1.0299	70.766
2	0.236285	16.236
3	0.076184	5.2348
4	0.038037	2.6136
5	0.025673	1.7641
6	0.021264	1.4611
7	0.009453	0.6495
8	0.008863	0.60898
9	0.005889	0.40464
10	0.002281	0.15672
11	0.001362	0.093558
12	0.000162	0.011165

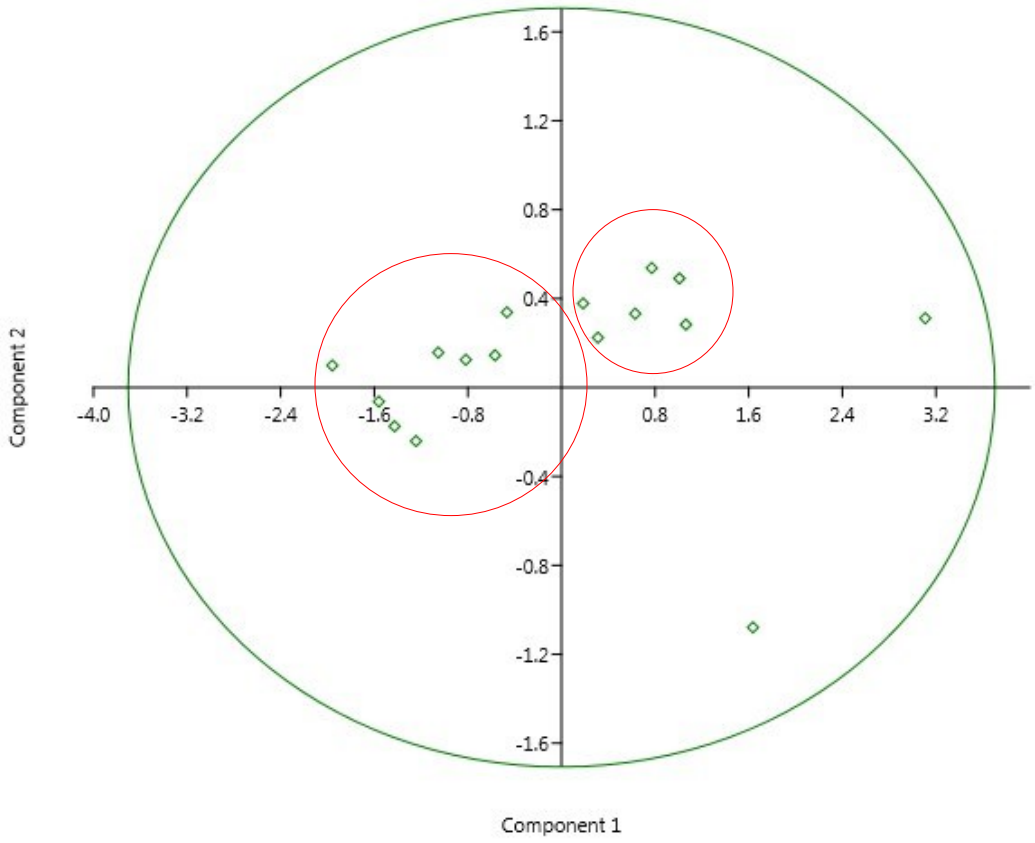

Figure 19: PCA scatter plot for Larus thayeri showing the first and second components of the PCA.

Figure 19 shows the scatter plot result for the *Larus thayeri* PCA. PC1 accounts for 75.0% of the variance and PC2 accounts for 8.5% (Table 9). PC 1 is strongly and positively correlated with the tarsometatarsus length. The other variables have an even and positive loading on PC1 (Table 8). Specimens on the right side of the graph will exhibit larger skeletal elements (with proportionally longer tarsometatarsus) than the ones on the left side (Fig. 20). PC 2 is strongly and positively correlated with the tibiotarsus width. The femur width and tarsometatarsus width have a positive loading on PC2. The tarsometatarsus length is strongly and negatively correlated with PC2 (Table 8). Specimens plotting on the upper part of the graph will exhibit wider tibiotarsus, femurs and short, wide tarsometatarsus. The graph shows two groups of specimens, which appear to be grouped based on the sex of the specimens. The females are plotting in the left group and the males plot in the right side group, suggesting that males will have longer, wider skeletal elements than females. There are two specimens of undefined sex and age that plot outside of either group (but are still within the 95% confidence interval).

Table 8: Loadings on PC 1 and 2 of the *L. thayeri* PCA

	PC 1	PC 2
left femur length	0.23684	-0.03124
left femur distal width	0.22752	0.16949
left femur midshaft radius	0.16808	0.32765
left tibiotarsus length	0.28747	-0.10218
left tibiotarsus distal width	0.32046	0.69335
left tarsometatarsus length	0.53972	-0.49719
left tarsometatarsus distal width	0.17204	0.31603
left humerus length	0.27423	-0.05442
left humerus distal width	0.25359	0.053689
left radius length	0.29769	-0.08644
left ulna length	0.30443	-0.09718
left ulna distal width	0.19194	-0.04405

Table 9: Eigenvalues and percent variance of each component of the *L. thayeri*

PC	Eigenvalue	% variance
1	1.03007	75.017
2	0.117041	8.5238
3	0.082964	6.0421
4	0.062398	4.5443
5	0.035736	2.6025
6	0.019041	1.3867
7	0.013863	1.0096
8	0.005431	0.39554
9	0.003536	0.25755
10	0.002201	0.16026
11	0.000763	0.055595
12	6.38E-05	0.004648

3.3 Gull cranial morphometric analysis

Figures 20 through 22 show the PCA results of the cranial morphometrics analysis for the dorsal view of the gull skulls. The analysis was conducted on four species of gulls using the dorsal photos taken. The PCA analysis was conducted using the landmark coordinates on two different views of the skull (dorsal and ventral). Appendix D shows the landmarks digitized on the ventral side of each skull. Component 1 explains 35.4% of the total variance. PC 2 explains 18.7% of variance. PC 3 explains 14.3% and PC 4 explains 6.9% of variance.

Table 10: percent variance of the each component of the dorsal geometric morphometric analysis

PC	Eigenvalue	% variance
1	0.000946	35.403
2	0.000501	18.762
3	0.000383	14.328
4	0.000187	6.994

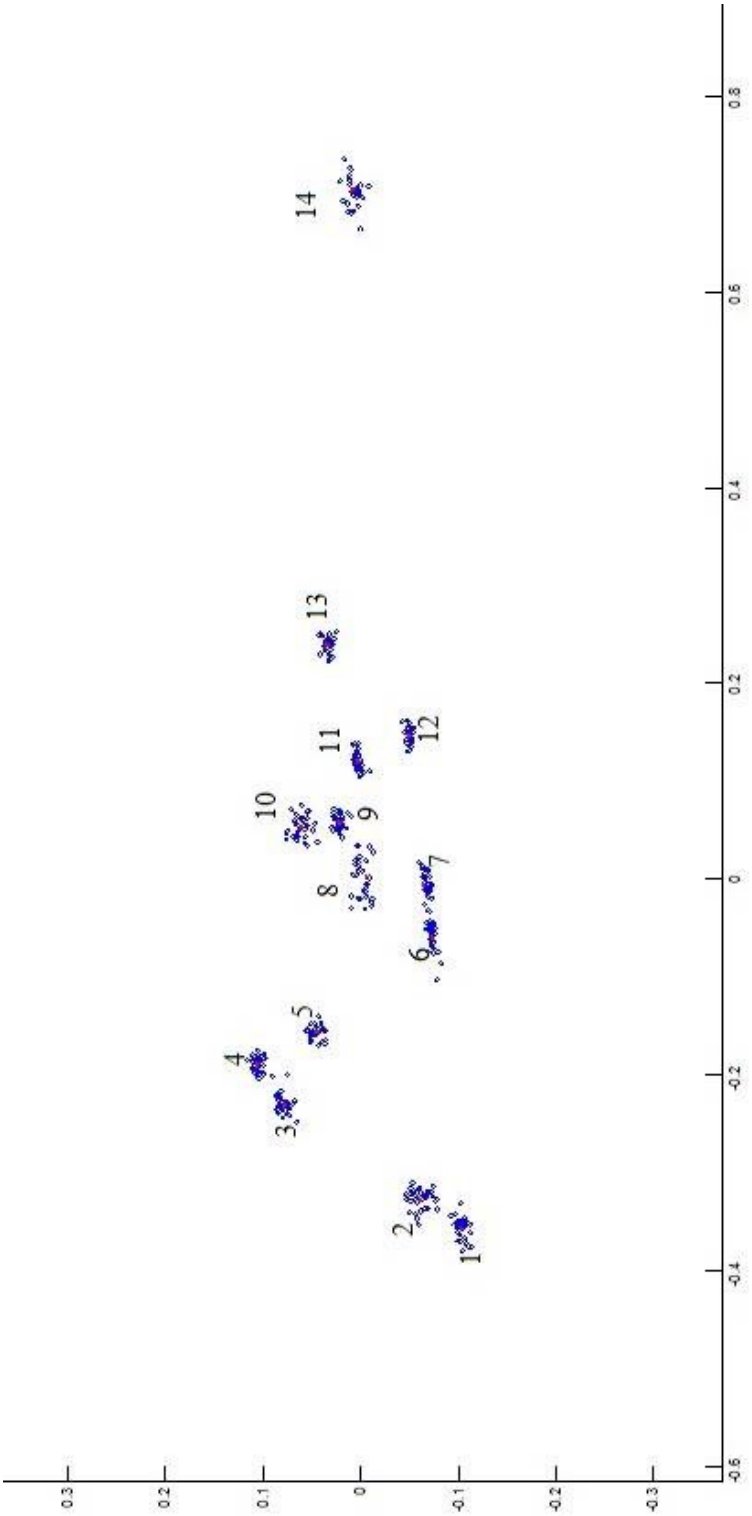

Figure 20: plot showing the distribution of all the landmarks digitized on the dorsal view of each gull skull. Each skull has been overlain on one graph to show the potential differences in morphologies among the species

Figure 20 shows the distribution of all the landmarks digitized on the dorsal view of each specimen. The landmarks do not exhibit much variation in position. The landmarks appear to be uniform in their position. They all appear to be grouped together. The variation in the position of each landmark can most likely be attributed to individual variations in skull shape. The landmark coordinates were used to conduct further PCA tests.

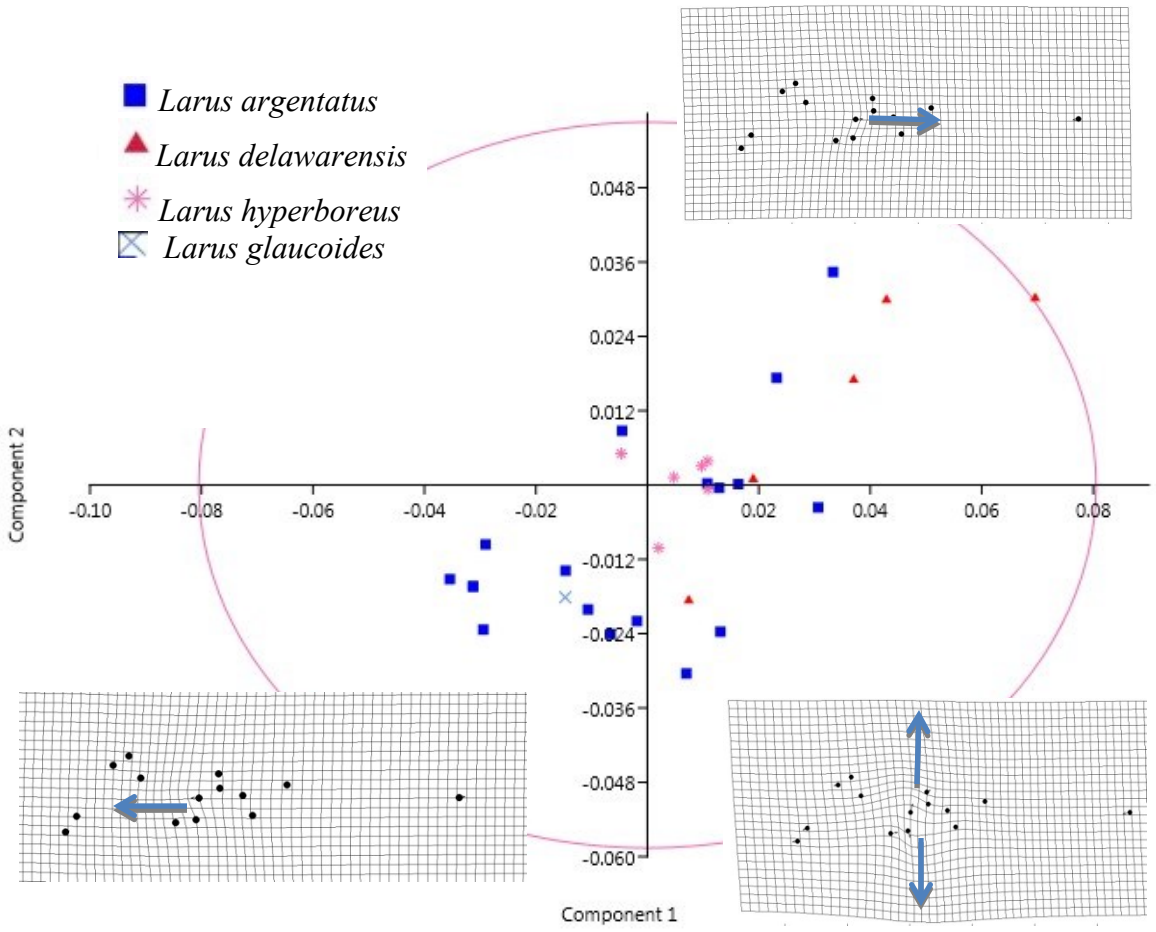

Figure 21: Scatter plot for the result of PCA for the gull dorsal cranial morphometrics analysis showing PC 1 and 2.

Figure 21 shows the scatter plot of the first two components of the dorsal landmark analysis. PC 1 accounts for approximately 35.4% of the total variance in the analysis. PC 2 explains approximately 18.7% (Table 10) of the total sample variance. Most of the specimens that were measured fell inside the 95% confidence interval. Those that remained inside do not appear to show any distinct groupings although there is some noticeable asymmetry to the distributions. There is a lot of overlap between the species. Some specimens of *L. argentatus* (blue squares) and *L. delawarensis* (red triangles) are plotting on the upper right quadrant.

It appears that most of the *L. argentatus* specimens are plotting on the left side of the graph and most of the *L. delawarensis* specimens plot on the right hand side of the graph. The deformation grids show the displacement of the landmarks and approximate deformation of the skulls. Specimens that plot on the lower left exhibit a slight compaction towards the anterior portion of the skull. Specimens plotting on the upper right exhibit the opposite effect: a slight compaction towards the rostral end of the skull. Specimens that plot on the lower right exhibit a widening in the skull (at the nasal-frontal contact).

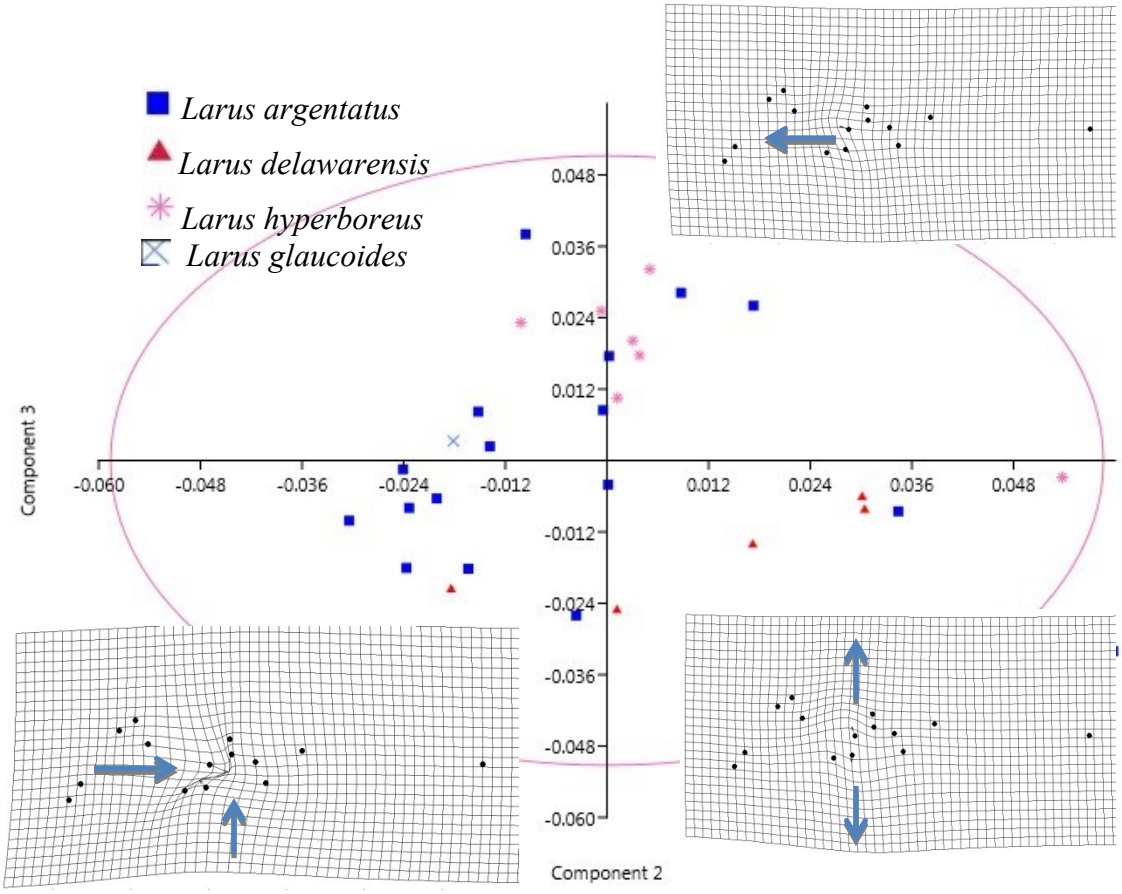

Figure 22: Scatter plot for the result of the PCA for the gull cranial morphometrics analysis. The graph shows the second and thirds components of the analysis.

Figure 22 shows the scatter plot comparing components 2 and 3. PC 3 explains approximately 14.3% of the variance in the analysis. As per the previous result, the specimens included in the analysis fell inside the 95% confidence interval. There is extensive overlap between the species analyzed. There are three specimens of *L. delawarensis* and one specimen of *L. argentatus* plotting on the bottom right quadrant of the graph. One specimen of *L. hyperboreus* is plotting on the right side of the plot (positive side of PC 2). Specimens that plot on the bottom left quadrant of the graph exhibit in the central portion of the skull (at the contact of the frontal and nasal). Specimens that plot on the upper right exhibit compaction towards the anterior of the skull. Specimens that plot on the bottom right exhibit widening of the skull.

Figures 23 through 25 show the PCA results for the ventral view of the gull skulls. Figure 23 shows the distribution of all the landmarks digitized on the ventral view of each specimen. The landmarks digitized on each specimen have all superimposed in the graph. PC 1 explains 79.6% of the variance. PC 2 explains10.9% of the variance and PC 3 explains 2.9% of the variance in the dataset.

Table 11: % variance and eigenvalues of each component of the ventral geometric morphometric analysis

PC	Eigenvalue	% variance
1	0.011982	79.668
2	0.001646	10.943
3	0.000438	2.9108

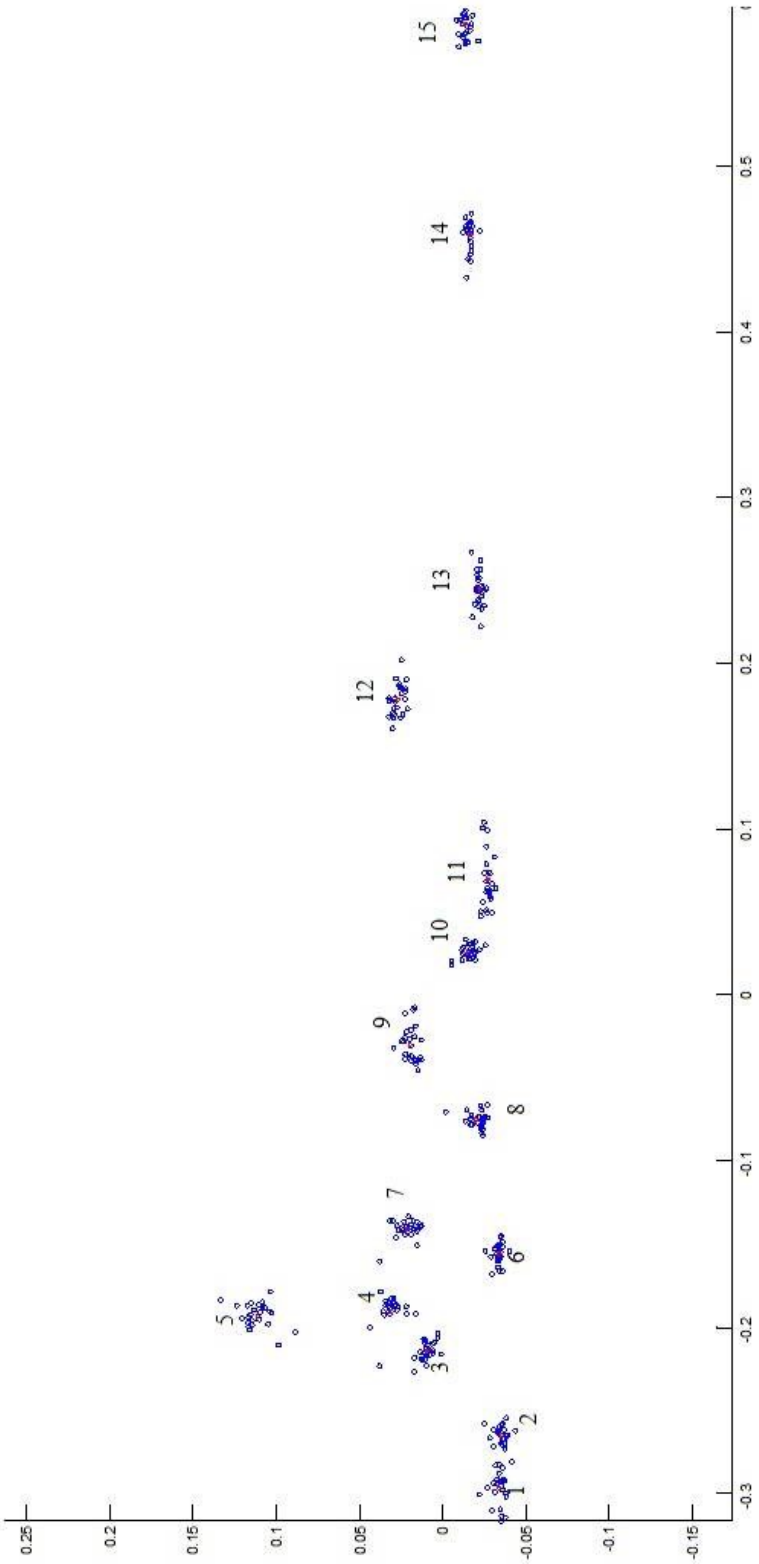

Figure 23: Plot showing all the digitized points on each gull skull in ventral view.

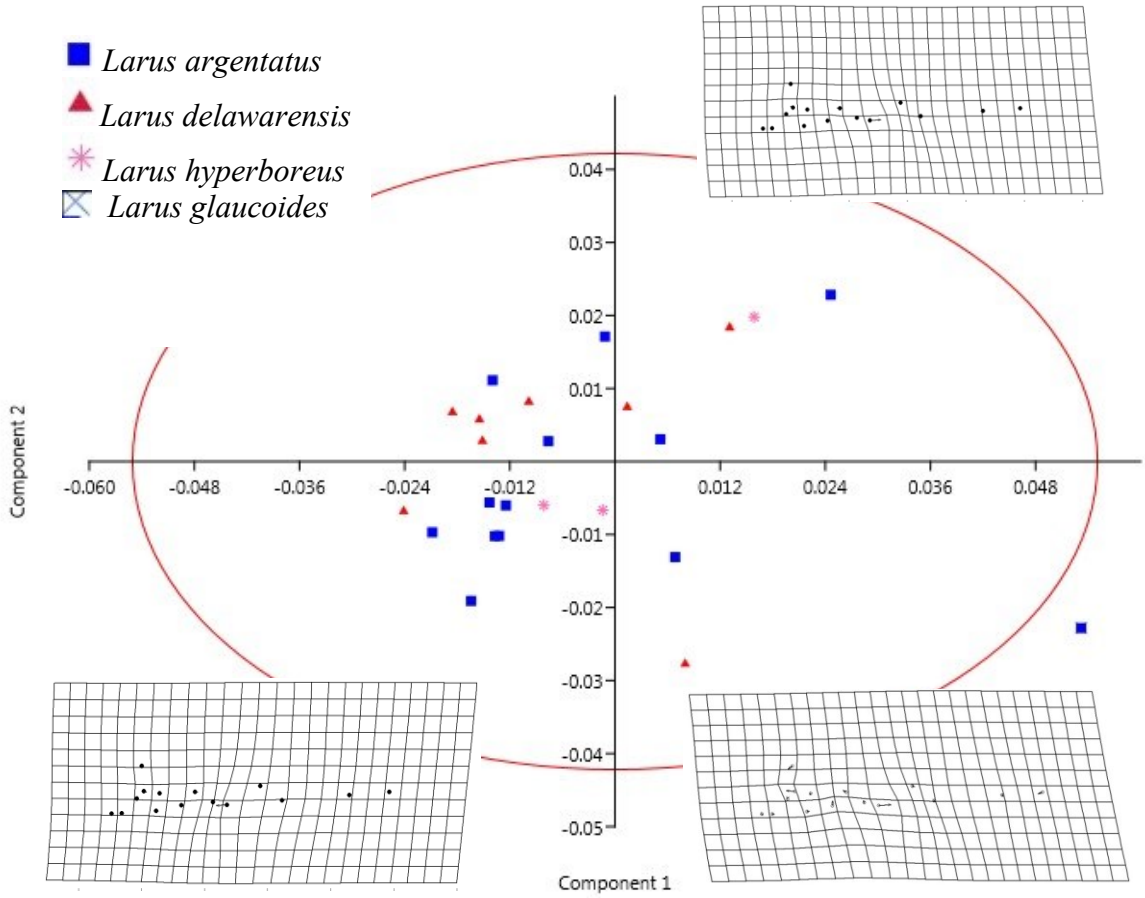

Figure 24: Scatter plot for the result of the PCA for the gull ventral cranial morphometrics analysis. The graph shows the results for PC 1 and PC 2.

Figure 24 shows the scatter plot of principal components 1 and 2 of the analysis. Principal component 1 comprises 79.7% of the total sample variance. Component 2 explains 10.9% of the total variance. The specimens that were analyzed fell inside the 95% confidence interval. The specimens are scattered throughout the plot in a cloud. The deformation grids show the deformation in the skulls. Specimens plotting on the bottom right portion of the graph exhibit compression in their skulls. Specimens plotting on the upper right exhibit elongation in their skulls. The specimens plotting on the bottom right also exhibit elongation in their skulls.

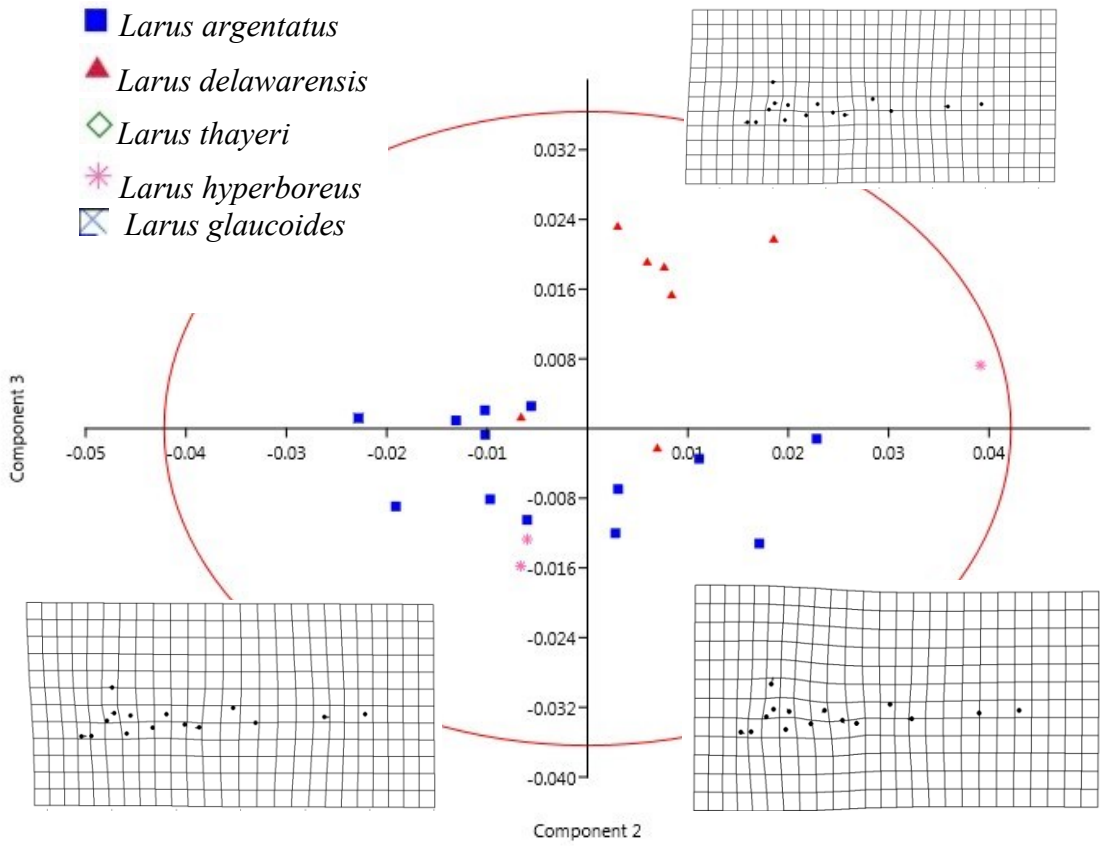

Figure 25: Scatter plot for the result of the PCA for the gull ventral cranial morphometrics analysis. The graph shows the results of components 2 and 3

Figure 25 shows the scatter plot of PC 2 and PC 3. Component 3 explains approximately 2.9% of the variance in the analysis. As per the previous result, the specimens included in the analysis fell inside the 95% confidence interval. *Larus argentatus* and *Larus delawarensis* are separated in this analysis. *L. argentatus* exhibits slight expansion and elongation of the skull and *L. delawarensis* exhibits slight compaction. Specimens plotting on the lower left exhibit slight compaction in the skulls. The specimens plotting on the upper right exhibit slight elongation. The ones plotting on the lower right exhibit slight narrowing of the skull.

3.4 Theropod morphometrics analysis

Four analyses were run were conducted on groups of fossil theropods: one includes all the tyrannosaurids (PC_{ty}; Figs. 26 and 27), the second includes all early bird specimens (PC_{m}; Figs. 28 and 29), the third includes all the maniraptorans (PC_{b}; Figs. 30 and 31) and the final analysis includes all of the theropod specimens available (PC_{th}; Figs. 32 and 33).

Table 10 shows the loadings of each component on the original variables. Table 11 shows the percent of variance that is explained by each principal component and the eigenvalues extracted from the PCA. The first component accounts for a large portion of the total variance (92.7% Table 12). The second component accounts for 3.6% (Table 12) of the total sample variance. The third PC explains 2.2% (Table 12) of the variance. The element that has the highest

positive loading (0.76) on the first component is the femur length. The element with the second highest loading (0.56) is the tibiotarsus length. This means that PC_{ty} 1 is highly correlated with the increase in femur and tibiotarsus length. For component 2, most of the variables have a correlation that is less than 0.5. The only variable that meets this criterion is the femur length, with -0.62. This means that PC_{ty} 2 is mainly characterized by a decrease in femur length.

Table 12: loadings of each component for the Tyrannosaurid PCA

	PC_{ty} 1	PC_{ty} 2	PC_{ty} 3
Humerus length	0.1994	0.46507	0.44925
Radius length	0.042251	0.37539	0.13324
Ulna length	0.063304	0.42609	0.27403
Femur length	0.75717	0.18166	-0.61479
Tibia length	0.55883	-0.1955	0.50769
mt III	0.26238	-0.62452	0.26384

Table 13: % variance and eigenvalues of each component of the tyrannosaurid PCA

PC_{ty}	Eigenvalue	% variance
1	130488	92.748
2	5170.65	3.6752
3	3105.97	2.2077
4	1480.55	1.0523
5	353.615	0.25134
6	91.9703	0.065371

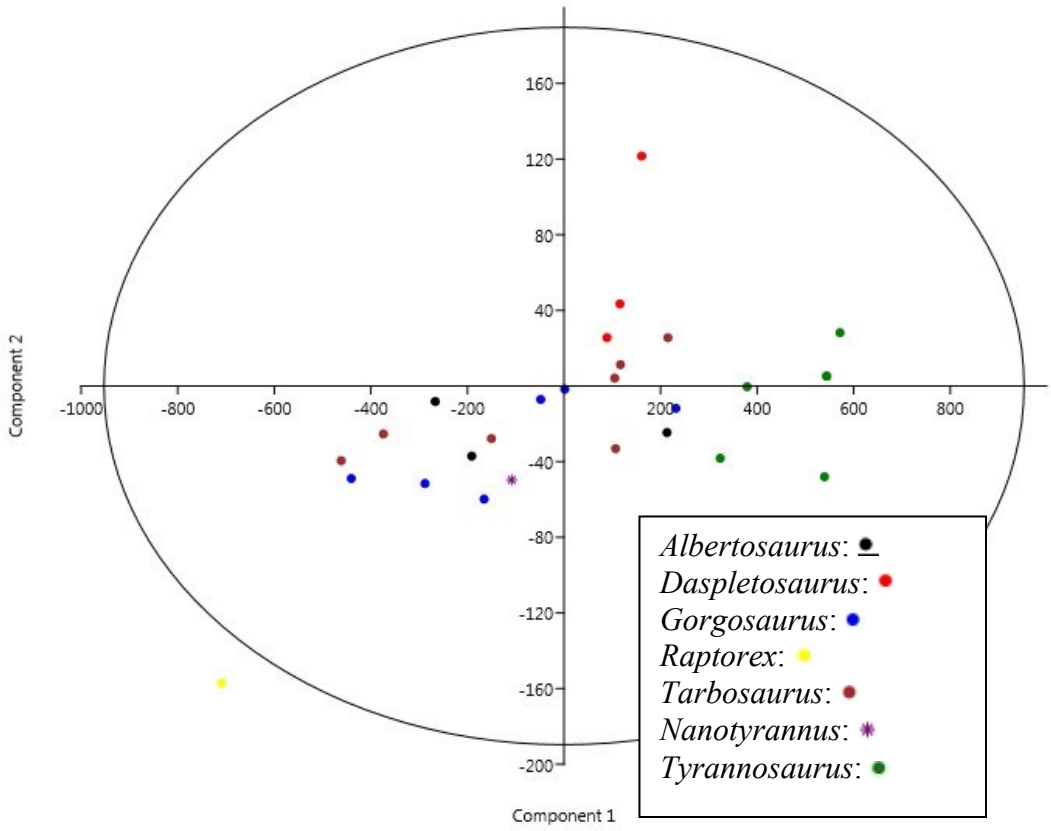

Figure 26: PCA results of the tyrannosaurid specimens showing PC_{ty} 1 and PC_{ty} 2.

Figure 26 show the PCA results for the large bodied tyrannosaurids for PC_{ty}1 and 2. The specimens used for the analysis were selected based on the completeness of their measurements. Due to the incompleteness of several specimens in Currie's database, only a few specimens were utilized for the PCA. *Raptorex* appears to plot away from all the other specimens of tyrannosaurids falling outside of the 95% confidence interval. This may be due to the fact that only a limited number of measurements were available the specimen. There were also a limited number of complete specimens available for the analysis. A more complete set of measurements would be needed for further speculations.

Most of the specimens plot as one large group. There appears to be a group of specimens plotting on the right hand side of the graph, the *Tyrannosaurus rex*. Their position on the right hand side of PC_{ty} 1 is due to their longer femora and tibiotarsi. *Albertosaurus*, *Gorgosaurus, Tarbosaurus* and *Nanotyrannus* and *Daspletosaurus* all show some separation, but have some overlap. *Daspletosaurus* is plotting on the positive part of component 2, suggesting it has larger metatarsi III. Their position to the left of *Tyrannosaurus rex* on the graph is indicative of their relatively shorter femora and tibiotarsi. It can also be seen that one of the specimens of *Daspletosaurus* is plotting away from the rest of the specimens, on the upper part of the second component. This indicates that the specimen has shorter metatarsi III than the rest of the *Daspletosaurus* specimens.

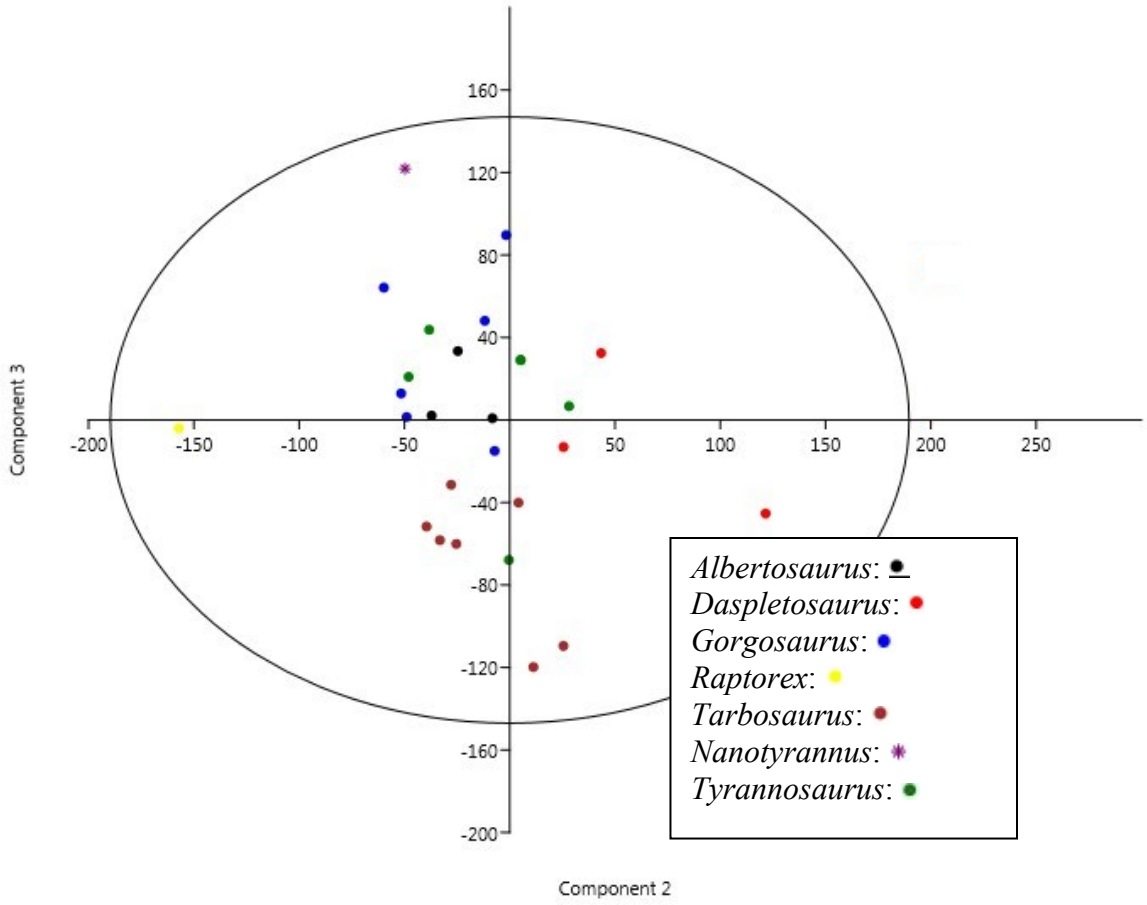

Figure 27: PCA results of the tyrannosaurid specimen showing PC_{ty} 2 and 3.

Figure 27 shows the second and third principal components of the Tyrannosaurid PCA. PC_t3 represents 2.2% of the total sample variance (Table 12). The tibia length has a loading that is 0.5 and the femur length has a loading of -0.61. This means that component 3 represents an increase in tibiotarsus length and a decrease in femur length. Specimens plotting on the upper portion of the graph will have shorter femurs and longer tibiotarsus. Interestingly, *Nanotyrannus* and *Raptorex* both plot away from the rest of the tyrannosaurid specimens. There is also a specimen of *Daspletosaurus* that is plotting away from the rest of the group. The *Daspletosaurus* plots far on the right hand side of the plot because it probably has a smaller length of the third Metatarsal. *Raptorex*, on the other hand, plots on the left hand side of component 2, which means it probably has a longer length of the third metatarsal. *Nanotyrannus* plots higher on the third component, which suggests that the specimen probably has longer tibiotarsus length and a shorter femur length.

Figures 28 and 29 show the PCA results for the small to medium sized theropods. Table 12 shows the loading on each component of the analysis. Table 13 shows the eigenvalues and the percent variation of each component. PC1 explains 97.1% of the total sample variance and is highly and positively correlated with the femur length. PC 2 describes 1.2% of the total sample variance and PC 3 explains 0.7%. Only the first two components will be considered.

Table 14: Loading of each component of the Maniraptora PCA (PC_b)

	PC_m 1	PC_m 2	PC_m 3
H. length	0.41131	-0.25676	0.29586
R. length	0.40863	-0.44386	0.061207
U. length	0.40781	-0.47974	-0.085235
F. length	0.40994	0.25438	-0.59584
T. length	0.40813	0.4067	-0.32997
mt III	0.40363	0.52612	0.66147

Table 15: % variance and eigenvalue of each PC of the Maniraptora PCA

PC_b	Eigenvalue	% variance
1	5.75557	95.926
2	0.149698	2.495
3	0.0418648	0.69775
4	0.0230166	0.38361
5	0.0188049	0.31341
6	0.0110432	0.18405

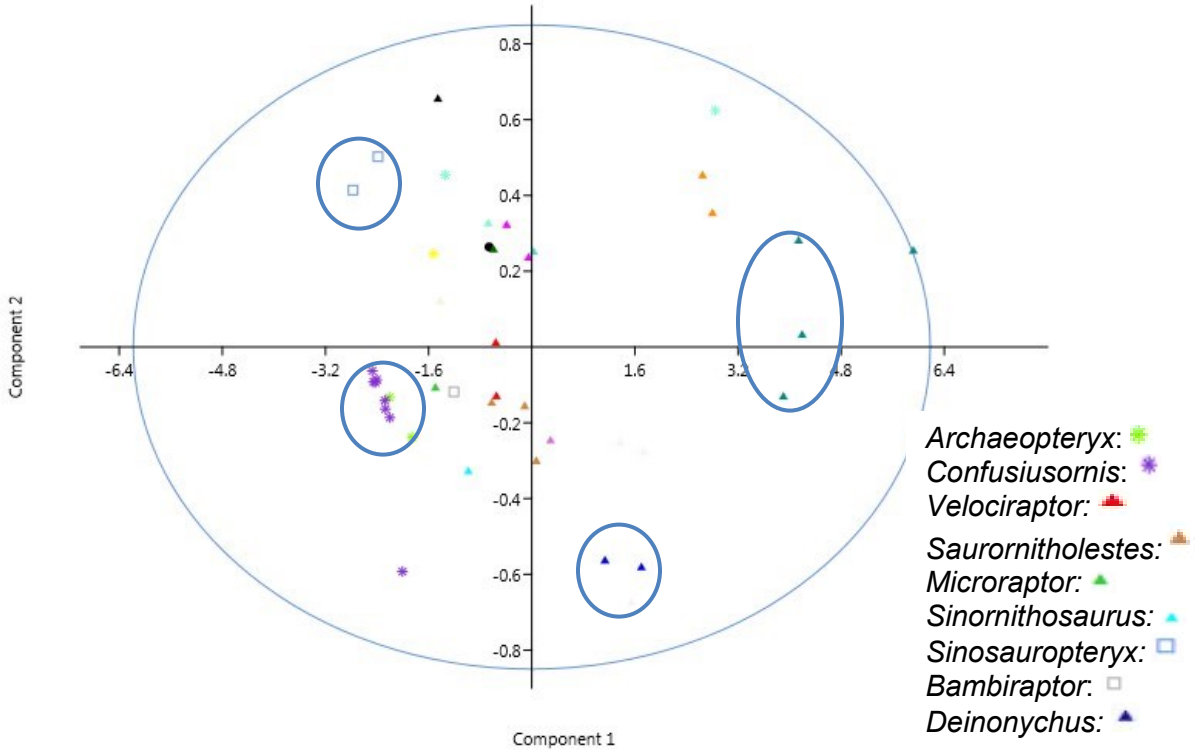

Figure 28: PCA results of the early bird specimen showing PC_b 1 and PC_b 2.

Figure 28 shows the PCA result for the small to medium sized theropods and compares PC_m1 and PC_m2. PC_b1 represents 95.9% of the total variance. PC_m2 represents 2.4% (Table 13). For component 1, all the variables show positive and nearly uniform loading, suggesting that PC_m1 is a size variable. Some grouping can be seen in the plot. *Archaeopteryx* and *Confuciusornis* appear to group in a tight cluster on the negative side of component 1, suggesting a smaller size compared to the other specimens.

The femur, tibia and metatarsus III lengths all have high positive loadings on the second component (PC_m2). The humerus, radius and ulna lengths all have negative loading on PC_m2. There is an inverse correlation between the elements of the hindlimbs and elements of the forelimb (Table 14). Specimens that plot on the upper part of the y-axis will have longer hindlimbs and shorter forelimbs. Specimens plotting on the lower part of the y-axis will exhibit shorter hindlimbs and shorter forelimbs (Fig. 29). *Deinonychus*, *Dromaeosaurus* and *Saurornitholestes* plot on the right side of the graph, suggesting they are larger in size compared to the species plotting on the left side. *Bambiraptor* and *Sinornithosaurus* plot on the bottom left of the graph, suggesting that they are smaller in size and have proportionally longer forelimbs (Fig. 31). *Sinosauropteryx* plots on the left side of the graph. This suggests that *Sinosauropteryx* was smaller in size compared to the other species examined and that it had larger hindlimbs. This is supported by previous analyses of skeletal anatomy of *Sinosauropteryx* (e.g., Ji and Ji, 1996). It also plots on the upper right, suggesting it has larger hindlimbs relative to forelimbs.

Combined theropod analysis

Figures 30 and 31 show the results of the PCA conducted using all available theropod specimens (PC_{th}). Table 16 shows the eigenvalues and percent of variance in each component of the PCA. Table 17 shows the loading of each variables on each PC_{th}.

Table 16: Eigenvalues and percent variance for components 1 to 6 of the theropod PCA

PC	Eigenvalue	% variance
1	4.65692	77.615
2	1.106	18.433
3	0.14062	2.3437
4	0.037662	0.6277
5	0.035306	0.58844
6	0.023496	0.3916

Table 17: loading of the principal components of the theropod PCA

	PC_{th} 1	PC_{th} 2	PC_{th} 3
H. length	0.96736	0.14083	-0.14452
R. length	0.79786	0.58806	0.0695
U. length	0.84193	0.52477	0.028512
F. length	0.88706	-0.39879	-0.19715
T. length	0.91872	-0.3621	-0.00159
mt III	0.863	-0.41811	0.27426

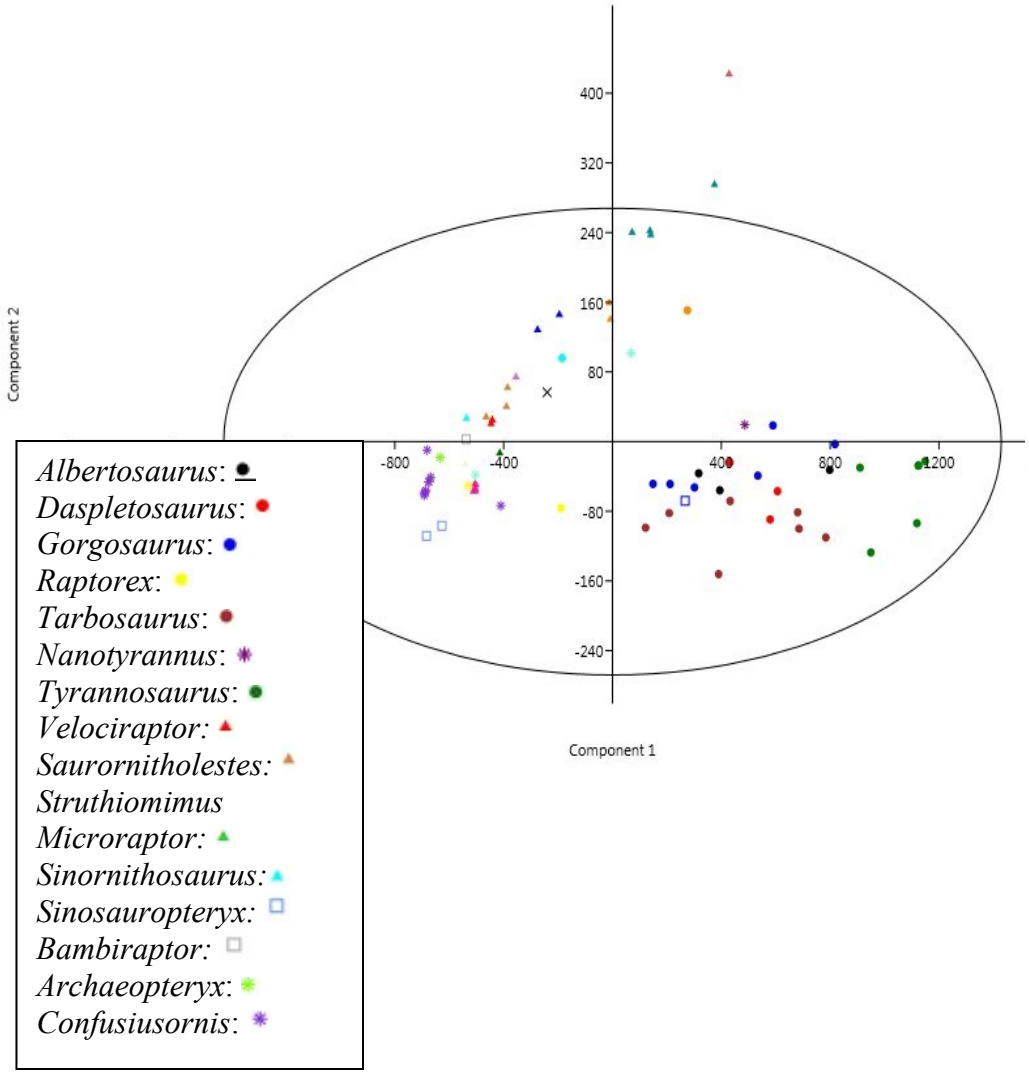

Figure 29: PCA results of all the theropod specimens showing PC 1 and 2.

Figure 29 shows the plot of $PC_{th}1$ and $PC_{th}2$. $PC_{th}1$ accounts for 77.6% of the total sample variance. $PC_{th}2$ accounts for 18.4% (Table16). Component 1 is highly, positively and uniformly correlated with all the variables (Table 17) suggesting that $PC_{th}1$ represents the size variation in the dataset. The radius and ulna lengths show strong and positive loading on $PC_{th}2$. The humerus length shows weak loading on $PC_{th}2$. The femur, tibia and metatarsal III lengths are strongly and negatively correlated with $PC_{th}2$ (Table 17). This shows an inverse correlation between elements of the hindlimb and elements of the forelimb. Two distinct groups can be seen in Figure 32. The small to mid-sized dinosaurs plot on the left-hand side of the graph (the early birds and maniraptorans). The right most group contains all the large bodied theropods (tyrannosaurids). There is some amount of overlap between the two groups. *Raptorex* plots closer to the left side of the graph, suggesting a smaller size compared to the other tyrannosaurids. The tyrannosaurids are also plotting in the bottom right portion of the graph (negative on the Y axis), which suggests that they have increased length of the hindlimb and decreased forelimb length. It is well documented that tyrannosaurids have highly reduced forelimbs and powerful hindlimbs (e.g., Sereno *et al*., 2009; Carpenter and Smith, 1995, Lipkin and Carpenter, 2008).

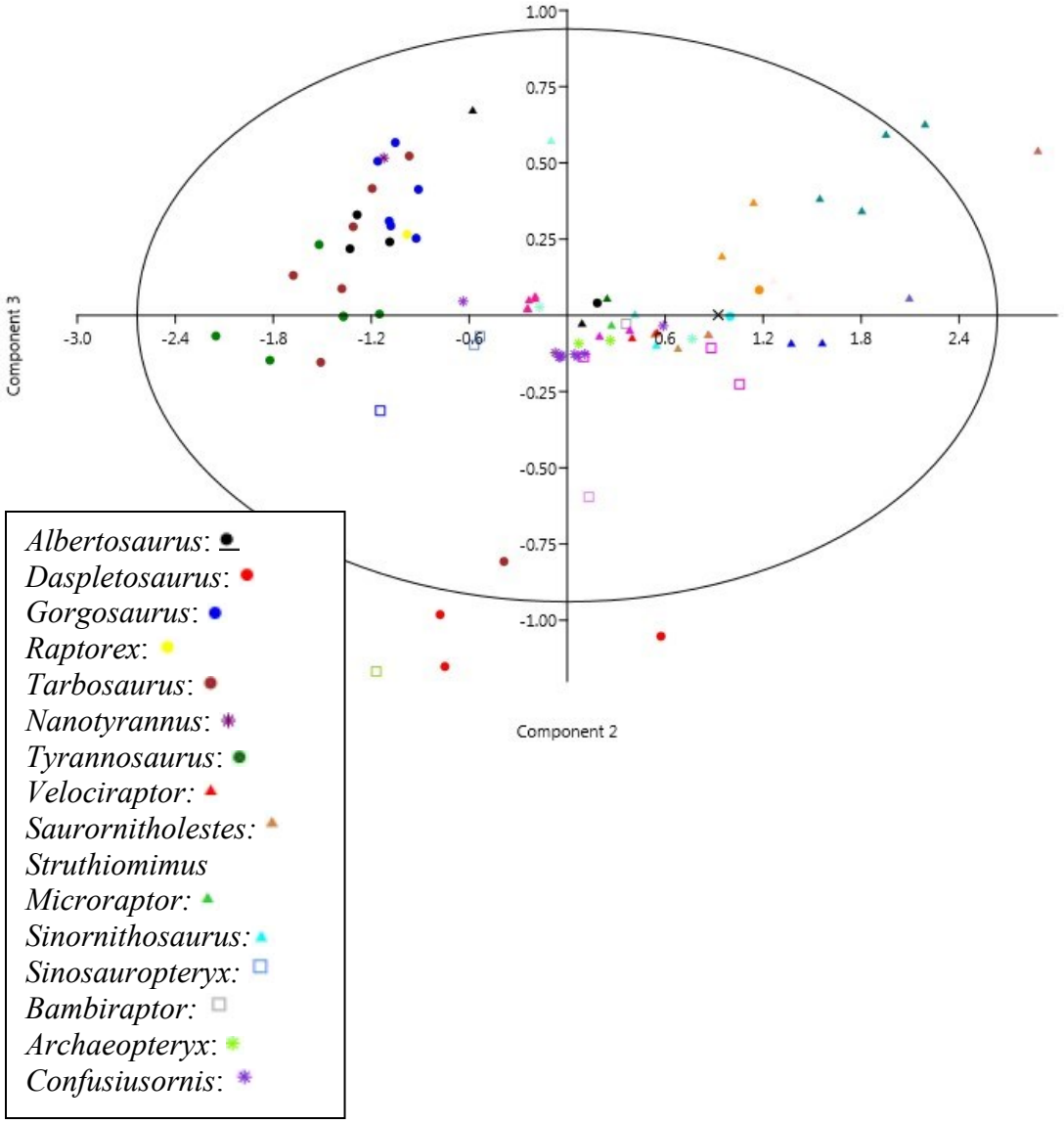

Figure 30: PCA results of all the theropod specimens showing PC 2 and 3.

Figure 30 shows the results for the second and third components of the theropod PCA analysis. PC_{th} 3 represents approximately 2.3% of the total sample variance (Table 16). Metatarsus III has a high and positive loading on PC_{th}3. The femora and humeri length have a strong and negative loading on PC_{th}3. The other variables do not exhibit significant loading on the component (Table17). This represents an inverse correlation between metatarsus III and the humerus and femur. Specimens plotting on the upper portion of the graph (positive on the Y axis) will have long metatarsus III and relatively shorter humerus and femurs. Two groups can be seen in Figure 33. Most of the tyrannosaurids (with the exception of *Daspletosaurus*) plot on the left side of the graph. The group on the right side is composed of the small theropods (maniraptorans and early birds). The tyrannosaurids show less variation along PC_{th}2 compared to the small theropods. Most of the tyrannosaurids plot on the upper part of the graph (positive on the Y axis) suggesting that they exhibit longer metatarsus III. *Daspletosaurus* and one specimen of *Tarbosaurus* plot on the bottom part of the graph. The *Daspletosaurus* specimens plot outside the 95% confidence interval and are therefore outliers. The three specimens of *Daspletosaurus* had incomplete measurements of their metatarsus III, radius and ulna. Considering that metatarsus III has the highest loading on PC_{th}3 (Table 17), incomplete or missing measurements of metatarsus III would explain why they fall outside the confidence ellipse.

The group on the right side is composed of the smaller theropods (the maniraptorans and early birds). These exhibit higher amounts of variation along

$PC_{th}2$ compared to the tyrannosaurids. Maniraptorans (and early birds) show greater diversity of body plan compared to tyrannosaurids. This could explain their higher variation along $PC_{th}2$, Some of the small theropod specimens, such as *Struthiomimus* and *Saurornitholestes* plot on the upper right portion of the graph. They exhibit larger metatarsus III and proportionally shorter humerus and femora.

Chapter 4: Discussion

Most living Aves are taxonomically defined based on legacy diagnoses more than one hundred years old (e.g., Brooks, 1915, Ridgeway and Friedman, 1919). These diagnoses are primarily based on some combination of soft tissue (e.g., plumage/color), behavior (e.g., song type), or size (e.g., Sibley 2003, Edwards 2007, Colwell 2010). In contrast their closest relatives (extinct, non-avian theropods) are diagnosed entirely on hard tissue (skeletal) characters. Since these sets of parameters have almost no overlap between the living and extinct groups, I tested to see if a selected group of skeletal parameters - the basis of all dinosaur diagnoses - could be used to support the distinctions between closely related birds (members of Laridae) showing similar morphologies. The hypothesis was that if the skeletal parameters could not differentiate the examined gulls, then we may be able to hypothesize that closely related, morphologically similar, extinct, non-avian theropods can also not be fully distinguished without access to additional, non-hard tissue features. Thus, the diversity of these extinct clades might be predicted to be much higher than what can be determined from data available from the fossil record alone, assuming the biological species concept.

During this project, six species of gulls (*L. argentatus, L. delawarensis, L. thayeri, L. glaucescens, L. glaucoides* and *L. hyperboreus*) were analyzed using traditional PCA, as well as, geometric morphometrics to test if selected parameters of the skull and postcrania (femora lengths, width and midshaft

radius, tarsometatarsi length and widths, tibiotarsi length and widths, humerus lengths and widths, radius length, ulna length and width) could be used to distinguish the taxa. A common explanation for the intraspecific shape variation seen is ontogeny (e.g., Carrier and Leon, 1990; Watanabe and Slice, 2014). As offspring grow to maturity, they undergo changes in the growth of their skeletal elements (e.g., Reece *et al*., 2013), with mature specimens having larger, better-developed elements. Studies conducted on the ontogeny of terns (e.g., Cane, 1993) show that their hindlimbs grow at elevated rates and comprise higher percent of body weight than forelimbs (Cane, 1993).

The interspecific size variation seen in Figure 15 has been well documented (e.g., Sibley, 2003; Colwell, 2010): *Larus delawarensis* is known for being a smaller species of gull and *L. hyperboreus* are typically much larger than other species. The highest amount of shape variation (PC_g3, Table 2) is captured in the tibiotarsus and it most likely reflects ontogenetic growth (Cane, 1993).

Analysis of shape (PC_g2 and PC_g3, Fig. 16) indicates that most of the variation is captured in the tarsometatarsus and the tibiotarsus. The results confirm that interspecific variation is very limited and these species are indistinguishable based on the shape of these parameters. Intraspecific shape variation is much more elevated, which may be caused by including varying ontogenetic stages in the analyses. *L. delawarensis* shows less variation than other species, but still has considerable overlap with the other species.

Separate analyses were then conducted on individual species *L. argentatus, L. delawarensis* and *L. thayeri*. The analysis for *L. argentatus* does

recover its known sexual dimorphism (Figs. 17), with the males plotting on the upper right and females plotting on the lower left. The analysis of *L. delawarensis* and *L. thayeri* did not recover sexual dimorphism, even though it has been reported in these species. Again, in all analyses, most of the variation is recorded in overall size of the skeletal elements. The most significant shape variation (PC2) was recorded in the tarsometatarsus (in *L. argentatus* and *L. thayeri*) and in the ulna (in *L. delawarensis*). Sexual dimorphism has also been reported in other species of gulls, such as the yellow-legged gull (*Larus michahellis*) (Bosch 1996) and the California gull (*Larus californicus*) (Schnell *et al*., 1985). These authors reported that most of the dimorphism was recorded on the skull, specifically on bill depth (Schnell *et al*., 1985) and skull length (Bosch 1996). In order to further analyze potential dimorphism in gulls, future measurements and analyses should be focused on the cranial region of the specimens.

Select skulls of *L. argentatus, L. delawarensis, L. thayeri* and *L. glaucoides* were analyzed using landmark-based morphometrics (Figs. 20 - 25) using the dorsal and ventral views. In dorsal view, most of the shape change is seen in the compression and elongation of the skull (both in Figs. 21 and 22). This can be illustrated using deformation grids that show the relative displacement of the landmarks. Specimens plotting on the bottom left of the graph exhibit slight compression towards the anterior of the skull. Those plotting on the lower right shower slightly broader skulls. The specimens plotting on the upper right show slight compression towards the front of the skull (Fig. 21). These variations are very slight and there is considerable overlap between each

species. Skull length and bill depth have been reported as a source of variation among species and have been used to sex gulls (e.g., Schnell *et al*., 1985; Bosch 1996).

The morphometrics analyses of the ventral view of the skull (Figs. 24 and 25) show the similar slight variations in shape as did the analysis of the dorsal view. Most of the variation is shown in the antero-posterior compression and expansion of the skull (skull length). The landmarks were selected to try and encompass as much of the shape of the skull as possible. A greater number of landmarks may be required to better show the skull variance. Different sets of landmarks might also be used to show the shape variation of different parts of the skull, such as the bill or the skull roof. Conducting geometric morphometrics on the lateral view of the skull might also show better species differentiation.

The postcranial analysis and cranial geometric morphometric analyses generated similar results indicating that the morphological parameters examined for the six gull species show very little appreciable morphological variation. This probably reflects that most of the gull species examined grow to similar adult sizes and share very similar lifestyles and habitats, e.g., gulls live near water bodies and all have skulls adapted to feed on small macroinvertebrates and fish (e.g., Sibley, 2003; Harris, 1964). Gulls are also very similar genetically and are known to interbreed where their breeding regions overlap (e.g., Hoffman *et al*., 1978; Mayr 1942). This project did not examine the issue of interbreeding, as the data was not recorded at the time of collection. Hybrids tend to show intermediate phenotypes and can be a significant source of uncertainty for

taxonomists (e.g., Hoffman *et al*., 1978; King and Carey, 1999; Barton and Hewitt, 1985). According to the biological species concept, if two populations interbreed freely and successfully wherever they come into contact, then they should be classified as conspecific. *L. hyperboreus* has been known to hybridize with *L. argentatus* (Vigfúsdóttir, 2008). There is no way of accounting for that when performing morphometrics analyses, as gull hybrids are very similar in morphology to their parents (Chu 2008).

The results presented here show that once size is factored out, modern gull species are difficult to differentiate using the skeletal parameters examined in this project. No interspecific shape variation was identified in either the appendicular skeleton or skulls. My results are consistent with the skeletal analyses results of Chu (1998) and Crochet *et al*. (2000). Crochet *et al*., (2000) went a step further and analyzed the phylogenetic relationships of gulls using molecular and plumage data. In that study, most of the gull species (i.e., *L. argentatus, L. hyperboreus, L. glaucoides, L. delawarensis* and *L. thayeri*) analyzed during the project all group within a homogeneous assemblage known as the 'white headed' gull species, with *L. delawarensis* determined to have originated from a more recent split from this group. My results also indicate the separation of *L. delawarensis* from the other taxa based at least on size and on slight shape variation of the hindlimb (Fig. 15, 16).

Morphometric analyses were conducted on select taxa of theropods to determine the extent of their known skeletal morphological variations. Analyses of the tyrannosaurid subgroup (Figs. 26 and 27; Tables 10 and 11) showed that

the highest variation was explained by the size of the animals ($PC_{ty}1$: 92%), which was primarily based on the lengths of their femurs and tibia (Table 10). *Tyrannosaurus rex*, which was the largest representative of the tyrannosaurids, plotted distinctly from other taxa in this theropod subgroup (e.g., Holtz *et al*., 2004). All other taxa exhibit significant overlap. In contrast, the shape analysis results indicate that all the theropod specimens, including the *T. rex* specimens plotted in one group with no clear distinction between individual species (Fig. 27). The highest loading is still represented by the femur and tibia (Table 10). *Nanotyrannus* is differentiated from the other theropod species in both analyses (Figs. 26 and 27). There has been considerable debate on the identity of *Nanotyrannus*, with most agreeing that it is a juvenile form of *Tyrannosaurus rex* (e.g., Yun, 2015). The position where this species plots suggests it had considerably longer tibia than femur (Fig. 27; Table 10), which is the immature condition in tyrannosaurids (Currie, 2008). Their tibia becomes proportionally shorter than the femur as their body size increases (Holtz, 2004 1995; Currie, 2008). Tyrannosaurid species are typically differentiated based on cranial characters and elements of the axial skeleton (e.g., Holtz, 2004). The tyrannosaurid species analyzed most likely shared the same ecological niches throughout their histories. Tyrannosaurids most likely filled the roll of top predators and may have occupied many predatory niches between hatchling and adulthood (Foster *et al*., 2001, Holtz, 2004).

Analysis of the limb elements of the small to medium sized theropods shows that they form relatively tight clusters (figure 28). *Archaeopteryx* and

Confuciusornis cluster together on the lower left of the plot. Both taxa are thought to have had adapted either gliding or limited flight abilities (e.g., Zhou *et al*., 2001; Chatterjee and Templin, 2003). *Deinonychus* plots on the lower part of the graph, suggesting it had larger and longer forelimbs compared to other species. The compsonganthid *Sinosauropteryx* plots on the upper left of the graph, suggesting it was smaller in size compared to the other species examined and had elongated hindlimbs (Ji and Ji, 1996). The number of specimens for each species was, unfortunately, limited. Most of the specimens in Currie's database were incomplete and had very few measurements taken on them. Only the most complete specimens were analyzed.

The analysis of all theropods (Figs. 29 and 30) showed discrimination between the tyrannosaurids and the rest of the theropods (maniraptorans and early birds) based on size and on elements of the forelimb (Table 16). The loading data show that the length of the femur and length of the tibiotarsus are highly correlated with component 1. This not unexpected because the tyrannosaurids are orders of magnitude larger than the other theropods and have proportionally larger hind legs, explaining why the femora and tibiotarsi show highly positive loading. Tyrannosaurids rely heavily on their hindlimbs for locomotion and, therefore, the selective pressure would be greater on their hindlimbs, suggesting they would have higher morphological variations in their hindlimb elements (e.g., Lipkin and Carpenter, 2008; Sereno *et al*., 2009).

The smaller theropods (maniraptorans and early birds) plot on the left side of the graph, which is explained by their relatively smaller size. *Struthiomimus* is

and ornithomimid and plots away from the other small-bodied theropod species (Fig. 30). The small early birds, *Archaeopteryx* and *Confuciusornis*, plot at the bottom part of the group, along with *Sinosauropteryx* and *Velociraptor*. It has been suggested that these small theropods used their hindlimbs for hunting prey (especially in *Velociraptor*) and may even be pack hunters (e.g., Li *et al*. 2007; Park *et al*., 2014; Manning *et al*., 2006). Although *Archaeopteryx* shares many features with modern birds, there is still debate as to whether it was capable of powered flight (e.g., Ruben, 1993; Speakman, 1993; Nudds *et al*., 2014; Burger and Chiappe, 1999). It has been suggested that it was capable of short distance flight by running and taking off from the ground (e.g., Speakman, 1993; Ruben, 1991; Longrich *et al*., 2012; Chatterjee and Templin, 2003). The specimens that plot on the upper part of the graph exhibit longer and differently shaped forearms. *Struthiomimus*, had highly developed, elongated forelimbs which it may have used for grasping prey (e.g., Nichols and Russell, 1985). The trend seen may indicate differing modes of locomotion or different feeding strategies in the theropod species analyzed. To further explore this, future analyses should include morphological measurements of the skulls (like measurements of jaw joints) to better reflect the lifestyles and feeding behaviour of each species.

Figure 33 shows the final PCA conducted using all theropod material and reflects shape variation. Again, the large bodied theropods were separated from the smaller theropods into two groups. The tyrannosaurids plot on the left side and the small theropods plot on the right. In a morphometrics analysis, comparing PC2 and 3 will typically show the shape variation in the dataset. This

analysis shows that, as expected, the tyrannosaurids vary significantly in shape compared to the small bodied theropods in the elements measured. The large bodied theropods have significantly larger and more robust hindlimb elements (Gatesy and Middleton, 1997; Dodson, 2004) and appear to group more tightly together than the small bodied theropods. They exhibit variations in the ratios of their femora to humeri lengths. Ratios of femoral length to humerus length can vary from approximately 2.8 in *Daspletosaurus* to 4.0 in *Tarbosaurus* (e.g., Holtz, 2004). The loading on $PC_{th}3$ (Table 16) shows that the femora and humeri exhibit the largest amount of variance. The species show significant overlap. However, the *Gorgosaurus* specimens and *Tyrannosaurus* plot together. Analyses conducted by Currie (2003) suggests that *Gorgosaurus* had slightly shorter and lower skulls, shorter ilia, longer tibiae, longer metatarsals and longer toes than tyrannosaurines of similar body sizes. Many studies support a split in Tyrannosauridae between the gracile Albertosaurinae (containing *Gorgosaurus*) and the more robust Tyrannosaurinae (containing *Tyrannosaurus*) (e.g., Currie, 2003; Holtz 2004; Paul, 1988). *Tyrannosaurus* and *Gorgosaurus* were split to account for these differences. The *Daspletosaurus* specimens all fell outside the 95% confidence interval. A lot of the measurements were missing from several elements, including the femur and humerus. This would explain why they are outliers.

The smaller maniraptorans plot together and show more variation in shape than the tyrannosaurids. As discussed previously, the species included in this analysis occupied varied ecological niches and had a wide variety of locomotor

modes. Some, like *Archaeopteryx* and *Confuciusornis*, were quite small and were possibly fliers or gliders. Others, like *Saurornitholestes,* had elongated hindlimbs and forelimbs and had specialized grasping claws for catching prey. The Ornithomimids, *Struthiomimus* and *Ornithomimus,* are separated from the other small bodied theropods based on elements of the hindlimb (femur and metatarsus III). They both belong to the Ornithomimosauria clade (Makovicky *et al*., 2004, Nicholls 1984) and are characterized by having elongate and slender forelimbs with non-raptorial manus and elongated hindlimbs adapted for fast running (Makovicky *et al*., 2004). The specimens plotting below the origin are members of Dromaeosauridae (like *Velociraptor* and *Deinonychus*) and Avialae (like *Archaeopteryx* and *Confuciusornis*). These species exhibit morphological characters adapted for active, predatory behavior. For example, *Velociraptor* and *Deinonychus* have a hyper-extendable claw on the second toe, which was most likely used for attacking preys (e.g., Norell and Makovicky, 2004; Kielan-Jaworwaska and Barsbold, 1972).

The results of the analyses show that shape variation in gulls is very conserved in the skeletal elements. They are genetically very similar and have very similar feeding behaviors. Gulls are morphologically too similar to be separated based on the shape of their elements. Analyzing similar elements in theropods show that size has a large impact on their variation (e.g., Fig. 27), but that shape of limb elements can distinguish more distantly related species (e.g., Fig. 33). These variations in limb shape and proportion have been attributed to different lifestyles and ecological niches (e.g., Holtz 2004; Makovicky, 2004;

Gatesy and Middleton, 1997). Species that share very similar lifestyles will exhibit overlaps in their skeletal morphologies and adaptations (e.g., Gatesy and Middleton, 1997; McGowan and Dyke, 2007). Even so, skeletal elements in the fossils will most likely not be able to account for species that are genetically (and morphologically) very similar. If the reproductive and molecular information of the gulls analyzed was not provided (and if the identity of the skeletons were unknown), it would become very difficult to quantitatively differentiate them using the limb elements. *Larus delawarensis* would be the most apparent differentiation based on its smaller size (Fig. 15). In the fossil record, size differences in a fossil group is usually attributed to sexual dimorphism (e.g., Chapman *et al*., 1997; Molnar 2005; Raath *et al*., 1990). Clearly, soft tissue and breeding potential are key aspects in species recognition.

Conclusions

The hypothesis to be tested for this project was whether closely related species of gulls could be differentiated exclusively based on their skeletal morphology. Based on the results of the PCA, the null hypothesis cannot rejected; closely related gull species sharing similar morphologies in their appendicular skeleton and skulls cannot be differentiated based on skeletal parameters examined in this project. This result is supported by the recent work of Chamero *et al.* 2013 who conducted a geometric morphometric analysis of pectoral girdle and forelimb variation in several extant taxa of Crocodylia, the closest living relatives of extinct, non-avian+avian dinosaurs. Their results

demonstrated that intraspecific variation in the limbs and pectoral element is very large, but that the interspecific variation is small or significant. They also show a high degree of overlap in forelimb shape between closely related crocodylians. Similar to modern birds, recognition of closely related crocodile species using skeletal anatomy has long been problematic (e.g., Eaton *et al*., 2009; King and Burke, 1989; Ross, 2006). Crocodiles have highly conserved morphology (e.g., Shirley *et al*., 2013) and taxonomic analyses rely more heavily on molecular data (e.g., Eaton *et al*., 2009; Dever *et al*., 2002; Hekkala, 2004).

My results show that gulls exhibit higher intraspecific variation in limbs and less interspecific variation (Figs. 15 and 16). Although this is a small data set, when combined with the results of the other avian, and non-avian dinosaur analyses (and from previous analyses of Crocodylia), it suggests that a percentage of modern archosaur diversity can actually only be recognized through the soft-tissue and behavioral characteristics that are not preserved in extinct dinosaurs. I would thus suggest that our understanding of the true diversity of non-avian theropods is hampered by our lack of non-skeletal characteristics for these animals. If the gulls being analyzed in this project were found as fossils, they would most likely not be recognized as separate taxa. The size difference of *L. delawarensis* would most likely be attributed to ontogeny or sexual dimorphism. Further analysis of the material is needed. Similar to the theropod analysis (e.g., Fig. 30), more distantly related species of shorebirds should be analyzed along with the gulls (e.g., the gulls and the skuas or terns). This analysis would give further insight into the extent of morphological variations

of related species. Gulls should also be analyzed and compared with other, distantly related birds of similar size (e.g., ducks or mallards).

Appendices

Appendix A Averaged measurements for the gull specimens

	left femur length	left femur dis width	left femur mids	left tbt length	left tbt distal width	left tmt length	left tmt distal width	L humerus length	left humerus	left radius length	left ulna length	left ulna distal width
z144	58.1	12.4	5.2	111.8	17.8	65.0	11.6	134.0	17.5	143.1	149.0	13.9
s5969	56.0	11.2	4.8	109.4	16.4	62.8	10.5	129.3	16.8	138.8	143.9	13.8
s3784	57.4	11.9	5.0	113.1	17.0	67.8	10.6	129.9	17.8	140.7	145.9	14.1
s3787	57.1	11.5	4.8	106.7	17.2	63.7	11.3	126.6	17.3	135.4	140.2	13.9
s3790	59.6	11.7	5.0	113.4	17.0	66.6	10.7	131.6	17.2	143.5	145.0	13.5
s3789	60.6	11.6	5.0	114.7	16.3	68.5	10.5	131.4	17.6	145.1	148.4	13.6
s3788	57.2	11.3	4.6	107.1	15.7	61.4	10.7	131.0	17.5	136.7	141.5	13.3
s3783	63.1	12.7	5.6	117.4	18.3	73.6	11.1	137.6	18.4	149.6	154.8	14.6
s484	60.5	12.4	5.0	111.7	16.8	64.0	11.4	133.9	17.4	139.6	144.3	13.5
S2153	62.5	12.5	5.3	115.9	18.6	70.0	12.6	133.5	17.8	144.3	148.9	14.4
S1090	56.2	12.0	5.1	108.3	17.3	62.1	12.8	125.8	17.6	135.4	140.9	14.2
S2152	64.5	13.5	4.7	122.3	19.1	72.8	12.6	130.0	17.5	145.0	142.0	15.3
S1099	60.1	11.0	4.7	107.5	16.6	65.1	10.9	131.6	17.2	139.8	144.8	14.1
S680	56.9	11.2	4.6	109.3	16.7	64.3	11.5	129.6	16.5	139.1	143.8	13.2
S1084	61.1	12.5	5.3	111.3	17.7	67.2	11.7	135.1	18.7	144.2	149.1	15.4
S3780	58.3	11.5	4.7	107.6	16.3	61.4	10.9	134.0	18.0	134.8	139.6	14.1
S5845	56.8	11.6	4.8	104.9	15.7	61.0	10.6	125.3	18.0	136.8	142.7	14.2
S5919	57.0	12.1	5.1	110.2	16.6	63.1	11.3	131.5	17.6	138.7	143.9	14.3
S5912	46.3	8.9	3.7	89.9	12.9	56.6	8.5	105.1	13.2	113.2	117.4	10.7
S6060	40.9	8.5	3.2	81.9	11.6	50.9	8.3	91.7	12.6	112.4	117.2	12.0
S5814	41.0	8.0	3.2	83.2	11.5	52.2	7.7	93.4	11.8	105.6	107.8	8.6
S5917	43.3	8.7	3.5	89.0	12.9	56.4	7.7	101.6	12.8	110.7	114.6	10.3
S5079	45.0	9.0	3.7	91.6	13.1	58.1	8.5	101.6	12.9	114.1	117.0	10.2
S5560	46.8	9.4	4.0	93.8	13.1	59.9	8.9	103.6	13.8	115.5	119.9	11.1
S5321	47.4	10.2	4.0	93.2	14.0	61.1	8.4	105.0	14.1	115.2	119.3	11.2
s6165	41.6	8.1	3.5	81.3	12.5	53.7	8.1	93.0	12.4	104.6	108.2	10.3
S3766	43.3	8.4	3.5	86.5	12.8	53.3	7.6	96.0	12.1	105.3	108.9	10.3
S3769	48.1	9.2	3.6	93.2	13.6	59.1	8.8	105.7	14.0	115.8	120.9	10.8
S3777	46.2	9.1	3.5	90.2	12.9	56.9	8.4	99.7	13.0	109.0	112.9	10.8
S3737	44.4	8.7	3.4	87.0	13.1	54.9	8.8	99.4	13.3	110.3	113.7	10.7
S3758	44.3	7.7	3.3	85.6	12.2	54.0	7.9	96.7	12.2	104.1	107.8	12.6

	Left femur length	Left femur dis width	Left femur mds radius	Left tbt length	Left tbt width	Left tmt length	Left tmt width	L humerus length	L humerus width	L radius length	L ulna length	L ulna width
S3748	46.4	9.3	3.8	93.1	13.6	59.0	9.0	105.3	13.7	115.4	119.8	11.5
ROM108931	56.9	12.3	4.9	106.4	17.8	61.3	11.3	124.4	17.4	133.0	137.4	14.1
ROM108932	61.8	13.2	5.1	118.1	19.2	70.5	12.5	138.7	18.3	152.3	160.7	15.3
ROM015149	57.0	11.2	4.8	108.4	17.6	62.8	11.1	126.3	17.6	135.6	140.6	14.4
ROM0151252	56.1	11.4	4.6	106.1	17.3	60.9	11.2	122.6	16.6	128.6	132.4	13.7
Rom115403	58.5	12.0	5.2	110.2	17.8	65.2	10.9	126.1	17.4	137.2	140.9	14.4
ROM115408	58.4	12.1	4.7	112.7	18.1	66.3	11.6	128.4	17.7	136.1	141.4	14.7
ROM158134	55.2	11.1	4.3	104.5	15.3	59.1	9.9	119.8	15.9	129.3	134.2	13.6
ROM0151283	55.4	11.0	4.7	103.1	16.6	54.1	10.1	117.5	16.3	125.9	130.4	13.6
ROM0151262	52.6	10.9	4.5	102.0	14.4	56.5	10.7	113.4	16.3	120.3	125.3	14.1
ROM124926	60.0	12.0	4.8	114.2	17.6	66.2	10.2	130.0	18.0	139.4	145.0	14.8
ROM124924	53.5	10.9	4.9	104.3	15.6	60.9	10.5	121.8	16.5	129.6	134.3	14.0
ROM125735	55.4	11.2	4.6	104.1	16.3	60.5	10.3	118.7	15.9	127.4	130.8	13.2
ROM124925	57.0	11.4	4.6	105.2	16.7	60.6	10.5	121.4	16.5	130.5	134.6	13.9
ROM125437	55.0	10.7	4.3	102.2	16.2	58.3	10.2	118.7	16.2	126.6	131.3	13.1
ROM125436	58.3	11.7	4.8	110.9	15.9	66.6	11.0	127.4	17.8	136.9	141.6	14.7
S2154	55.5	11.6	4.4	104.3	16.3	59.3	10.8	124.0	16.8	132.1	136.9	14.0
S6055	59.3	12.0	4.6	113.4	17.9	65.8	11.0	130.9	17.4	138.0	142.7	14.0
S1785	57.9	11.4	4.5	107.0	16.2	64.1	10.7	124.4	16.7	133.2	136.1	13.8
S563	66.8	13.7	5.9	126.8	19.3	70.4	13.6	155.1	21.5	165.8	170.5	17.5
S2151	67.0	14.0	5.3	122.1	16.2	71.7	12.7	141.2	19.6	149.7	155.5	17.1
S5853	60.6	13.3	5.5	117.7	18.4	64.2	12.3	144.5	18.2	156.5	155.5	16.0
ROM0151260	72.2	14.7	5.5	132.6	21.4	76.2	14.0	154.4	21.5	165.8	172.4	17.6
ROM0151266	70.4	15.1	6.5	132.3	22.3	74.6	13.7	155.1	21.5	167.5	170.0	17.5
ROM0151263	70.5	14.8	5.9	132.1	21.3	74.8	13.2	153.6	20.9	162.2	165.7	17.1
S930	69.4	14.8	5.5	130.8	21.3	74.9	13.4	149.7	19.7	156.5	170.5	15.6
S564	66.7	13.7	5.5	127.7	20.1	70.4	13.5	144.3	18.2	155.0	155.5	15.2
S2155	66.9	13.9	5.3	122.7	16.4	71.9	12.6	141.2	19.5	149.7	155.5	16.2
S5586	64.1	13.1	5.6	119.2	18.8	66.5	11.9	140.2	19.2	152.1	155.5	15.9
S3791	58.5	11.9	4.5	107.1	17.5	60.8	11.1	124.7	17.3	130.4	134.2	14.5
S893	61.8	10.9	4.8	96.2	16.4	56.8	10.4	113.1	16.0	117.8	122.5	13.3
S7955	66.9	13.8	5.5	130.3	20.9	75.6	12.3	142.6	18.7	150.1	154.7	15.3
S5532	56.9	11.3	4.5	108.0	16.9	63.2	10.5	119.5	16.4	129.0	133.7	13.5
S5531	62.5	12.7	5.3	120.8	19.6	68.9	12.0	131.2	18.0	139.9	145.0	14.0

S5553	56.9	11.7	4.6	108.5	17.3	62.8	10.9	117.5	15.0	125.0	129.7	12.9

Appendix B Standardized gull measurements

	left femur length	left femur dis width	left femur mids	left tbt length	left tbt distal width	left tmt length	left tmt distal width	left humerus	left humerus	left radius length	left ulna length	left ulna distal width
z144	0.2	0.2	0.7	0.3	0.5	0.3	0.5	0.6	0.3	0.5	0.6	0.1
s5969	-0.1	-0.5	0.2	0.1	-0.1	-0.1	-0.2	0.3	0.0	0.3	0.3	0.1
s3784	0.1	0.2	0.4	0.4	0.2	0.7	-0.1	0.3	0.4	0.4	0.5	0.2
s3787	0.0	0.0	0.1	-0.1	0.2	0.0	0.3	0.1	0.2	0.1	0.1	0.1
s3790	0.4	0.1	0.4	0.4	0.2	0.5	-0.1	0.4	0.2	0.6	0.4	-0.1
s3789	0.5	0.0	0.4	0.5	-0.1	0.8	-0.2	0.4	0.4	0.7	0.6	-0.1
s3788	0.1	-0.1	-0.1	-0.1	-0.4	-0.3	-0.1	0.4	0.3	0.2	0.2	-0.3
s3783	0.8	0.7	1.1	0.7	0.7	1.6	0.2	0.8	0.7	0.9	1.0	0.5
s484	0.5	0.5	0.4	0.3	0.1	0.1	0.4	0.6	0.3	0.3	0.4	-0.1
S2153	0.7	0.6	0.8	0.6	0.8	1.0	1.1	0.5	0.4	0.6	0.6	0.3
S1090	-0.1	0.3	0.6	0.0	0.3	-0.2	1.3	0.1	0.4	0.1	0.2	0.2
S2152	1.0	1.1	0.0	1.1	1.0	1.5	1.1	0.3	0.3	0.7	0.2	0.8
S1099	0.4	-0.3	0.0	0.0	0.0	0.3	0.1	0.4	0.2	0.3	0.4	0.2
S680	0.0	-0.2	-0.1	0.1	0.0	0.1	0.5	0.3	-0.1	0.3	0.3	-0.3
S1084	0.6	0.5	0.8	0.3	0.5	0.6	0.6	0.6	0.8	0.6	0.7	0.9
S3780	0.2	0.0	0.0	0.0	-0.1	-0.3	0.1	0.6	0.5	0.0	0.1	0.2
S5845	0.0	0.0	0.1	-0.2	-0.3	-0.4	-0.1	0.0	0.5	0.2	0.3	0.2
S5919	0.0	0.3	0.5	0.2	0.0	-0.1	0.3	0.4	0.4	0.3	0.3	0.3
S5912	-1.4	-1.4	-1.3	-1.4	-1.5	-1.1	-1.4	-1.2	-1.5	-1.3	-1.3	-1.6
S6060	-2.1	-1.7	-2.0	-2.0	-2.0	-2.0	-1.6	-2.0	-1.7	-1.3	-1.3	-0.9
S5814	-2.1	-2.0	-2.0	-1.9	-2.0	-1.8	-1.9	-1.9	-2.1	-1.7	-1.9	-2.7
S5917	-1.8	-1.6	-1.6	-1.4	-1.5	-1.1	-1.9	-1.4	-1.6	-1.4	-1.5	-1.8
S5079	-1.5	-1.4	-1.3	-1.2	-1.4	-0.9	-1.4	-1.4	-1.6	-1.2	-1.3	-1.8
S5560	-1.3	-1.2	-0.9	-1.1	-1.4	-0.6	-1.2	-1.3	-1.2	-1.1	-1.1	-1.4
S5321	-1.2	-0.7	-0.9	-1.1	-1.0	-0.4	-1.5	-1.2	-1.1	-1.2	-1.2	-1.3
s6165	-2.0	-1.9	-1.7	-2.0	-1.7	-1.6	-1.7	-1.9	-1.8	-1.8	-1.9	-1.8
S3766	-1.8	-1.8	-1.6	-1.6	-1.5	-1.6	-2.0	-1.8	-2.0	-1.8	-1.8	-1.8
S3769	-1.1	-1.3	-1.5	-1.1	-1.2	-0.7	-1.2	-1.2	-1.2	-1.1	-1.1	-1.5
S3777	-1.4	-1.4	-1.6	-1.4	-1.5	-1.0	-1.5	-1.5	-1.6	-1.5	-1.6	-1.5
S3737	-1.6	-1.6	-1.8	-1.6	-1.4	-1.4	-1.3	-1.6	-1.4	-1.5	-1.5	-1.6
S3758	-1.6	-2.1	-1.9	-1.7	-1.8	-1.5	-1.8	-1.7	-1.9	-1.8	-1.9	-0.6
S3748	-1.4	-1.2	-1.2	-1.1	-1.2	-0.7	-1.1	-1.2	-1.3	-1.1	-1.1	-1.2
ROM108931	0.0	0.4	0.2	-0.1	0.5	-0.4	0.3	0.0	0.2	-0.1	-0.1	0.2
ROM108932	0.6	1.0	0.6	0.8	1.0	1.1	1.0	0.9	0.6	1.1	1.4	0.8

ROM015149	0.0	-0.2	0.1	0.0	0.4	-0.1	0.2	0.1	0.3	0.1	0.1	0.3
	left femur	left femur	left femur	left tbt length	left tbt distal	left tmt length	left tmt distal	left humeru	left humeru	left radius	left ulna	left ulna
ROM0151252	-0.1	-0.1	-0.1	-0.1	0.3	-0.4	0.3	-0.1	-0.1	-0.3	-0.4	0.0
Rom115403	0.2	0.3	0.7	0.2	0.5	0.3	0.0	0.1	0.3	0.2	0.1	0.3
ROM115408	0.2	0.3	0.0	0.4	0.6	0.4	0.5	0.2	0.4	0.1	0.2	0.5
ROM158134	-0.2	-0.3	-0.5	-0.3	-0.5	-0.7	-0.6	-0.3	-0.4	-0.3	-0.3	-0.1
ROM0151283	-0.2	-0.3	0.0	-0.4	0.0	-1.5	-0.5	-0.4	-0.2	-0.5	-0.5	-0.1
ROM0151262	-0.5	-0.3	-0.3	-0.4	-0.9	-1.1	-0.1	-0.7	-0.2	-0.8	-0.8	0.2
ROM124926	0.4	0.3	0.1	0.5	0.4	0.4	-0.4	0.3	0.5	0.3	0.4	0.6
ROM124924	-0.4	-0.3	0.2	-0.3	-0.4	-0.4	-0.2	-0.2	-0.1	-0.3	-0.3	0.1
ROM125735	-0.2	-0.1	-0.1	-0.3	-0.1	-0.5	-0.3	-0.4	-0.4	-0.4	-0.5	-0.3
ROM124925	0.0	-0.1	-0.1	-0.2	0.1	-0.5	-0.2	-0.2	-0.1	-0.2	-0.2	0.1
ROM125437	-0.2	-0.5	-0.6	-0.4	-0.1	-0.8	-0.4	-0.4	-0.2	-0.5	-0.4	-0.3
ROM125436	0.2	0.1	0.1	0.2	-0.3	0.5	0.1	0.2	0.5	0.2	0.2	0.5
S2154	-0.2	0.0	-0.3	-0.3	-0.1	-0.7	0.0	0.0	0.0	-0.1	-0.1	0.1
S6055	0.3	0.3	-0.1	0.4	0.5	0.4	0.1	0.4	0.3	0.2	0.3	0.1
S1785	0.1	0.0	-0.3	-0.1	-0.2	0.1	-0.1	0.0	0.0	-0.1	-0.1	0.0
S563	1.3	1.2	1.5	1.5	1.1	1.1	1.7	1.9	2.0	1.9	2.0	2.0
S2151	1.3	1.4	0.8	1.1	-0.2	1.3	1.2	1.0	1.2	1.0	1.0	1.7
S5853	0.5	1.0	1.0	0.8	0.7	0.1	1.0	1.2	0.6	1.4	1.0	1.2
ROM0151260	2.0	1.8	1.1	1.9	2.0	2.0	2.0	1.8	2.0	1.9	2.1	2.0
ROM0151266	1.8	2.0	2.4	1.9	2.3	1.8	1.8	1.9	2.0	2.0	1.9	2.0
ROM0151263	1.8	1.9	1.6	1.9	1.9	1.8	1.5	1.8	1.7	1.7	1.7	1.7
S930	1.6	1.9	1.0	1.8	1.9	1.8	1.6	1.5	1.3	1.4	2.0	1.0
S564	1.3	1.2	1.1	1.5	1.4	1.1	1.7	1.2	0.6	1.3	1.0	0.8
S2155	1.3	1.4	0.8	1.2	-0.1	1.4	1.1	1.0	1.2	1.0	1.0	1.3
S5586	0.9	0.9	1.2	0.9	0.9	0.5	0.7	0.9	1.0	1.1	1.0	1.1
S3791	0.2	0.2	-0.3	-0.1	0.4	-0.4	0.2	0.0	0.2	-0.2	-0.3	0.4
S893	0.7	-0.4	0.1	-0.9	-0.1	-1.1	-0.3	-0.7	-0.3	-1.0	-1.0	-0.2
S7955	1.3	1.3	1.0	1.7	1.7	1.9	1.0	1.1	0.8	1.0	1.0	0.8
S5532	0.0	-0.1	-0.3	0.0	0.1	0.0	-0.2	-0.3	-0.2	-0.3	-0.3	-0.1
S5531	0.7	0.7	0.7	1.0	1.2	0.9	0.7	0.4	0.5	0.4	0.4	0.1
S5553	0.1	0.1	-0.1	0.1	0.3	-0.1	0.1	-0.4	-0.8	-0.6	-0.5	-0.4

Appendix C Measurements of Theropod Specimens

Species	Specimen #	source	H. length	R. length	U. length	F. length	T. length	mt III
Albertosaurus sarcophagus	NMC 11315	Currie pers. obs. and Russell 1970	222	96.2	119.5	680	690	445
Albertosaurus sarcophagus	ROM 807	Parks 1928; Currie pers. obs.	305	134	165	1020	980	595
Albertosaurus sarcophagus	TMP 1986.64.1	Currie pers. obs.	209	99	114	729	750	475
Daspletosaurus torosus	TMP 2001.36.1	Currie pers. obs., some from field	360	135	169	960	905	486
Daspletosaurus torosus	UALVP 52981	field measurements	305	125	175	965	870	456
Gorgosaurus libratus cf.	Children's Museum 2001.89.1	Currie pers. obs., cast	303	94	182	830	885	538
Gorgosaurus libratus	NMC 2120 (type Gorgo)	Currie pers. obs.	324	156	180	1030	980	615
Gorgosaurus libratus	TMP 91.36.500	Currie pers. obs.	167	96	120	645	714	456
Raptorex kriegsteini	Long Hao Inst. Geol. Pal. LH PV18	Sereno et al. 2009	99	52	56.8	338	382	
Tarbosaurus baatar	CMMD1 (Central Museum of Mongolian Dinosaurs)	P. Currie pers. Obs. 120605	212	98.6	120.5	785	740	486
Tarbosaurus baatar	MPC 940823-Bgt-1	Currie pers. obs.	130	126	92	630	615	412
Tarbosaurus baatar	MPC-D107/02	Currie pers. obs.	285	123	135	1120	890	530
Tarbosaurus baatar	PIN 552-1/Ulan Batar	Maleev 1974	255	110	115	995	870	550
Tyrannosaurus rex	FMNH PR2081 (Sue)	Currie pers. obs. & Brochu 2003	385	175	222	1321	1140	671
Tyrannosaurus rex	MOR 0555 "Wankel"	Currie pers. obs.	385	161	201	1280	1150	670
Guanlong wucaii	IVPP V14531 holotype	Miyashita pers.obs. 2013	217	160	179	343	380	189.2
Yutyrannus huali	ZCDM V5001, IVPP FV1961	Xu et al., 2012; cast from SVP auction	320	219	255	650	655	350
Aucasaurus	MCF-PBPH-236	Currie pers. obs.	248	79	92	700	640	346
Carnotaurus sastrei	MACN-CH 894	Bonaparte et al, Currie pers. obs.	284	76	82	1024		
Acrocanthosaurus atokensis	NCSM 14345	Currie pers. obs.	370	220	255	1277	952	439e

Allosaurus fragilis	MOR 693	Currie pers. obs.	318	200	254	742	702	345
Allosaurus fragilis	Wyoming Dinosaur Center baby (Pohl)	Currie pers. obs. 120813, cast	176	110	137	450	407	205
Allosaurus fragilis	USNM 4734 (topotype)	Gilmore 1920, Carrano database	310	222	263	850	690	327
Suchomimus	BM R16013	cast at BMHN	545	257	327	1037	945	
Sinosauropteryx prima	NIGP 127586/NGNC 2123	Currie pers. obs.	20.3	12.4	16.9	53.2	61	40
Sinosauropteryx prima	NIGP 127587	Currie pers. obs.	35.5	20.1	28.2	86.4	97	63.9
Bambiraptor	AMNH FARB 30556 (FIP 000001)	Currie pers. obs.	103	85	93	118	165.7	80
Deinonychus antirrhopus	AMNH 3015	Ostrom 1976	237	172	186	284	312	151
Deinonychus antirrhopus	MCZ 4371	Ostrom 1976	254	192	208	336	368	164.4
Dromaeosaurid Sayn Shand	MPC-D100/22	PJC2002, 150901	186	134	146	228	278	132.4
Microraptor gui	Wendy 1	Currie pers. obs.	88.3	78.7	79.4	105.7	132.7	70.3
New IVPP from Tugumu		Currie pers. obs.	119	87.5	96	192	211	136.5
Saurornitholestes langstoni	MOR 660	Currie pers. obs.	162	122.8	123.1	225	245.5	113
Julieraptor	ROM 53680	Currie pers. obs.	140	105.6	107.5	165	207	101.4
Saurornitholestes langstoni	UALVP 55700	field measurements	170	129	144	220	249	120
Sinornithosaurus millenii	IVPP V12811	Xu Xing, Currie pers. obs.	139	89	110	137	125	92
Velociraptor mongoliensis	MPC-D100/0025	Barsbold & Osmolska 1999	145	96	106	172	229	112.5
Velociraptor mongoliensis	MPC-D100/0054 skull	Currie pers. obs.150829	130.3	104.4	117.3	187	214	100.9
Wendy 2	Wendy 2; poached, ?in Korea	Currie pers. obs.	84	68	75	92	141	
Protarchaeopteryx	GMV 2125	Ji&Ji, Currie pers. obs.	88	71	73	122	160	85
Avimimus	Complete Currie pers. obs. on display	Currie pers. obs.	99	93	105	210	239	124
Caudipteryx zhoui	NGMC 97-9-A	Currie pers. obs.	70	56	59	149	188	107
Caudipteryx zoui	NGMC 98-7-8	Currie pers. obs.	68.5	55	59	145	182	105
Caudipteryx zoui	private collection	cast in Fukui	71.3	60	62	142.5	187	113
Caudipteryx zoui	BPM 0001	Zhou, Wang, Zhang, Xu, 2000; Currie pers.	72	59	63.5	145.4	188	113

		obs.						
Caudipteryx sp.	IVPP 12430	Zhou, Wang, Zhang, Xu, 2000; Currie pers. obs.	69	56	61.8	146	187	112
Anzu wyliei	CM 78000 Triebold & Nus #1	Lamanna et al. 2014, casts, Carnegie 150115	338	274	280	533	650	
Citipati n.sp.	MPC-D100/42	Currie pers. obs. in Denmark	205	180	188	305	380	180
Citipati osmolskae	MPC-D100/978 holotype	Currie pers. obs.	230	189	200	345	397	192
Citipati osmolskae	MPC-D100/979	Currie pers. obs.	215	198	214	405		177
Conchoraptor gracilis	MPC-D110/21	Currie pers. obs.	61.3	54.6	55	131	164	
Heyuannia huangi	HYMV1-2 (Heyuan Museum)	Lu 2005	130	110	127	255	315	135
Ingenia yanshini	MPC-D100/32	Currie pers. obs.	140	110.5	115.2	254	294	132
Ingenia yanshini	MPC-D100/33	Currie pers. obs.	128	94.7	99	233	267	124.5
Khaan mckennai	MPC D-100/1127 holotype, "Sid"	Currie pers. obs. 120315	110.2	87	95.5	183	215	
Deinocheirus mirificus Therizino 3	MPC-D100/127 KID447	Currie pers. obs.	993	650	655	1150	1140	655
Gallimimus bullatus	MPC-D100/11	Osmolska et al, Currie pers. obs.	530	350	380	665	695	530
Ornithomimus edmontonicus	ROM 851	Parks 1933, Clive Coy, Russell 72, PJC 2005; Carrano database	279	177	206	435	475	310
Ornithomimus edmontonicus	TMP 95.110.1	Currie pers. obs.	275	200	211	425	465	332
Struthiomimus altus	AMNH 5257	Currie pers. obs.	358	261	261	512	555	370
Struthiomimus altus	BHI 1266 "Claws"	Currie pers. obs.	395	313	326	655	700	475
Struthiomimus altus	TMP 90.26.1	Currie pers. obs.	310	260	280	467	506	375
Struthiomimus altus	UCMZ (VP) 1980.1	Currie pers. obs.	362	239	256	502	556	398
Sinornithoides youngi	IVPP V9612	Currie pers. obs.	83	59.1	65	137	194	111
Limusaurus inextricabilis	IVPP V15923 holotype	Xu et al., 2009; Currie pers. Obs. 120807	82.2	45	44.3	208	245	157
Sinosaurus triassicus	ZLJ0057 (Previously LDM L10)	Currie pers. obs.	285	155	218	545	482	295
Eoraptor	PVSJ 512	Currie pers. obs.	81.5	61	62	152	155	73.5
Herrerasaurus ischigualestensis	PVSJ 373	Currie pers. obs.	175	152	167	345	315	164

Archaeopteryx lithographica	Berlin	Wellnhofer 74	63.5	54.4	55	52.6	68.5	37
Archaeopteryx lithographica	Solnhofen	Wellnhofer 93, 95	83	69	72	70	89.5	47.8
Confuciusornis sanctus	GMV 59a	Currie pers. obs.	63	50	56	55	59	29
Confuciusornis sanctus	GMV 59b	Currie pers. obs.	66	54	59	55.8	66.5	30.4
Confuciusornis sanctus	IVPP V11374 bird 1	cast (check original later)	53.1	42.6	45.3	44.8	50.5	24.3
Confuciusornis sanctus	Nathan, right one of pair	Currie pers. obs.	55.4	44.6	46.1	47.8	54.4	27.7
Confuciusornis sanctus	Nathan, left one of pair	Currie pers. obs.	53.9	43.9	46.1	48.3	51.3	25.7
Confuciusornis sanctus	TMP 98.14.1	Currie pers. obs.	64	51.3	51.5	51.6	60.4	30.9
Confuciusornis sanctus	TMP 98.14.2	Currie pers. obs.	49.8	42.5	42.7	44.6	50.2	26.2
Protopteryx?	IVPP V11665	Currie pers. obs.	26.8	26.4	27.4	19.8	28.8	16.5

Appendix D Loading of PC 1 and 2 of each analysis

PC1

PC2

Gulls

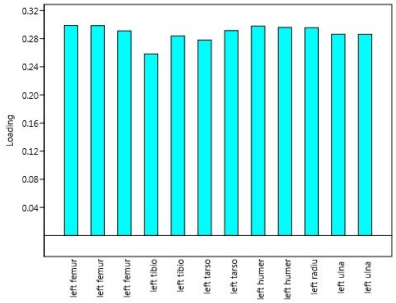

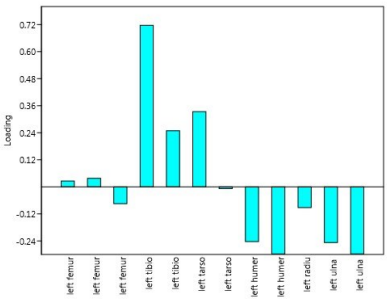

Small bodied theropods

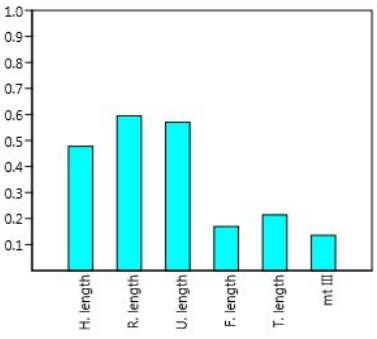

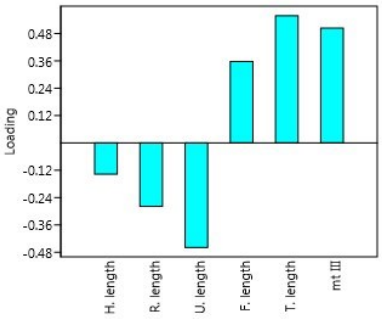

Tyrannosaurid

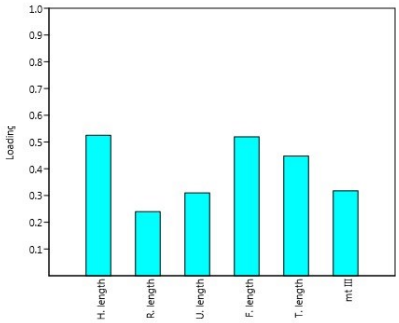

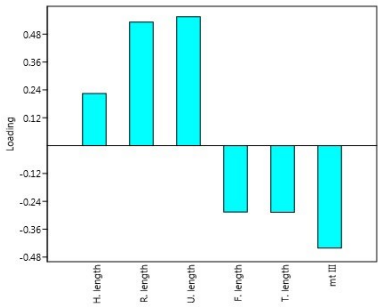

All Theropods

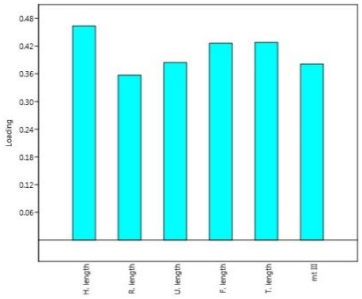

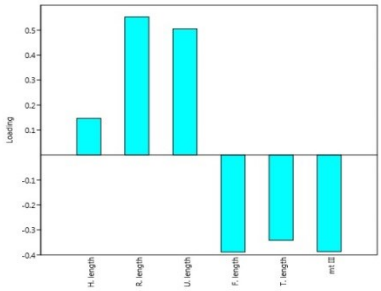

Appendix E Landmarks digitized on *Larus* skulls

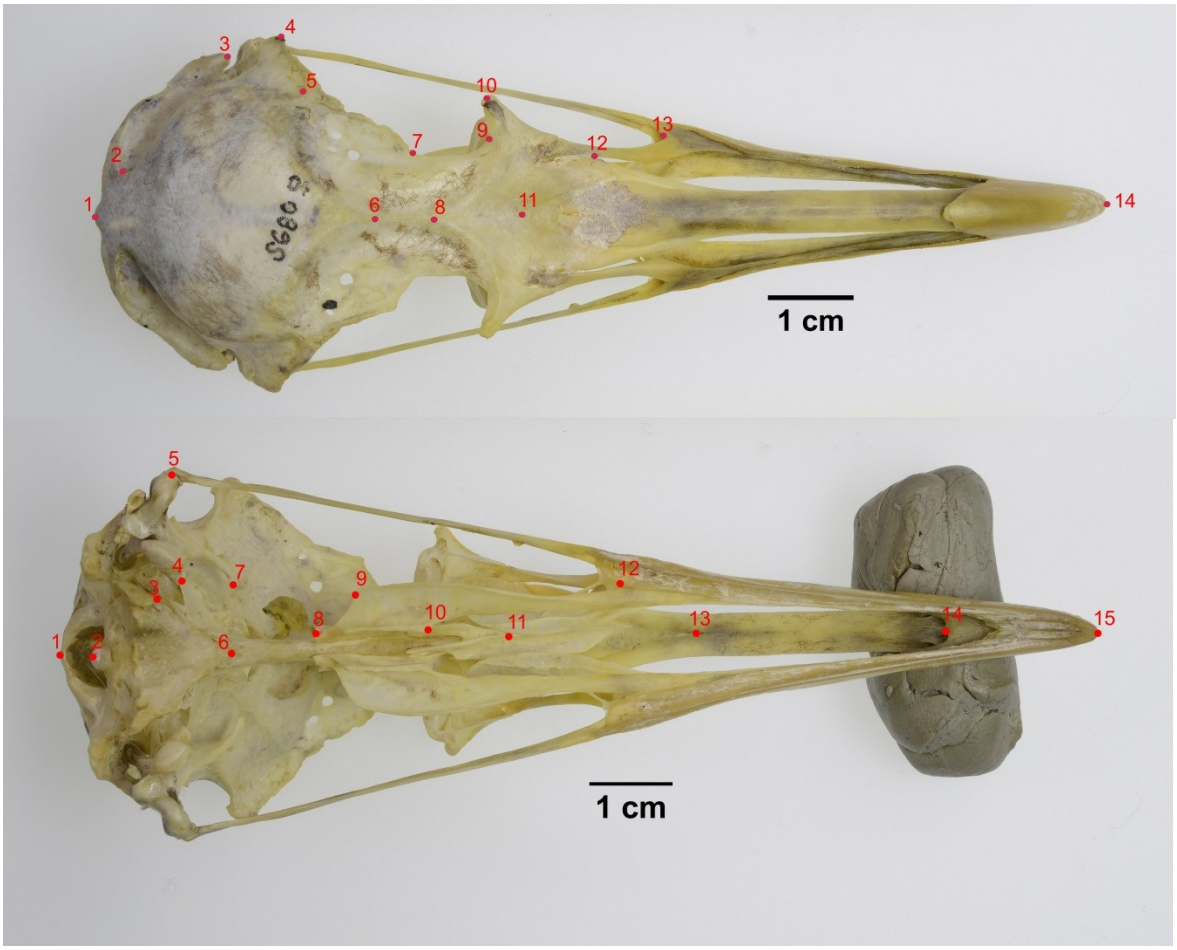

Appendix F Landmark location

Number	Dorsal Landmarks
1	Foramen magnum dorsal extreme
2	‘Highest’ curvature of fossa temporalis
3	Distal end of the occipital process
4	‘point’ of the postorbital process
5	Edge of the frontal
6	Tip of frontal crest
7	Sharpest curvature of orbit
8	Tip of nasal crest
9	Sharpest curvature of the lacrimal
10	Tip of the lacrimal bone
11	Suture of nasals and premaxilla
12	posterior curvature of nasal opening
13	Sharpest curvature of jugal
14	Tip of beak

Number	Ventral Landmarks
1	Foramen magnum ventral extreme
2	Occipital condyle tip
3	Edge of basioccipital
4	Suture of quadrate and pterygoid
5	Suture of quadratojugal and jugal
6	suture of parasphenoid and Basitemporal
7	Tip of squamosal
8	Contact of pterygoid and palatine
9	Sharpest curvature of external edge of palatine
10	Contact of vomer and palatine
11	Contact of vomer and palatine
12	Contact of premaxillary process of palatine and palatine process of premaxilla
13	Ventral suture of premaxilla and nasal
14	Choanal fossa
15	Tip of beak

References

Agnolin, F. L., & Novas, Fernando E. (2013), *Avian ancestors: a review of the phylogenetic relationships of the theropods Unenlagiidae, Microraptoria, Anchiornis and Scansoriopterygidae*, Springer Science & Business Media

Bada, J. L., Wang, X. S., Poinar, H. N., Paabo, S. and Poinar, G. O. (1994), Amino acid racemization in amber-entombed insects: Implications for DNA preservation, *Geochimica et cosmochimica acta*, vol. 58, No. 14, pp. 3131-3135

Bakker, R. J. and Bradley, R. D. (2006), Speciation in mammals and the genetic species concept, *Journal of Mammalogy*, vol. 87 (4), pp. 643-662

Bakker, R. J. and Bradley, R. D. (2006), Speciation in mammals and the genetic species concept, *Journal of Mammalogy*, vol. 87 (4), pp. 643-662

Bakker, R. T. (1986), *The dinosaur heresies*, William Morrow.

Barrett, P. M. (2009), The affinities of the enigmatic dinosaur *Eshanosaurus deguchiianus* from the Early Jurassic of Yunnan Province, People's Republic of China, *Palaeontology*, 52(4), 681-688

Barton, N. H., & Hewitt, G. M. (1985), Analysis of hybrid zones, *Annual review of Ecology and Systematics*, 113-148.

Benson, R. B. (2009), An assessment of variability in theropod dinosaur remains from the Bathonian (Middle Jurassic) of Stonesfield and New Park Quarry, UK and taxonomic implications for *Megalosaurus bucklandii* and *Iliosuchus incognitus*, *Palaeontology*, 52(4), 857-877

Benson, R. B., Carrano, M. T., & Brusatte, S. L. (2010), A new clade of archaic large-bodied predatory dinosaurs (Theropoda: Allosauroidea) that survived to the latest Mesozoic. *Naturwissenschaften*, 97(1), 71-78

Benton, M. and Harper, D. (2009), *Introduction to paleobiology and the fossil record*, Blackwell publishing

Benton, M. J. (2004), Origin and relationships of Dinosauria, *The Dinosauria*, 2nd edition, pp. 7-19.

Bookstein, F. L. (1997), Landmark methods for forms without landmarks: morphometrics of group differences in outline shape. *Medical image analysis*, 1(3), 225-243.

Bosch, M. (1996), Sexual Size Dimorphism and Determination of Sex in Yellow-Legged Gulls (Dimorfismo Sexual de Tamaño y Determinación del Sexo en *Gaviotas Patiamarillas*), *Journal of Field Ornithology*, 534-541.

Brett-Surman, Michael K., Thomas R. Holtz, and James O. Farlow, eds. (2012) *The complete dinosaur*, Indiana University Press

Brooks, W. S. (1915), *Notes on birds from east Siberia and arctic Alaska*, *Mus. Comp. Zool*. Vol. LIX, No. 5. pp. 361-413

Bryant, H. N., & Russell, A. P. (1992), The role of phylogenetic analysis in the inference of unpreserved attributes of extinct taxa. *Philosophical Transactions of the Royal Society of London B: Biological Sciences*, 337(1282), 405-418.

Burgers, P., & Chiappe, L. M. (1999), The wing of Archaeopteryx as a primary thrust generator, *Nature*, 399(6731), 60-62.

Burnham, D. A., Derstler, K. L., Currie, P. J., Bakker, R. T., Zhou, Z. and Ostrom, J. H., (2000), Remarkable new birdlike dinosaur (Theropoda: Maniraptora) from the upper Cretaceous of Montana, *The University of Kansas Paleontological Contributions*, number 13

Cane, W. P. (1993), The ontogeny of postcranial integration in the common tern, *Sterna hirundo*, *Evolution*, 1138-1151

Cane, W. P. (1994), ontogenetic evidence for relationships within the Laridae, *the auk* 111(4):873-880

Carpenter, K. (2013), A Closer Look at the Hypothesis of Scavenging versus Predation by *Tyrannosaurus rex*, *Tyrannosaurid Paleobiology*, 265-77.

Carpenter, K., & Smith, M. B. (1995), Osteology and functional morphology of the forelimb in tyrannosaurids as compared with other theropods (Dinosauria), *Journal of Vertebrate Paleontology*, 15, 530.

Carrano, M. T., & Sampson, S. D. (2008), The phylogeny of Ceratosauria (Dinosauria: Theropoda), *Journal of Systematic Palaeontology*, 6(02), 183-236

Carrano. M. T., Benson, R. B. J. and Sampson, S. D. (2012), The phylogeny of Tetanurae (Dinosauria: Theropoda), *Journal of Systematic paleontology*, 10(2), pp. 211-300

Carrier, D., & Leon, L. R. (1990), Skeletal growth and function in the California gull (*Larus californicus*), *Journal of Zoology*, 222(3), 375-389.

Chamero, B., Buscalioni, Á. D. and Marugán-Lobón, J. (2013), Pectoral girdle and forelimb variation in extant Crocodylia: the coracoid–humerus pair as an evolutionary module, *Biological Journal of the Linnean Society*, 108, 600–618

Chatterjee, S. (1997). The rise of birds. *Baltimore: Johns Hopkins Univ. Pr*.

Chatterjee, S., & Templin, R. J. (2003), The flight of *Archaeopteryx*, *Naturwissenschaften*, 90(1), 27-32.

Chiappe, L. M. and Dyke, Gareth J. (2002), The Mesozoic Radiation of Birds, *Annual Review of Ecology and Systematics*, 33, pp. 91-124

Chiappe, L. M., Norell, M. A., & Clark, J. M. (1996), Phylogenetic position of *Mononykus* (Aves: Alvarezsauridae) from the Late Cretaceous of the Gobi desert, *Memoirs-Queensland Museum*, 39, 557-582.

Chu, P. (1998), A Phylogeny of the Gulls (Aves: Larinae) Inferred from Osteological and Integumentary Characters, *Cladistics* 14, 1–43

Codd, J. R., Manning, P. L., Norell, M. A. and Perry, S. F. (2008), Avian-like breathing mechanics in maniraptoran dinosaurs, *Proceedings of the Royal Society of London B: Biological Sciences*, 275(1631), pp. 157-161

Colwell, M. A. (2010), *Shorebird ecology, conservation, and management*, University of California press

Cooper, A. and Penny, D. (1993), Mass Survival of Birds Across the Cretaceous-Tertiary Boundary: Molecular Evidence, *Science*, 275(5303), pp. 1109-1113

Crochet, P.-A., Bonhomme, F., and Lebreton, J. D., (2000), Molecular phylogeny and plumage evolution in gulls (Larini), *Journal of Evolutionary Biology,* 13 (1), pp. 47-57

Cullen, T. M., Fraser, D., Rybczynski, N., & Schröder-Adams, C. (2014), Early evolution of sexual dimorphism and polygyny in Pinnipedia. *Evolution*, 68(5), 1469-1484.

Currie, P. J. (2003), Allometric growth in tyrannosaurids (Dinosauria: Theropoda) from the Upper Cretaceous of North America and Asia, *Canadian Journal of Earth Sciences*, 40(4), 651-665.

Dever, J. A., Strauss, R. E., Rainwater, T. R., McMurry, S. T., & Densmore, L. D. (2002), Genetic diversity, population subdivision, and gene flow in Morelet's

crocodile (*Crocodylus moreletii*) from Belize, Central America, *Copeia*, 2002(4), 1078-1091.

Dodson, P. (1993), Comparative craniology of the Ceratopsia, *American Journal of Science*, 293, pp. 200-234

Dodson, P. (2003). Allure of El Lagarto—Why do dinosaur paleontologists love alligators, crocodiles, and their kin? *The Anatomical Record Part A: Discoveries in Molecular, Cellular, and Evolutionary Biology*, 274(2), 887-890.

Dwight, J. (1925). The gulls (Laridae) of the world; their plumages, moults, variations, relationships, and distribution, *Bulleting of the American Museum of Natural History*, 52, pp. 63–408

Eaton, M. J., Martin, A., Thorbjarnarson, J., & Amato, G. (2009), Species-level diversification of African dwarf crocodiles (Genus *Osteolaemus*): a geographic and phylogenetic perspective, *Molecular Phylogenetics and Evolution*, 50(3), 496-506.

Edwards, S. V., Jennings, B. W., Shedlock, A. M., (2005), Phylogenetics of modern birds in the era of genomics, *Proceedings of the Royal Society B*, 272, pp. 979-992

Eernisse, D. J. and Kluge, A. G. (1993), Taxonomic Congruence versus Total Evidence, and Amniote Phylogeny Inferred from Fossils, Molecules, and Morphology, *Molecular Biology and Evolution*, 10 (6), pp. 1170-1195

Erickson, G. M., Currie, P. J., Inouye, B. D., & Winn, A. A. (2006), Tyrannosaur life tables: an example of nonavian dinosaur population biology.*Science*, 313(5784), 213-217.

Foth, C. and Rauhut, W. M. (2013), Macroevolutionary and Morphofunctional Patterns in Theropod Skulls: A Morphometric Approach, *Acta Palaeontologica Polonica*, 58(1):1-16

Fountaine, T. M. R., Benton, M. J., Dyke, G. J. and Nudds, R. L. (2005), The quality of the fossil record of Mesozoic birds, *Proceedings of the Royal Society of London B*, 272, 289–294

Fowler, D. W., Woodward, H. N., Freedman, E. A., Larson, P. L., & Horner, J. R. (2011), Reanalysis of "*Raptorex kriegsteini*": a juvenile tyrannosaurid dinosaur from Mongolia. *PLoS One*, 6(6), e21376.

Gatesy, S. M. (1991), Hind Limb Scaling in Birds and Other Theropods: Implications for Terrestrial Locomotion, *Journal of Morphology,* 209, pp. 83-96

Gauthier, J. (1986), Saurischian monophyly and the origin of birds, *Memoirs of the California Academy of Sciences*, 8, pp. 1-55

Gianechini, F. A. and Apesteguía, S. (2011), Unenlagiinae revisited: dromaeosaurid theropods from South America, *Anais da Academia Brasileira de Ciências,* 83(1), pp. 163-195

Godefroit, P., Sinitsa, S. M., Dhouailly, D., Bolotsky, Y. L., Sizov, A. V., McNamara, M. E., Benton, M. J., Spagna, P. (2014), A Jurassic ornithischian dinosaur from Siberia with both feathers and scales, *Science*, 345(6195), pp. 451-455

Griffiths, R., Double, M. C., Orr, K. and Dawson, R. J. G. (1998), A DNA test to sex most birds, *Molecular Ecology*, 7, pp. 1071 – 1075

Gündüz, İ., Jaarola, M., Tez, C., Yeniyurt, C., Polly, P. D., & Searle, J. B. (2007). Multigenic and morphometric differentiation of ground squirrels (*Spermophilus*, Scuiridae, Rodentia) in Turkey, with a description of a new species. *Molecular phylogenetics and evolution*, *43*(3), 916-935.

Gunnerus, J. E. (1767), Leem, K. (1975). *Larus albus gunnerus* in Leem's *Beskrivelse over Finmarkens Lapper*, 1767. Rosenkilde og Bagger, International Boghandel og Forlag.

Hackett, S. J. (1989), Effects of varied electrophoretic conditions on detection of evolutionary patterns in the Laridae, *Condor,* 91, 73–90.

Hackett, S. J., Kimball, R. T., Reddy, S., Bowie, R. C. K., Braun, E. L., Braun, M. J., Chojnowski, J. L., Cox, W. A., Han, K.-L., Harshman, J., Huddleston, C. J., Ben D. Marks, Kathleen J. Miglia, William S. Moore, Frederick H. Sheldon, David Steadman, W., Witt, C. C., Yuri, T., (2008). A phylogenomic study of birds reveals their evolutionary history. *science*, 320(5884), 1763-1768.

Haddrath, O. and Baker, A. J. (2001), Complete mitochondrial DNA genome sequences of extinct birds: ratite phylogenetics and the vicariance biogeography hypothesis, *Proceedings of the Royal Society of London*, 268, pp. 939 – 945

Harris, M. P. (1965), The food of some *Larus* gulls, *Ibis*, 107(1), 43-53.

Hayman, P., Marchant, J. and Prater, T. (1986), *Shorebirds, an identification guide to the waders of the world*, Houghton Mifflin

Hebert, P. D. N., Stoeckle, M. Y., Zemlak, T. S., Francis, C. M. (2004), Identification of Birds through DNA Barcodes, *PLoS Biology*, 2(10), pp. 1657-1663

Hedrick, B. P. and Dodson, P. (2013), Lujiatun Psittacosaurids: Understanding Individual and Taphonomic Variation Using 3D Geometric Morphometrics, 8(8), e69265

Hekkala, E. R. (2004), Conservation genetics at the species boundary: case studies from African and Caribbean crocodiles (Genus: *Crocodylus*), *New York, NY: Columbia University*.

Hendrickx, C., Hartman, S. A., & Mateus, O. (2015), An overview of non-avian theropod discoveries and classification, *PalArch's Journal of Vertebrate Palaeontology*, 12(1)

Hoffman, W. (1984), Phylogeny, feeding behavior, and wing structure in gulls, terns, and allies (Laroidea), Ph.D. thesis, University of South Florida, Tampa

Hoffman, W., Wiens, J. A., & Scott, J. M. (1978), Hybridization between gulls (*Larus glaucescens* and *L. occidentalis*) in the Pacific Northwest, *The Auk*, 441-458

Holliday, C. M. and Witmer, L. M. (2008), Cranial kinesis in dinosaurs: intracranial joints, protractor muscles, and their significance for cranial evolution and function in diapsids, *Journal of Vertebrate Paleontology*, 28(4), pp. 1073-1088

Holtz Jr, T. R. (2000), A new phylogeny of the carnivorous dinosaurs, *Gaia*, 15, 5-61

Holtz, T. R. (2004), Tyrannosauroidea, in *The Dinosauria* 2004

Holtz, T. R. (2012) Theropods, in *The Complete Dinosaur*, Indiana University press

Holtz, T. R. and Osmolska, H. (2004), Saurischia, *The Dinosauria*, 2004, pp. 21-24

Hoyo, J., Elliott, Andrew, Sargatal, Jordi, Christie, David A. (2013), Handbook of the birds of the world, Lynx Edicion

Hu, D., Hou, Lianhai, Zhang, Lijun & Xu, Xing (2009), A pre-*Archaeopteryx* troodontid theropod from China with long feathers on the metatarsus, *Nature*, 461 (7264), pp. 640-643

Hudson, G. E., Hoff, K. M., Vanden Berge, J. M., and Trivette, E. C. (1969), A numerical study of the wing and leg muscles of Lari and Alcae. *Ibis ,* 111, 459–524

Hugot, J. P., Morand, S. and Vassart, M. (1991), Morphological study of *Contracaecum magnicollare* (Nematoda, Anisakidae) from *Anous minutus* (Aves, Laridae), *Systematic Parasitology*, 20, pp. 229-236

Hurum, J. H., & Sabath, K. (2003), Giant theropod dinosaurs from Asia and North America: skulls of Tarbosaurus bataar and Tyrannosaurus rex compared. *Acta Palaeontologica Polonica*, 48(2).

Hutson, J. D., & Hutson, K. N. (2015), An examination of forearm bone mobility in *Alligator mississippiensis* (Daudin, 1802) and *Struthio camelus* Linnaeus, 1758 reveals that *Archaeopteryx* and dromaeosaurs shared an adaptation for gliding and/or flapping, *Geodiversitas*, 37(3), 325-344

Ingolfsson, A. (1970), Hybridization of glaucous gulls *Larus hyperboreus* and herring gulls *L. argentatus* in Iceland, *Ibis*, 112(3), 340-362

Irmis, R. B. (2010), Evaluating hypotheses for the early diversification of dinosaurs, *Earth and Environmental Science Transactions of the Royal Society of Edinburgh*, 101, pp. 397-426

Janke, A. and Ulfir Amason (1997), The Complete Mitochondrial Genome of Alligator mississippiensis and the separation Between Recent Archosauria (Birds and Crocodiles), *Molecular Biology and Evolution*, 14(2), 1266-1272

Jetz, W., Thomas, G. H., Joy, J. B., Hartmann, K. and Mooers, A. O. (2012), The global diversity of birds in space and time, *Nature,* 491, pp. 444-448

Ji, Q. and Ji, S. (1996), On the Discovery of the earliest fossil bird in China (Sinosauropteryx gen. nov.) and the origin of birds, *Chinese Geology*, 233, pp. 30-33

Ji, Q., Ji, S. A., Lü, J., You, H., Chen, W., Liu, Y. and Liu Y. (2005), first avialan bird from China, *Geological bulleting of china*, 24, 197-210

Ji, Q., Norell, M. A., Gao, K. Q., Ji, S. A., & Ren, D. (2001), The distribution of integumentary structures in a feathered dinosaur, *Nature*, 410(6832), 1084-1088.

Kielan-Jaworowska, Z., and Barsbold, R. (1972) Narrative of the Polish-Mongolian paleontological expeditions 1967– 1971, *Palaeontologia Polonica* 27: 5– 13

King, J. R., & Carey, G. J. (1999), Slaty-backed Gull hybridization and variation in upperparts colour, *Birder's Journal*, 8, 88-93.

Kischlat, E. E. (2000), Tecodoncios: A aurora dos Arcosaurios no Triassico. in Holz and De Rose (eds.), *Paleontologia do Rio Grande do Sol*. 273-316.

Kubetzki, U. and Garthe, S. (2003), Distribution, diet and habitat selection by four sympatrically breeding gull species in the south-eastern North Sea, Marine Biology, 143, pp. 199-207

Langer, M. C., Rincón, A. D., Ramezani, J., Solórzano, A., & Rauhut, O. W. (2014), New dinosaur (Theropoda, stem-Averostra) from the earliest Jurassic of the La Quinta formation, Venezuelan Andes, *Royal Society open science*, 1(2), 140184.

Larson, D. (2008), Diversity and variation of theropod dinosaur teeth from the uppermost Santonian Milk River Formation (Upper Cretaceous), Alberta: a quantitative method supporting identification of the oldest dinosaur tooth assemblage in Canada, *Canadian Journal of Earth Sciences*, 45, pp. 1455-1468

Larson, P. (2013), The case for *Nanotyrannus*, *Tyrannosaurid Paleobiology*, pp. 15-53

Larsson, H. C., Sereno, P. C., & Wilson, J. A. (2000), Forebrain enlargement among nonavian theropod dinosaurs, *Journal of Vertebrate Paleontology*, 20(3), 615-618

Lemme, I., and Erbacher, M., (2013), Molecules and morphology suggests cryptic species diversity and an overall complex taxonomy of fish scale geckos, genus *Geckolepis*, *Organisms Diversity and Evolution*, 13(1), pp. 87-95

Li, R., Lockley, M. G., Makovicky, P. J., Matsukawa, M., Norell, M. A., Harris, J. D., & Liu, M. (2008), Behavioral and faunal implications of Early Cretaceous deinonychosaur trackways from China, *Naturwissenschaften*, 95(3), 185-191

Linnaeus, C. (1758). Systema Naturae, Ed. 10, Vol. 1. 824 pp. *Salvii, Holmiae*.

Lipkin, C., & Carpenter, K. (2008), Looking again at the forelimb of *Tyrannosaurus rex*, *Tyrannosaurus rex, the tyrant king*, 166-189.

Livezey, B. C. (2010), Phylogenetics of modern shorebirds (Charadriiformes) based on phenotypic evidence: analysis and discussion, *Zoological Journal of the Linnean Society*, 160 (3), pages 567–618

Livezey, B. C., & Zusi, R. L. (2007), Higher-order phylogeny of modern birds (Theropoda, Aves: Neornithes) based on comparative anatomy. II. Analysis and discussion, *Zoological Journal of the Linnean Society*, 149(1), 1-95

Longrich, N. (2006), Structure and function of hindlimb feathers in Archaeopteryx lithographica. *Paleobiology*, 32(03), 417-431.

Longrich, N. R., Vinther, Jakob, Meng, Qingjin, Li, Quangguo, and Russell, Anthony P. (2012) Primitive Wing Feather Arrangement in *Archaeopteryx lithographica* and *Anchiornis huxleyi*, *Current Biology,* 22, 2262–2267

Maiorino L., Farke, A. A., Piras, P., Ryan M. J., Terris, K. M. and Kotsakis, T. (2013), *Journal of Vertebrate Paleontology*, 33(6), pp. 1385-1393

Makovicky P. J., Apesteguía S. and Agnolín F. L. (2005), The earliest dromaeosaurid theropod from South America, *Nature*, 437: 1007–1011

Makovicky, P. J., Kobayashi, Y. and Currie, P. J. (2004), Ornithomimosauria, in *The Dinosauria: second edition*, University of California Press

Manning, P. L., Payne, D., Pennicott, J., Barrett, P. M., & Ennos, R. A. (2006), Dinosaur killer claws or climbing crampons? *Biology Letters*, 2(1), 110-112.

Martin, L. D., Zhou, Z. H., Hou, L., & Feduccia, A. (1998), *Confuciusornis sanctus* compared to Archaeopteryx lithographica, *Naturwissenschaften*, 85(6), pp. 286-289.

Mayden, R. L. (1997), A hierarchy of species concepts: the denouement in the saga of the species problem, In *Species, The Units of Biodiversity*, ed. MF

Mayr, E. (1942), *Systematics and the origin of species, from the viewpoint of a zoologist*, Harvard University Press.

Mayr, E. (1957), Species concepts and definitions, pp. 1- 22. In E. Mayr (ed.), The Species Problem, *American Association for the Advancement of Science Publ*. 50, Washington, D.C

Mayr, E. (1982), *The growth of biological thought: Diversity, evolution, and inheritance*, Harvard University Press.

Mayr, E. (1963), *Animal species and evolution* (Vol. 797), Cambridge, Massachusetts: Belknap Press of Harvard University Press.

McGowan, A. J. & Dyke, G. J. (2007), A morphospace-based test for competitive exclusion among flying vertebrates: did birds, bats and pterosaurs get in each other's space? *Trustees of the Natural History Museum*, 20, pp. 1230-1236

Meganathan, P. R., Dubey, B., & Haque, I. (2009), Molecular Identification of Indian Crocodile Species: PCR-RFLP Method for Forensic Authentication, *Journal of forensic sciences*, 54(5), 1042-1045.

Meyer, B., & Wolf, J. (1822), *Taschenbuch der deutschen Vögelkunde* (Vol. 1). F.

Moyniham, M. (1959), A revision of the family Laridae (aves) *American Museum Novitates*, no. 1958

Naish D., (2012) Birds, in *The Complete Dinosaur*, Indiana University press

Naumann, J. A., & Naumann, J. F. (1822), *Naturgeschichte der Vögel Deutschlands: nach eigenen Erfahrungen entworfen*, 10, p 351. Fleischer

Nesbitt, J. S., Irmis, R. B. and Parker, W. G. (2007), A critical re-evaluation of the Late Triassic dinosaur taxa of North America, *Journal of Systematic Paleontology*, 5, issue 2, pp. 209-243

Nicholls, E. L., & Russell, A. P. (1985), Structure and function of the pectoral girdle and forelimb of *Struthiomimus altus* (Theropoda: Ornithomimidae), *Palaeontology*, 28(4), 643-677.

Norell, M. A. and Makovicky. P. J. (2004) Dromaeosauridae, in *The Dinosauria, second edition*, University of California press

Norell, M. and Xu, Xing (2005), Feathered Dinosaurs, *Annual Review in Earth and Planetary Science*, 33, pp. 277-299

Nudds, R. L. (2014), Reassessment of the wing feathers of *Archaeopteryx lithographica* suggests no robust evidence for the presence of elongated dorsal wing coverts, *PloS one*, 9(4), e93963.

O'Connor, J. and Zhou, Z. (2015), Early evolution of the biological bird: perspectives from new fossil discoveries in China, *Journal of Ornithology*, 73(1) pp. 1-10

Ord, G. (1815), North American Zoology, in Guthrie, W., *A New Geographical, Historical and Commercial Grammar: Philadelphia, Johnson and Warner*, *2nd American edition*, 2, 292.

Ostrom, J. H. (1976), Archaeopteryx and the origin of birds, Biological Journal of the Linnean Society. 8: 91-182

Padian, K. (2004) Basal Avialae, *The Dinosauria second edition*, pp. 210-231

Park, J., Lee, J., Lee, J., Kim, K. S., & Kim, S. (2014), Raptor: Fast bipedal running and active tail stabilization, *In Ubiquitous Robots and Ambient Intelligence (URAI), 2014 11th International Conference on* (pp. 215-215). IEEE.

Paul G. S. (1988), *Predatory Dinosaurs of the World: A Complete Illustrated Guide*. Simon and Schuster,

Pons, J. M., Hassanin, A., & Crochet, P. A. (2005), Phylogenetic relationships within the Laridae (Charadriiformes: Aves) inferred from mitochondrial markers, *Molecular phylogenetics and evolution*, 37(3), 686-699.

Pontoppidan, E. (1763), *Den Danske Atlas eller Konge-Riget Dannemark*, Trykt hos Kongelig Universitets Bogtrykker AH Godiche.

Prum, R. O., Berv, J. S., Dornburg, A., Field, D. J., Townsend, J. P., Lemmon, E. M. and Lemmon, A. R. (2015), A comprehensive phylogeny of birds (Aves) using targeted next-generation DNA sequencing, *Nature*, 526, pp. 569-573

Rauhut, O. W. (2003), Special Papers in Palaeontology, The Interrelationships and Evolution of Basal Theropod Dinosaurs, 69. Blackwell Publishing

Reece, J. B., Urry, Lisa A., Cain, Michael L., Wasserman, Steven A., Minorsky, Peter V., Jackson, Robert B. (2011), *Campbell biology*, ninth edition, Pearson Higher Education AU.

Reynolds, S. J., Martin, G. R., Wallace, L. L., Wearn, C. P. & Hughes, B. J. (2008), Sexing sooty terns on Ascension Island from morphometric measurements, *Journal of Zoology*, 274, 2–8

Reynolds, S. J., Martin, G. R., Wallace, L. L., Wearn, C. P. & Hughes, B. J.

Ridgway, R., & Friedmann, H. (1919), *The birds of North and Middle America: a descriptive catalogue of the higher groups, genera, species, and subspecies of birds known to occur in North America, from the Arctic lands to the Isthmus of Panama, the West Indies and other islands of the Caribbean sea, and the Galapagos Archipelago*, 50(8) Govt. Print. Off.

Rising, J. D. and Somers, Keith M. (1989), The Measurement of Overall Body Size in Birds, *The Auk*, 106(4), pp. 666-674

Ruben, J. (1993), Powered flight in Archaeopteryx: response to Speakman, *Evolution*, 47(3), 935-938.

Ryan, M. J., Evans, D., C., Currie, P. J., Brown, C. M., Brinkman, D. (2012), New leptoceratopsids from the Upper Cretaceous of Alberta, Canada, Cretaceous Research, 35, pp. 69-80

Schmidt-Nielsen, K. (1984), Scaling, why is animal size important? Cambridge University press

Schnell, G. D. (1970a), A phenetic study of the suborder Lari (Aves) I. Methods and results of principal components analyses, *Systematic Zoology*, 19, pp. 35 – 57

Schnell, G. D. (1970b), A phenetic study of the suborder Lari (Aves) II. Phenograms, discussion, and conclusions, *Systematic Zoology*, 19, pp. 264 – 302

Schnell, G. D., Worthen, G. L. and Douglas, M. E. (1985), Morphometric Assessment of Sexual Dimorphism in Skeletal Elements of California Gulls, *The Condor*, 87(4) (Nov., 1985), pp. 484-493

Sereno, P. C. (1997), The origin and evolution of dinosaurs, *Annual Review of Earth and Planetary Sciences*, 25(1), 435-489.

Sereno, P. C., & Brusatte, S. L. (2008), Basal abelisaurid and carcharodontosaurid theropods from the Lower Cretaceous Elrhaz Formation of Niger, *Acta Palaeontologica Polonica*, 53(1), 15-46.

Sereno, P. C., Forster, C. A., Rogers, R. R. and Monetta, A. M. (1993), Primitive dinosaur skeleton from Argentina and the early evolution of Dinosauria, *Nature*, 361, pp. 64-66

Sereno, P. C., Tan, L., Brusatte, S. L., Kriegstein, H. J., Zhao, X., & Cloward, K. (2009), Tyrannosaurid skeletal design first evolved at small body size, *Science*, 326(5951), 418-422.

Shirley, M. H., Vliet, K. A., Carr, A. N., & Austin, J. D. (2014), Rigorous approaches to species delimitation have significant implications for African crocodilian systematics and conservation, *Proceedings of the Royal Society of London B: Biological Sciences*, 281(1776), 20132483.

Sibley, D. A. (2003) *The Sibley field guide to birds of Eastern North America*, Knopf Doubleday Publishing group

Sibley, D. A. (2003) *The Sibley field guide to birds of Eastern North America*, Knopf Doubleday Publishing group

Sibley, J., C. G. and Ahlquist, J. E. (1990), Phylogeny and Classification of Birds: A Study in Molecular Evolution, Yale University Press, New Haven

Simpson, G. G. (1951), The species concept, *Evolution*, *5*(4), 285-298.

Smith, J. B., Vann, D. R., & Dodson, P. (2005), Dental morphology and variation in theropod dinosaurs: implications for the taxonomic identification of isolated teeth. The Anatomical Record Part A: Discoveries in Molecular, Cellular, and Evolutionary Biology, 285(2), 699-736.

Snell, R. R. (1989), Status of *Larus* Gulls at Home Bay, Baffin Island, *Colonial Waterbirds*, 12(1), pp. 12-23

Snively, E., & Russell, A. P. (2007), Functional variation of neck muscles and their relation to feeding style in Tyrannosauridae and other large theropod dinosaurs, *The Anatomical Record*, 290(8), 934-957

Speakman, J. R. (1993), Flight capabilities in Archaeopteryx, *Evolution*, 47(1), 336-340.

Starrfelt, J., & Liow, L. H. (2016), How many dinosaur species were there? Fossil bias and true richness estimated using a Poisson sampling model. *Phil. Trans. R. Soc. B*, 371(1691), 20150219

Strauch, J. G., JR. (1978), The phylogeny of the Charadriiformes (Aves): A new estimate using the method of character compatibility analysis, *Transcripts of the Zoological Society of London*, 34:263-345

Thomas, G. H., Wills, M. A., Szekely, T. (2004), Phylogeny of shorebirds, gulls, and alcids (Aves: Charadrii) from the cytochrome-b gene: Parsimony, Bayesian inference, minimum evolution, and quartet puzzling, *Molecular Phylogeny and Evolution*, 30, pp. 516-526

Thomas, G. H., Wills, Matthew A., Szekely, Tamas (2004), A supertree approach to shorebird phylogeny, *BMC Evolutionary Biology*, 4 (28), pp. 1-18

Timmennann, G. (1957), Studien zu einer vergleichenden Parasitologie der Charadriiformes oder Regenpfeifervogel. 1: Mallophaga, *Parasitologische Schriftenreihe* 8(204), p 1-15

Tuinen, M. (2009), Birds (Aves), *The Timetree of Life*, Oxford University Press, New York, pp. 409-411

Vigfúsdóttir, F., Pálsson, S., & Ingolfsson, A. (2008), Hybridization of glaucous gull (*Larus hyperboreus*) and herring gull (*Larus argentatus*) in Iceland: mitochondrial and microsatellite data, *Philosophical Transactions of the Royal Society of London B: Biological Sciences*, 363(1505), 2851-2860.

Wang, S. C. and Dodson, Peter (2006), Estimating the diversity of dinosaurs, *Proceedings of the National Academy of Sciences of the United States of America*, vol. 103 (37), pp. 13601-13605

Watanabe, A., & Slice, D. E. (2014), The utility of cranial ontogeny for phylogenetic inference: a case study in crocodylians using geometric morphometrics, *Journal of evolutionary biology*, 27(6), 1078-1092.

Webster, M., & Sheets, H. D. (2010), A practical introduction to landmark-based geometric morphometrics, *Quantitative Methods in Paleobiology*, 16, 168-188

Weishampel, D. B. Dodson, P., Osmólska, H. (2004), The *Dinosauria: Second Edition*, University of California Press

Wellhnofer, P. (1992), A new specimen of *Archaeopteryx* from the Sonlnhofen Limestone, *Natural History Museum of Los Angeles County*, 36, pp. 3-23

Wellnhofer, P. (1993), The seventh specimen of Archaeopteryx from the Solnhofen Limestone. *Archaeopteryx*, 11, pp. 1-47

Wetmore, A. (1960), A classification for the birds of the world, *Smithsonian Miscellaneous Collection*, 139(11), pp. 1-37

Witmer, L. M. (1990). The craniofacial air sac system of Mesozoic birds (Aves), *Zoological Journal of the linnean Society*, 100(4), 327-378.

Witmer, L. M. (1995), The Extant phylogenetic Bracket and the importance of reconstructing soft tissues in fossils, *Functional morphology in vertebrate paleontology*, first edition, pp. 19-33

Witmer, L. (2002) The debate on avian ancestry: phylogeny, function, and fossils. In: Chiappe, L. & Witmer, L. (eds.), *Mesozoic Birds: Above the Heads of Dinosaurs*, 3-30.

Wold, S., Esbensen, K., & Geladi, P. (1987), Principal component analysis, *Chemometrics and intelligent laboratory systems*, 2(1-3), 37-52.

Xing, L., Buckley, L. G., McCrea, R. T., Lockley, M. G., Zhang, J., Piñuela, L., Klein, H., Wang, F. (2015), Reanalysis of *Wupus agilis* (Early Cretaceous) of Chongqing, China as a Large Avian Trace: Differentiating between Large Bird and Small Non-Avian Theropod Tracks, *PLOS One*

Xu, X. and Pol, D. (2014), *Archaeopteryx*, paravian phylogenetic analyses, and the use of probability-based methods for palaeontological datasets, Journal of Systematic Palaeontology, 12 (3), 323–334

Xu, X., Wang, K., Zhang, K., Ma, Q., Xing, L., Sullivan, C., Hu, D, Cheng, S & Wang, S. (2012), A gigantic feathered dinosaur from the Lower Cretaceous of China.*Nature*, 484(7392), 92-95.

Xu, X., You, H., Du, K. & Han, F. (2011), An *Archaeopteryx*-like theropod from China and the origin of Avialae, Nature, 475, pp. 465-470

Xu, X., Zhao, Qi, Norell, M., Sullivan, C., Hone, D., Erickson, G., Wang, X., Han, F. & Guo, Y. (2008), A new feathered maniraptoran dinosaur fossil that fills a morphological gap in avian origin, *Chinese Science Bulletin*, 54(3), pp. 430-435

Yun, C.-C., (2015), Evidence points out that *Nanotyrannus* is juvenile *Tyrannosaurus rex*, *PeerJ Preprints*, 3, e1052

Zelditch, M. L., Swiderski, D. L., & Sheets, H. D. (2012), *Geometric morphometrics for biologists: a primer*, Academic Press.

Zhang, F., Kearns, Stuart L., Orr, Patrick J., Benton, Michael J., Zhou, Zhonghe, Johnson, Diane, Xu, Xing & Wang, Xiaolin (2010), Fossilized melanosomes and the colour of Cretaceous dinosaurs and birds, Nature, 463, pp. 1075-1078

Zheng, X., O'Connor, Jingmai, Wang, Xiaoli, Wang, Min, Zhang, Xiaomei, and Zhou, Zhonghe (2014), On the absence of sternal elements in *Anchiornis* (Paraves) and *Sapeornis* (Aves) and the complex early evolution of the avian sternum, *PNAS*, 111(38), pp. 13900-13905

Zheng, X.-T., You, Hai-Lu, Xu, Xing & Dong, Zhi-Ming (2009), An Early Cretaceous heterodontosaurid dinosaur with filamentous integumentary structures, *Nature*, 458(19), pp. 333-336